

# 國立交通大學

電子物理學系

## 博士論文

異向性超導體之渦旋物質的熱力學性質-Ginzburg - Landau 理論

Ginzburg-Landau theory—  
The thermodynamic properties of the anisotropic superconductors

研究生：林佩真

指導教授：儒森斯坦 教授


中華民國九十七年六月

異向性超導體之渦旋物質的熱力學性質-Ginzburg - Landau 理論  
Ginzburg-Landau theory—  
The thermodynamic properties of the anisotropic superconductors

研 究 生：林佩真  
指 導 教 授：儒森斯坦

Student : Pei-Jen Lin  
Advisor : Baruch Rosenstein

國 立 交 通 大 學  
電 子 物 理 學 系  
博 士 論 文



A Thesis  
Submitted to Department of Electrophysics  
College of Science  
National Chiao Tung University  
in partial Fulfillment of the Requirements  
for the Degree of  
Doctor of Philosophy  
in  
Electrophysics

June 2008

Hsinchu, Taiwan, Republic of China

中華民國九十七年六月

# 異向性超導體之渦旋物質的熱力學性質 ---Ginzburg - Landau 理論

學生：林佩真

指導教授：儒森斯坦

國立交通大學電子物理學系博士班

## 中文摘要

本論文主旨要探討在熱微擾下二類超導體在大磁場下的物理性質，以增廣超導應用上的知識。主要研究的材料是針對高溫超導和新的非傳統超導，此類材料在空間上的異向性很強，強烈的影響到費米面的不對稱性，使得材料在超導態的物理性質與傳統超導體有很大的不同。在磁場下超導所形成的奈米級的『渦旋物質』，它們可以大小彼此間的影響力是可以由調變溫度和磁場所控制，此外它們的活動深深影響在臨界區的物理現象。超導態的相變屬於二類相變的範疇，因此我們採用 Ginzburg - Landau 理論作為基本模型，根據不同的系統加以變化，並以統計力學的技巧考慮高溫效應和雜質的影響在一項性強的材料下的物理性質。

材料在空間異相性可以分為  $x$   $y$  平面上的異相性和  $z$  軸上層狀結構。在  $x$   $y$  平面上的異相性我們探討了四方長柱形底材的渦旋物質之結構相變。根據我們的計算發現可以藉由調變磁場強度控制渦旋物質結構使其產生由菱形到矩形的相變。在此研究中我們分別考慮了純系統和無序系統下對此結構相變的影響，結果顯示雜質影響下原本為第二類相變結構相變成為第一類相變，同時雜質也影響了結構相變曲線的溫度相依性等其他現象。

在研究  $z$  軸上層狀結構我們探討此異性相對超導反磁性的影響。所採用的模型有 Laerence-Doniach 模型和準二維的 Ginzburg - Landau 模型。一般勻稱的材料在  $H_{c2}(T)$ 附近的強磁場區裡物理量在不同磁場下的溫度特性曲線會有最低 Landau 能級的 scaling 行為，我們發現底材層狀結構和在準二維系統強大的熱擾動皆會破壞這個 scaling 行為，尤其在臨界曲線附近一般常用的最低 Landau 能級的近似法無法使用描述具有強熱效應的準二維系統。我們將理論的結果與很多實驗比照得到很好的應證。

# Ginzburg-Landau theory—The thermodynamic properties of the anisotropic superconductors

Student : Lin, Pei-Jen

Advisors : Prof. Rosenstein, B

Department of Electrophysics  
National Chiao Tung University

## ABSTRACT

Vortex matter plays an important role in superconductivity state especially for high- $T_c$  cuprate superconductors with layered structure. For an homogeneous system, the isotropic repelled vortices form the Abrikosov lattice. It was first proposed by Abrikosov for temperatures close to  $T_c$ , and then it was extended to all temperatures [56]. These theories ignore the fluctuations of the order parameter, called mean-field theory. It is a very good approximation for the conventional superconductors. However, under fluctuations influence at high temperature, the motions of vortices are responsible for the thermodynamic properties and transport properties of systems especially for those unconventional superconductors due to its strong anisotropic magnetic properties.

The most efficient way to study the mesoscopic phenomena is the effective Ginzburg-Landau (GL) functional. Unfortunately, because of the nonlinear term, even having the effective functional one can hardly calculate the free energy exactly. It is a typical problem for the critical phenomena. Lowest Landau level approximation (LLL) is a common way to simplify the question and its practical region is valid all the way down to  $H = H_{c2}(T)/13$  [89]. The LLL degeneracy results in a high field scaling was observed in many experiments. For various physical quantities (static quantities such as magnetization curves, specific heat etc. and dynamic quantities such as electrical conductivity etc.) as function of temperature will collapse to a scaling function for various fields. However, recent experiments show the failure of high field scaling behavior and the GL model is under examination. To understand them, in this thesis, we consider two cases in liquid phase: For strongly quasi 2D system, higher Landau levels contribution is taken into account. For the layered superconductors, the coupling between layers which changes the dimensionality of the system is considered. Our results show a good agreement with several experiments.

In the second part of this dissertation, the structural transition of vortex solid state is discussed. For a 4-fold symmetric system, it transpires that the coupling between magnetic flux and underlying crystal lattice influences the vortex lattice configuration in a complicate way. The distortion of vortex lattice from hexagonal lattice to square lattice depends on an external magnetic field which enhances the effect of anisotropy and temperature. At a sufficient high field, the configuration is a perfect square lattice.

Temperature dependency of the structural phase transition is under debate. Experiments shows that even for small  $G_i$  materials, the structural phase transition has a strong temperature dependency which is inconsistent with theoretical prediction base on the thermal fluctuations influences. It is found that quenched disorder is responsible for the departure from the mean field result in clean sample. Thermal fluctuations merely smear the anisotropy effect at the vicinity of its melting line.



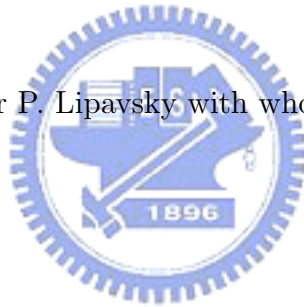
# Acknowledgements

I wish to express my deepest gratitude to Professor B. Rosenstein for his guidance and support throughout my research. I appreciate the scientific collaboration with him.

My special thanks to Professor D. Li for his help on some parts of my work.

I would like also to thank Dr. G. Bel for his fruitful, guidance and friendship throughout my research.

Finally I thank Professor P. Lipavsky with whom I had an inspiring collaboration.



# Contents

Approval ii

Abstract iii

Acknowledgements vi

Contents vii



1 Introduction 1

1.1 Superconductivity . . . . .	5
1.2 Spontaneous Symmetry Breaking and Phase Transitions . . . . .	10
1.3 Thermal fluctuations in anisotropic/ disordered superconductors . . . . .	12

2 Mesoscopic description of superconductor in magnetic field 17

2.1 Landau Expansion of the Free Energy in homogeneous Superconductors . . . . .	18
2.2 Landau Expansion of the Free Energy in Anisotropic Superconductors . . . . .	20
2.3 Applicability of Lowest Landau level approximation within the mean field approach . . . . .	24
2.4 Optimized perturbation approach and the Bore-Padé approximation. . . . .	26
2.5 Disorder . . . . .	30

3 Magnetization in Layered Superconductors	33
3.1 Introduction	33
3.2 Basic equations and assumptions	35
3.3 Dimensionality effects of layered superconductors	40
3.4 Sum of contributions of all Landau levels in quasi-2D systems. The 1... OPA method	42
3.5 All Landau level contributions in quasi-2D systems. An effective LLL model	45
3.6 Results and Comparisons with Experiments	48
3.7 Discussion	52
4 Structural Phase transition in Fourfold Symmetric Superconductors	54
4.1 Introduction	54
4.2 Basic equations and symmetries	56
4.3 Structure of the vortex lattice in the clean system and its phase transition	57
4.4 Effects of weak disorder on structural phase transition	60
4.5 Spectrum of rhombic lattice in a clean system	63
4.6 Hartree-Fock-like approximation and Replica trick in disordered system	66
4.7 Results	71
4.8 Discussion	74
5 Summary	79
Bibliography	81



# Chapter 1

## Introduction

A two steps transition from the superconducting to the normal state with two critical fields was first observed in the magnetization of superconducting alloys by De Haas and Casimir-Jonker back in 1935 [2]. It was originally “explained away” by inhomogeneity of their samples. Correct explanation proposed on 1957 when Abrikosov predicted theoretically the existence of type II superconductors that magnetic field can penetrate into a superconducting material [4]. Each “individual” magnetic flux is quantized by surrounding supercurrent thus to form a vortex. Abrikosov also suggested a periodic magnetic field distribution, transverse to the applied field, occurs near the critical region of superconducting -normal transition. Due to this structure, the mixed state is sometimes called “the vortex lattice phase”. The existence of the vortex lattice was not widely accepted at that time. In 1964, at the suggestion of De Gennes & Matricon, Cribier, Jacrot, Rao and Farnoux performed the first experiment in which the triangular vortex configuration in a single crystal was observed by neutron scattering [11]. At different magnetic field  $H$  and temperature  $T$ , multitude of vortex lattice configurations were observed in  $Nb$  which has a simple cubic underlying atomic crystalline structure. All the vortex lattices were locked in a certain crystal direction [13]. Theoretically, the energy difference between various lattices is very small. For example, it amounts to just 2% between the square and the triangular lattices. In real substances, the crystalline symmetry can make the square lattice more favorable. In 1966, Neumann and Tewordt proposed to incorporate nonlocal effects

by including higher order derivatives terms in the general GL model which reflect the material anisotropies. Since in original GL or London model, to incorporate anisotropy terms is via local effective mass tensor,  $\mathbf{m}$ . And *Nb* has cubic crystalline atomic structure whose  $\mathbf{m}$  is isotropic, thus the nonlocal effect is important [12]. In the new class of heavy fermion and cuprate superconductors, one would expect even richer behaviors of vortex configuration as these materials exhibit highly anisotropic electronic structures and order parameters with unconventional symmetries involving nodes in superconducting gap. Microscopically, the Fermi surface anisotropy, anisotropy of the effective mass, and asymmetry in the superconducting gap remove the degeneracy of vortex lattice orientation with respect to atomic lattice and also other lattice configurations will appear. Renewed interest in the vortex configurations is due to experimental observations of the rhombic-to-square lattice transition in high- $\kappa$  materials in *s*-wave superconductors, such as Boracabides ( $RE = Er, Y, Lu$ )  $Ni_2B_2C$  [14],  $V_3Si$  [15] and *Nb* [13], and in *d*-wave high  $T_c$  superconductors, such as  $La_{2-x}Sr_xCuO_4$  [16] and  $YBa_2Cu_3O_7$ [18], and in recently discovered *d*-wave heavy fermion superconductor such as  $CeCoIn_5$ [19]. Roughly speaking, for a system with a four-fold symmetry, magnetic field will enhance the coupling with underlying crystal, therefore, square vortex lattice appears at higher magnetic fields, compare with the magnetic fields where triangular lattices were observed. The current puzzling issue is whether the temperature dependence of the structural phase transition (SPT) line is a consequence of thermal fluctuations of vortex lattice or not. This contrasts with the situation in low- $T_c$  superconductors, such as Boracabides etc. in which the thermal fluctuation influence is negligible. In the present thesis, I studied how both the thermal fluctuation and the quenched disorder influence the structural phase transitions in the vortex lattice based on the extension of the GL model for 4-fold symmetric system[22][26]. Unlike the existing theoretical interpretations[23][24] [20], we proposed that quenched disorder dominates the temperature dependence of SPT transition. Near the mean field SPT line, while having a square lattice structure at low temperatures, rhombic lattice is restored at a higher temperature region in the vicinity of  $H_{c2}(T)$ [21][25]. In addition to the in-plane anisotropy which results in the struc-

tural phase transition in vortex solid state, the anisotropy in  $c$ -direction dramatically enhances the thermal fluctuations in the presence of magnetic field at high temperatures. It is typical for high- $T_c$  layered superconductors that thermal fluctuations change the morphology of vortex matter. The intrinsic properties of the high- $T_c$  superconductor which enhanced fluctuations of order parameter are (a) the high- $\kappa$ , the ratio between coherence length and magnetic penetration depth, and (b) the large effective distance (or weak coupling) between superconducting layers and (c) high critical temperature  $T_c$  and (d) high critical field  $H_{c2}$ . A widely accepted way to characterize the thermal fluctuations influence of a material is using a dimensionless quantity  $Gi$  (see section 1.3). Due to the relatively large  $Gi$  of high- $T_c$  layered superconductor (compare to conventional superconductor), an additional critical scaling behavior which is very different from the ordinary universality of critical phenomena arise from thermal fluctuations. In 1991, the magnetization and resistivity in  $YBa_2Cu_3O_7$  by Welp *et al* [28] reported scaling behaviors in the variable of  $(T - T_c(H)) / (TH)^{2/3}$  around the critical temperature in the vicinity of the  $H_{c2}(T)$ . The temperature dependent physical quantities of various magnetic fields collapse into a single scaling function (see Fig. 3.4). The scaling function is universal for various anisotropy 3D materials. Li and Suenaga noticed that the magnetization of highly anisotropic  $Bi_2Sr_2Ca_2Cu_3O_{10}$  crystals can be described by the 2D version of the scaling function in the variable  $(T - T_c(H)) / (TH)^{1/2}$  [29]. Due to the scaling behavior, there exist a crossing point  $(T^*, H^*)$  where  $T$  dependent physical quantity curves,  $O(T, H)$ , of various  $H$  (or  $T$ ) interact at the point for a given dimension. The fixed point characterize the dimensionality of the system. The scaling called Lowest Landau level (LLL) scaling is due to the situation that the fluctuations near  $H_{c2}(T)$  can be represented in terms of the GL field theory on a degenerate manifold spanned by the LLL for Cooper pairs. The LLL scaling is formally valid in a wide range of the  $H - T$  parameters space (see section 2.3 for details). Therefore, LLL approximation is a general adopted approximation to simplified the nonlinear GL theory[48, 89, 83]. However, when the interaction term in the GL theory is larger than the cyclotron gap of Cooper pairs and the fluctuations from excited Landau levels become significant. For

layered materials such as *LaSCO* [32], *HgBCCO*[31] and underdoped *YBCO*[86], while the coherence length  $\xi_c(T)$  is comparable to interlayer spacing  $d$  at certain temperature near  $H_{c2}(T)$ , the change of dimensionality of the system results in the breaking of the general LLL scaling. Namely, the crossing point of the magnetization curves can "moves" from its 2D to 3D position while approaching  $H_{c2}(T)$  from the superconducting phase. In 2000, underdoped *LaSCO* experiment by Huh shows the motion of crossing points in the opposite directions to that predicted theoretically and eventually it exceed  $T_c$  [32]. We mathematically define the intersection point and study its motion base on a layered model, the LD model. It is shown that the intersection point always occurs below  $T_c$  [36]. And the theory is in agreement with other recent experiments on layered superconductors on *HgBCCO*[31] and *LaSCO* [32]. Recently experiments on strongly anisotropic quasi-2D material *BSCCO* done by Ong *et al.* on 2005 provided a "new" behavior of High- $T_c$  superconductors[30], in which the data has been found to be in disagreement with the theory based on the thermal fluctuations scenario. In this study, we proposed that the anomalous behavior is due to the thermal fluctuations from excited Landau levels in which we take into account the contribution from all Landau levels and use resummation technique to obtain the theoretical curves. In the following, the basic idea and the current understanding of the vortex matter in type II superconductor are discussed in this chapter. The second chapter will discuss the various modifications of homogeneous GL model for particular materials. In section 2.3, the valid region of LLL approximation is discussed. In section 2.4, an efficient approach, the optimization variational approach, and a resummation technique, a Borel-Pade approximation, are introduced and the convergency of the series is discussed. In section 2.5 the disorder model which will be used in SPT is discussed. The fluctuations influence of different dimensionality high- $T_c$  superconductors are presented in Chapter 3. The structural phase transition will be discussed in Chapter 4. As a result I can state that the "mystery" part at the critical regime of high- $T_c$  superconductivity can be understood as the thermal fluctuations of order parameter.

## 1.1 Superconductivity

Superconductivity was first discovered in 1911 by H. Kamerlingh Onnes in Leiden [1]. A few years after he had first liquefied helium and reach temperatures of a few degrees of Kelvin, he observed that the electrical resistance of various metals such as mercury, lead, and tin disappeared completely in a small temperature range at a critical temperature,  $T_c$ , which is characteristic of the material. This perfect conductivity is the first traditional hallmark of superconductivity.

The next hallmark to be discovered was perfect diamagnetism, found in 1933 by Meissner and Ochsenfeld [7]. They found that not only does magnetic field not enter a superconducting sample, as might be explained by perfect conductivity, but also that a field in an originally normal sample is expelled as the sample is cooled through  $T_c$ . The existence of such a reversible Meissner effect implies that superconductivity will be destroyed by a magnetic field above certain critical field  $H_c$ . The new thermodynamic state is call superconducting state. This critical field, named as thermodynamic critical field, is determined by the difference in free energies of the superconducting state and the normal state.

The disappearance of the electrical resistance below  $T_c$ , has numerous important applications. Since it allows the existence of non-decaying electric currents, supercurrent, stay permanently inside the material. It makes possible the production of many important devices such as extremely powerful electromagnets, energy reservoirs, and much more. However, the supercurrent density allowed to flow through a sample is limited by a critical value  $J_c$ , which is an upper limit of the current consumption of these devices and, therefore, on their maximum output power.

Various theories were suggested in order to describe and explain superconductivity. In 1935 F. and H. London [5][6] proposed a phenomenological theory based on classical Maxwell electromagnetism, which was able to describe the basic electromagnetic properties of a homogeneous superconductor. The London theory and its future generalizations [10] introduced two important scales: the concepts of correlation length,  $\xi$ , and penetration depth,  $\lambda$ . Those two parameter characterize many physical properties

of a system.

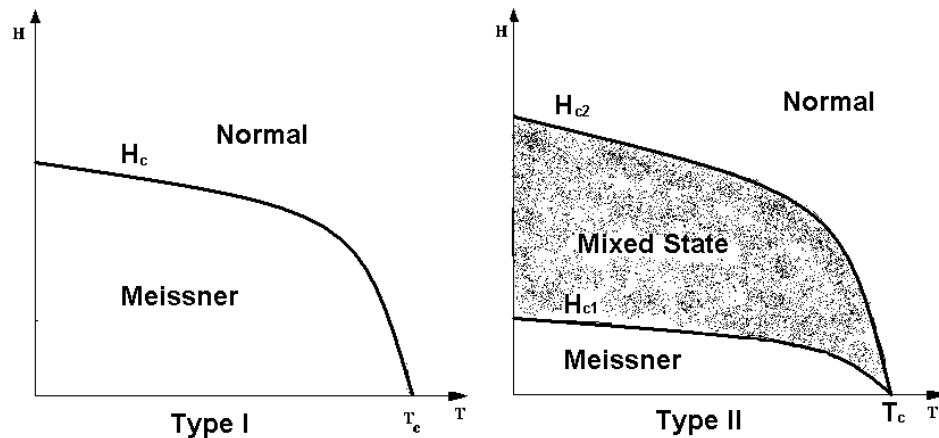


Figure 1.1: The H-T phase diagram of Type I and Type II superconductors

Even though the two quantities are both material and temperature-dependent, their quotient is effectively temperature-independent and can be considered as a material characteristic. The new dimensionless quantity is called the *Ginzburg-Landau parameter* and is denoted by  $\kappa = \lambda/\xi$ . As was shown by Abrikosov [4], two types of superconductors exist, differing by the value of  $\kappa$  and behaving differently in the presence of a magnetic field. Superconductors with  $\kappa < 1/\sqrt{2}$  are called Type-I, and those with  $\kappa > 1/\sqrt{2}$  are called Type-II. The value  $1/\sqrt{2}$  is an exact solution where the interface energy (between superconductivity and normal state) vanished.

Type-I superconductors can exist in one of two thermodynamically stable states - either in the normal, or in the superconducting state. The superconducting state is energetically favorable at  $T < T_c$  and  $H < H_c$ .  $H_c$  and  $T_c$  are mutually dependent, see Fig. 1.1. Applying an external magnetic field to the system turns on the surface supercurrents, which screen the field from the interior of the superconductor. It does not allow external magnetic field to penetrate deeper than  $\lambda$ . This phenomenon is called the *Meissner effect* [7], and the whole state is sometimes called the *Meissner state*. In this state the material has perfect diamagnetism. The magnetization defined as  $4\pi M = B(r) - H$  (where  $B = 0$  in Meissner state) is negative and proportional to up to  $H_c$ . In an ideal sample, it has a reversible hysteresis curve.

When the external magnetic field approaches  $H_c$  and the screening surface supercurrents approach  $J_c$  ( $H_c$  and  $J_c$  are therefore mutually dependent), the superconducting state is no longer energetically favorable, and a second order phase transition into the normal state takes place. The opposite process is possible as well. The quantity  $H_c^2/8\pi$  is the condensation energy density of the system. It should be emphasized that this scenario is exact only for the case of an infinite cylinder, while arbitrary geometry Type-I superconductors transform into an *intermediate state* [50, 51], consisting of large superconducting and normal domains separated by domain walls.

Unlike Type-I, Type-II superconductors have an extra thermodynamically stable state - the *mixed state* [4], in which the external magnetic field partially penetrates the bulk of the superconductor, locally destroying superconductivity. In this case two critical magnetic fields exist,  $H_{c1}$  and  $H_{c2}$  (see Fig. 1.1).  $H_{c1}$  is the lower critical magnetic field, at which the magnetic field starts penetrating into the bulk of the superconductor and superconductivity begins to decline, and  $H_{c2}$  is the upper critical field, at which the magnetic field fills the whole sample, i.e. superconductivity is destroyed while the normal metallic state is recovered. The  $H_{c1}$  is mainly determined by the London penetration depth  $\lambda$ , which is the length scale determining the electromagnetic response of the superconductor. From the London equation set, one got  $H_{c1} = (\Phi_0/4\pi\lambda^2) \log(\kappa)$ . The upper critical field  $H_{c2}$  is determined by the coherence length  $\xi$  of superconductor, which determines the spatial response of the macroscopic field  $\Psi$ . The relation between  $H_{c2}$  and  $\xi$  are given by  $H_{c2} = \Phi_0/2\pi\xi^2$ , where  $\Phi_0$  is a fluxon. The transition to normal state is of second order.

The differences in the behavior of Type-I and Type-II superconductors can be explained if one examines the transitional energy between the normal and the superconducting domains, which is positive in Type-I and negative in Type-II superconductors. In this study, we have interest on physics of the mixed state.

In the mixed state, the penetration of the magnetic flux into the superconductor takes place in the form of long thin flux lines, called *Abrikosov vortices* or *fluxons* (see Fig.1.2). At the center of each vortex a normal core exists, bearing the magnetic flux



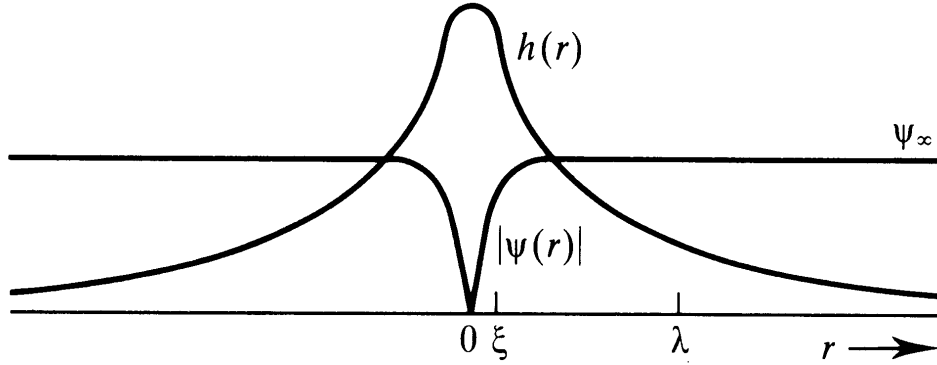


Figure 1.2: The order parameter and the magnetic field profiles of a single Abrikosov vortex

created by supercurrents moving around the core. The characteristic radius of the core, i.e., the radius at which the order parameter decay from its maximal value to zero is  $\xi$ , while the magnetic field and the supercurrents, which surround the core, spread as far as  $\lambda$  from it. The amount of magnetic flux  $\Phi$  carried by each vortex is quantized and equal to an integer number of unit quanta  $\Phi_0 = hc/2e = 2.07 \cdot 10^{-7} (G \cdot cm^2)$  [61]. For a single vortex, with magnetic field,  $H$ , apply to  $z$  direction, the induced magnetic field

$$B(\mathbf{r}) = \frac{\Phi_0}{2\pi\lambda^2} K_0\left(\frac{|r|}{\lambda}\right)$$

where  $K_0$  is Hankel function has the following properties:

$$K_0\left(\frac{r}{\lambda}\right) \approx \begin{cases} \log(\kappa) & , r \leq \xi \\ -\log(r/\lambda) & , \xi \ll r \ll \lambda \\ \left(\frac{\pi\lambda}{2r}\right)^{1/2} e^{-r/\lambda} & , r \gg \lambda \end{cases}$$

The core cutoff is introduced to prevent unphysical divergence of magnetic field.

Vortex interaction consists of two parts, electromagnetic interaction due to the Lorentz force acting between the current loops, and interaction due to the gradient of the order parameter in the vicinity of the core. The electromagnetic interaction between fluxons and antfluxons (fluxons with an opposite direction of supercurrent and magnetic field) is attractive, while the electromagnetic interaction between fluxons of the same sign is repulsive. The cores interaction is always attractive but is usually neglected due to



the fact that it decays over short distance compare to the electromagnetic interaction, in extremely Type II superconductors ( $\kappa \gg 1$ ). Let's look at a simplified model in London limit where the validity is  $r \gg \xi$ . Consider two parallel straight vortices, the London equation is linear in magnetic field within range of its validity. The interaction line energy density (Gibbs energy) between two straight vortices line which is defined as  $\Delta g = g(\mathbf{x}_1, \mathbf{x}_2) - g(\mathbf{x}_1) - g(\mathbf{x}_2)$  where  $\mathbf{x}_i$  is the position of the core  $i$  is

$$\Delta g = \frac{\Phi_0^2}{8\pi^2\lambda^2} K_0\left(\frac{r}{\lambda}\right).$$

The interaction force per unit length is

$$f_{force} = -\frac{dg}{dr} = \frac{\Phi_0^2}{8\pi^2\lambda^2} \begin{cases} r^{-1} & , \xi \ll r \ll \lambda \\ \frac{1}{2} \left(\frac{\pi}{2\lambda r}\right)^{1/2} e^{-r/\lambda} & , r \gg \lambda \end{cases}.$$

One can see that the vortex repulsion is isotropic. In dense region, the vortex should form the hexagonal Abrikosov lattice, which provides the maximal vortex spacing for a given flux density  $B/\Phi_0$ . For interaction of curving vortices line please find the detail in [99].

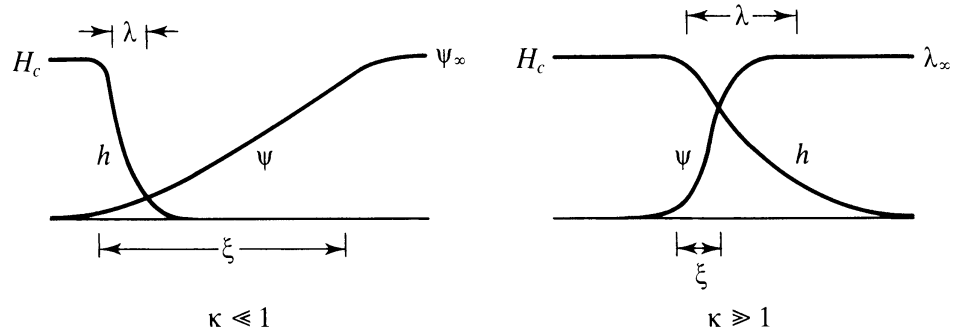


Figure 1.3: Profiles of correlation length  $\xi$  and penetration depth  $\lambda$  of Type-I ( $\kappa \ll 1$ ) and Type-II ( $\kappa \gg 1$ ) superconductors on a normal-superconducting interface the magnetic field profiles of a single Abrikosov vortex

## 1.2 Spontaneous Symmetry Breaking and Phase Transitions

Phase transitions [120] are usually described with an *order parameter* function, retain a finite value at the ordered (non-symmetric) phase and vanish in the disordered (symmetric) phase. The order parameter depends on the system it describes, and bears the symmetries of the ordered state. As an example, one can think of a conventional superconductor, whose order parameter is a complex scalar having the  $U(1)$  symmetry, which matches the local gauge invariance of superconductors (for detailed discussion of the order parameter properties see discussion below).

There are two kinds of phase transitions, named the *first order* and the *second order*. The difference between them is that during a first order phase transition the system changes its state immediately rather than gradually, i.e., the order parameter is discontinuous at the transition point. The liquid-gas transition is a typical example of such a process where the density serves as an order parameter, and at the critical pressure there is a sudden increase in the density even if the pressure changes slightly. This, however, is not the case for the second order phase transition where various physical quantities either vanish or diverge at the transition point continuously. The order parameter declines smoothly as the system nears the transition point, while completely disappearing at the point itself. In the critical region, the scale of correlation is unbounded, namely, large scale correlation such as universality is observed. In the language of field theory, one is approaching a zero mass theory. At such point the first derivative of the free energy-like entropy, volume, magnetization, etc.-behave continuously. Note that is possible there is no change in symmetry at transition point. For example the critical point of the gas-liquid transition involves no symmetry change at all.

Second order phase transitions can be modeled with a potential, proposed by Landau [3]:

$$V = \alpha |\Psi|^2 + \frac{\beta}{2} |\Psi|^4 \quad (1.1)$$

where  $\Psi$  is the order parameter function and  $a$  and  $b'$  are phenomenological parameters.

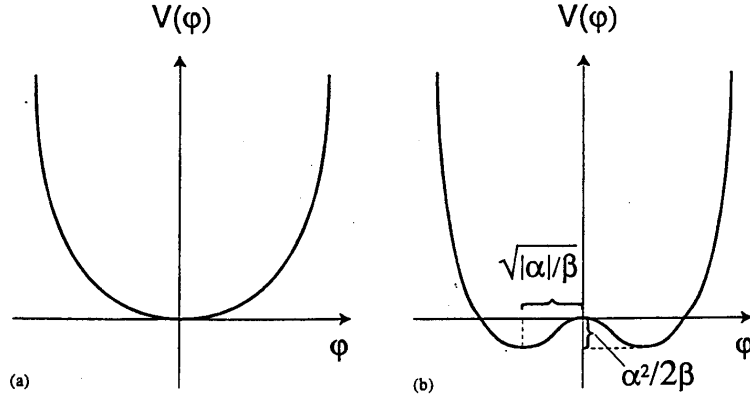


Figure 1.4: The effective potential  $V(\varphi)$  describing second order phase transitions

Minimizing the potential one can find the values of  $|\Psi|$  corresponding to the vacuum state (see Fig.1.4). Given  $b' > 0$  (a necessary condition for the existence of a minimum), this potential has two modes differing by the sign of  $a$ . If  $a > 0$  there is only one minimum at  $|\Psi| = 0$ , and this mode corresponds to the disordered phase. However, if  $a < 0$ , the minimum is at  $|\Psi| = \sqrt{|a|/b'}$ , while  $|\Psi| = 0$  turns into a maximum, and this mode corresponds to the ordered phase.  $\alpha$  is therefore a crucial parameter that triggers the phase transition. The condensation energy is  $(\alpha T_c)^2 / 2b'$ . It is temperature dependent and has the following form at  $T \sim T_c$ :

$$a(T) \simeq \alpha T_c \left( \frac{T}{T_c} - 1 \right) \quad (1.2)$$

As the temperature declines and passes through  $T_c$  the vacuum state of the system changes, although it is possible that the new vacuum has a degeneracy. The type of this degeneracy strongly depends on the properties of the order parameter in the ordered phase. In a ferromagnet, for example, the order parameter is a real vector, namely the vector of magnetization, but its energy, according to Eq. (1.1), is not affected by the direction of magnetization, only by its magnitude. In 1D ferromagnets this situation corresponds to a 2-fold degeneracy of the ordered state - the magnetization vector points either up or down. The order parameter of a conventional superconductor is a complex scalar. Looking at Eq. (1.1) one finds that the superconducting vacuum state is infinitely degenerate, since the phase of order parameter does not appear in the potential and

therefore does not affect the energy.

Abrikosov vortices is a kind of topological defect. The systems with a complex order parameter are *strings* -  $1D$  objects that are encircled by areas of different order parameter phase in such a way that its total change around the string at every point of its length is equal to  $2\pi n$ , where  $n$  is an integer. The latter condition is required in order to ensure that the order parameter is a single-valued function.

### 1.3 Thermal fluctuations in anisotropic/ disordered superconductors

The main phenomenon determining the physics of the vortex lattice is thermal motion of vortices about their equilibrium position. At high temperature thermal fluctuation increase the amplitude of the vortices vibration. I first exemplify the qualitatively the phenomenon using the London approximation limit, which is different from the so called lowest Landau level approximation limit mainly employed in the following sections. An isolated flux line acting as a stretched string can undergo both longitudinal or transverse vibrations. At the region of parameter space in which vortices are densely packed the vibrations are more localized along the length of the vortex core with numerous nearby vortices participating in collective. The vortex motion strongly depends on the material characteristics, impurities, external magnetic field and temperature.

A naive idea to estimate the influence of thermal fluctuation is via a characteristic length  $L_T$  of segment of the vortex associated the quantized flux energy to the thermal energy. The energy  $U_M$  of magnetic field in a region of volume  $V$  is given by

$$U_M = \frac{\Phi_0^2}{8\pi} \frac{V}{A^2},$$

where  $B = \Phi_0/A$  and  $A$  is the area of the unit cell of the vortex lattice. If this is equated to the thermal energy  $k_B T$  for a quantum flux, and if we write  $A^2/V = 2\pi L_T$ , we obtain the characteristic length

$$L_T = \frac{\Phi_0^2}{16\pi^2 k_B T} = \frac{1.79}{T (\text{Kelvin})} \text{cm}.$$

This is much larger than other characteristic lengths, such as  $\xi$  and  $\lambda$ , except in the case of temperature extremely close to  $T_c$  both  $\xi$  and  $\lambda$  diverged as  $(T_c - T)^{-1}$ . Therefore, fluctuation can be expect to be small when at low temperature. In high temperature cuprates several factors combine to enhance the effects of thermal fluctuations: (1) higher transition temperature, (2) shorter coherence length  $\xi$ , (3) large magnetic penetration length  $\lambda$  (4) quasi- $2D$ - dimensionality, and (5) high anisotropy.

A proper fundamental material parameter describing the strength of thermal fluctuations is the Ginzburg number  $Gi = (T_c/F_{con})^2 / 2$  [62], which is the ratio of the minimal ( $T = 0$ ) condensation energy  $F_{con} = (H_c^2/8\pi) \xi_c \xi^2$  within a coherence volume ( $\xi_c \xi^2$ ) and the critical temperature  $T_c$ . It is a dimensionless quantity. For typical superconducting metals  $Gi$  is very small (of order  $10^{-6}$ ). It becomes significant for relatively isotropic high  $T_c$  cuprates *YBCO* ( $10^{-3}$ ) and even quite large for strongly anisotropic cuprates *BSCCO* (up to  $Gi = .1 - .5$ ).

Disorder of a sample originally comes from point defect, dislocation, oxygen vacancy, grain boundary...etc.. It can change the local properties of the sample, such as critical temperature, the effective mass and coupling between vortices. A vortex will experience a short range pinning force that hold the core of a vortex at a defect. The pinning energies have been reported in the range of hundreds of  $meV$ . When sufficient pinning center are present, the spatial structure of vortices will reflect the distribution of pinning center and the long-range order of vortex lattice is disturbed. It will result in glassy state.

Disorder dramatically influence the vortex motion. Fig 1.5 shows the glass transition in the driven case. In the flux-flow regime, the driven lattice hits the defects and pushes the vortex from the pinning centre. The onset motion of vortex is determined by competition between driving forces, usually Lorentz forces, and pinning force. In the steady-state motion, the viscous force which result in dissipation are present. In the presence of thermal excitations, vortices can undergo thermal hopping between pinning centers.

Theoretical study of those phenomena predict a complicate phase diagram of vortex matter shown in Fig.1.6, which is more complicate than the mean field diagram for clean

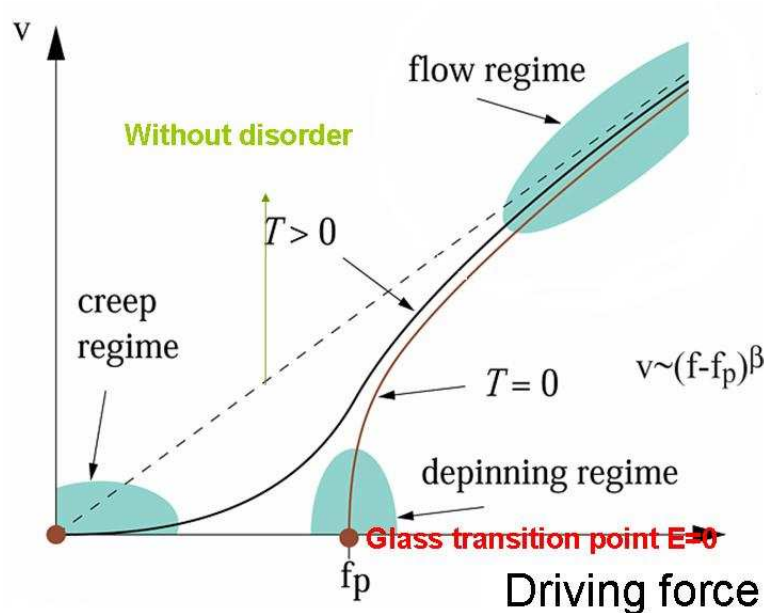


Figure 1.5: Diagram of Vortex Motion

idea sample. There are five main distinct phases: unpinned solid (solid), pinned solid (Bragg glass), pinned liquid (vortex glass or amorphous solid), weakly pinned solid with marginal glassy dynamics, and unpinned liquid (or simply liquid). With anisotropic effect on  $a - b$  plane, the phase diagram will have additional complexity, the vortex solid will encounter structural phase transition.

Melting of the vortex lattice happened when thermal agitation induces a wandering of vortex filaments and leads to an entangled flux liquid phase. Pairs of flux lines passing close to each other can be cut, exchanged, or reattached. Qualitatively, according to Lindermann criterion, melting occurs when the root mean-square fluctuation amplitude  $u_{rms}$  exceed the quantity  $\approx 10^{-1}s$ , where  $s$  is the average vortex separation distance. Evidence of the first-order vortex-lattice melting transition is confirmed by experiments in single crystals of  $YBa_2Cu_3O_y$ [44] [33][28][39],  $Bi_2Sr_2CaCu_2O_y$  [94][34], and  $La_{2-x}Sr_xCuO_y$ [40][41][42] and other high- $T_c$  materials. The transition type be determined by magnetization jumps [94], spikes in specific heat [33], SQUID[34] and etc..

The order-disorder (ODO) transition is defined as the moment of the loss of the

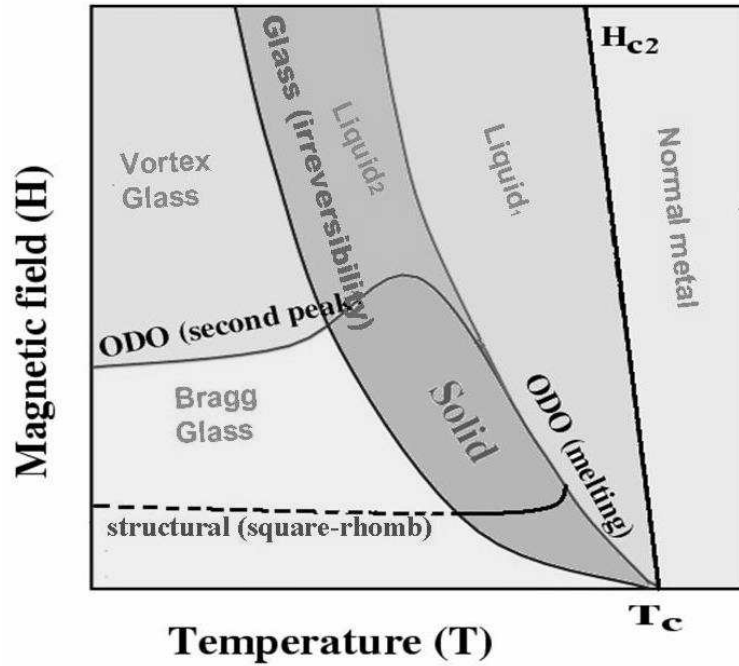


Figure 1.6: Phase diagram of vortex matter: The complexity of the phase diagram is due to the influence of thermal fluctuations, disorder and anisotropy.

translation and rotation symmetry. The intensity of the first Bragg peak can be used as an order parameter. The first order ODO line has two parts: the melting segment and the “second magnetization peak” segment, separates the homogeneous and the crystalline phases. The broken symmetry is not directly related to pinning, but the location of the line is sensitive to the strength of disorder. Thermal fluctuations, on one hand side, make quenched disorder less effective in destroying crystalline structure, thereby favoring solid, but, on the other hand, they themselves destabilize vortex lattice. The low temperature segment of the ODO line, the second peak line, is disorder dominated and weakly depends on temperature.

The memory effect is one of characteristics in glass state. The history-dependent property was observed by Müller at the beginning of the high- $T_c$  era. The irreversibility line is not very sensitive to the type and distribution of defects, although these defects have a pronounced effect on the critical current density. Moreover, there are two distinguishable liquid phases (refers as liquid 1 and liquid 2) which are classified by its

dynamic properties. This feature receives a natural explanation within the developed description. The line separating two regimes coincides with the melting line of a clean sample. The theoretical argument can be found in [47].





## Chapter 2

# Mesoscopic description of superconductor in magnetic field

A phenomenological description, typically valid near the transition temperature, was originally proposed by the Ginzburg and Landau [3] to describe any second order transition. The remarkable success of GL theory is due to the long-range character of critical fluctuations leading to universality of the critical properties at the vicinity of transition temperature. The effective theory can be derived from a microscopic one which determines the limited number of coefficients of the GL. The GL model is by far more efficient to study mesoscopic phenomena rather than a microscopic theory. The originally proposed GL model described a material which is homogeneous in all direction. Microscopically it followed from assumptions of the spherical Fermi surface and isotropic pairing potential. Most of the newly discovered type II superconductors addressed in this work (like high  $T_c$  cuprates, borocarbides etc.) are far from being isotropic. The symmetry of the underlying structure influences profoundly the mesoscopic behaviors. Here we introduce various commonly used modifications of the GL model describing the anisotropy.

Within the GL approach the free energy is expanded in order parameter up to a quartic term in potential, namely becomes a  $\phi^4$  type theory. As a nonlinear field theory the model is still nontrivial and further simplifications and approximations are required.

The most commonly used is the lowest Landau level approximation. We will show that the bifurcation expansion on distance between the S-N phase transition line works well down to  $H = H_{c2}(T)/13$  which is used very far from transition line [89]. In the last section, we will demonstrate a resummation technique, the Borel-Padé series, to extract more physics from a expansion coefficients of a function of coupling. The factorial growth of the power series is taken into account by means of Borel transformations. As quotients of polynomials, the Padé approximate can describe functions with poles in lowest order. And a sequence of Padé approximates, which converges outside the region of power series, can be used to define an analytical continuation of the function outside the converge region of a power series.

## 2.1 Landau Expansion of the Free Energy in homogeneous Superconductors

The GL theory has both quantum and phase-transitional properties. It describes superconductivity as a gauge-invariant quantum phenomenon, and that its nucleation in a normal domain can be treated as a second order phase transition from the disordered (normal) to the ordered (superconducting) state. The basic feature of the theory is that the change in the Gibbs free energy density functional between normal and superconducting states can be expanded in powers of the *order parameter*. Since the electrons forming the Cooper pairs are charged particles, the electromagnetic vector potential  $\mathbf{A}$  must also be introduced. In the case of conventional superconductivity, this expansion has the form

$$F_{cond} = F_s - F_n = \frac{\hbar^2}{2m^*} |\mathbf{D}\psi|^2 - a(T) |\psi|^2 + \frac{1}{2} b' |\psi|^4 + \frac{1}{8\pi} (\nabla \times \mathbf{A})^2 \quad (2.1)$$

where  $F_n$  is the free energy of the normal state and  $\mathbf{D} = \nabla - i \frac{e^*}{\hbar c} \mathbf{A}$  is the covariant derivative,  $B_j \equiv (\nabla \times \vec{A})_j$  is the magnetic induction. The magnetic energy term is also present.  $m^*$  and  $e^*$  are the effective mass and charge of the Cooper pair, respectively;  $c$  is the speed of light; and  $a(T) = \alpha (T - T_c)$  and  $b'$  are the Ginzburg-Landau coefficients.

All those coefficient can be obtained from a microscopic theory. The stability of the superconducting state requires that  $b'$  is always positive, while  $a(T)$  is temperature dependent and can be either positive (superconducting state) or negative (normal state), as shown in the Introduction.

Varying the free energy functional with respect to  $\psi^*$  and  $\mathbf{A}$  and equating the variation to zero the two steady state *Ginzburg-Landau equations* are achieved:

$$a(T) \psi + b' |\psi|^2 \psi + \frac{\hbar^2}{2m^*} \left( -i\nabla - \frac{e^*}{\hbar c} \mathbf{A} \right)^2 \psi = 0 \quad (2.2)$$

$$\frac{c}{4\pi} \nabla \times \nabla \times \mathbf{A} \equiv \mathbf{J}_s = -\frac{ie^*\hbar}{2m^*} (\Psi^* \nabla \Psi - \Psi \nabla \Psi^*) - \frac{e^{*2}}{2m^*c} |\Psi|^2 \mathbf{A} \quad (2.3)$$

where  $\mathbf{J}_s$  is the supercurrent density or simplily  $\mathbf{J}_s = \frac{e^*\hbar}{m^*} |\psi|^2 (\nabla\phi - \frac{e^*}{\hbar c} \mathbf{A})$ . It is clear that in the absence of fields (Meissner state) these equations have a homogeneous solution  $\psi = \sqrt{|\alpha|/\beta} \exp(i\phi)$ , where  $\phi$  is constant. It is no longer the case in the mixed state. While at the center of the vortex core the order parameter  $\psi$  vanishes, at distances sufficiently far from it the absolute value of the order parameter is again constant  $|\psi| = \sqrt{|\alpha|/\beta}$ , but not the phase.

Requiring the supercurrents to encircle the core (i.e.,  $\nabla \cdot \mathbf{J}_s = 0$ ) and choosing a gauge in which  $\nabla \cdot \mathbf{A} = 0$ , one obtains the following equation for the order parameter phase:  $\nabla^2 \phi = 0$ . Making another requirement of azimuthal symmetry, this equation has the following solution:  $\phi = n\varphi + \varphi_0$ , where  $\varphi_0$  is a constant,  $\varphi$  is the azimuthal angle and  $n$  is an integer, since  $\phi(\varphi) = \phi(\varphi + 2\pi)$  is a periodic function. From this result the quantization of magnetic flux in a superconductor is deduced:

$$\Phi = \oint_C \mathbf{A} \cdot d\mathbf{l} + \frac{4\pi\lambda^2}{c} \oint_C \mathbf{J}_s \cdot d\mathbf{l} = n\Phi_0 \quad (2.4)$$

This phenomenon was first observed by Little and Parks [61] and confirmed by numerous experiments [75].

The quantization of magnetic flux in superconductors imposes an important constraint - the *topological charge* conservation. The topological charge of the Abrikosov vortex is defined as:

$$n = \frac{\Phi}{\Phi_0} = \frac{1}{2\pi} \oint_C |\psi|^2 \nabla\phi \cdot d\mathbf{l} \quad (2.5)$$

where the integration is performed over an arbitrary path that encircles the vortex and lies infinitely far from its core. The topological charge conservation means that vortices can appear and disappear only by crossing the domain boundaries or, alternatively by vortex-antivortex pair production or annihilation.

The GL free energy has the property of *local gauge invariance*, which leaves the GL equations invariant under the following simultaneous gauge transformations:

$$\psi \rightarrow \psi \exp(i\chi), \quad \mathbf{A} \rightarrow \mathbf{A} + \frac{\hbar c}{2e} \nabla \chi, \quad \mu \rightarrow \mu - \frac{\hbar}{2e} \frac{\partial}{\partial t} \chi. \quad (2.6)$$

One can see that these transformations do not affect the physical quantities, such as the Cooper pair density  $|\psi|^2$ , the magnetic induction  $\mathbf{B} = \nabla \times \mathbf{A}$  or the supercurrent density  $\mathbf{J}_s$ . In order to eliminate the additional degree of freedom, appearing because of the local gauge invariance, Eqs.(2.2-2.3) must be accompanied by a gauge condition. In the absence of applied electric field a gauge that eliminates the scalar potential is used, demanding  $\mu = 0$  as well as  $\nabla \cdot \mathbf{A} = 0$ .

## 2.2 Landau Expansion of the Free Energy in Anisotropic Superconductors

For isotropic superconductors, the GL model discussed in previous section is sufficient. However, in real materials, even in conventional superconductor such as *Nb* [13], experimental evidence had shown complicate behaviors of vortex matter. The symmetries of superconductors are strongly related to the crystallographic symmetry group of the material, producing an anisotropy of the Fermi surface, and to the effective attraction mechanism of Cooper pairing [69, 70]. Both of these are omitted from the Gor'kov equations and so does the GL model as Eq.( 2.1).

All High- $T_c$  superconductivity arises in a family of layered copper oxides that all feature weakly coupled square-planar sheets of *CuO<sub>2</sub>* Fig. 2.1 which are separated by other materials. According to the current understanding, it seems that most of the properties are determined by electrons moving within the copper-oxide planes. The remaining

components play structural roles and provide screening and doping environments. It may be considered as an experimental fact that the copper-oxide plane that determines the Fermi surface and low-energy electronic properties.

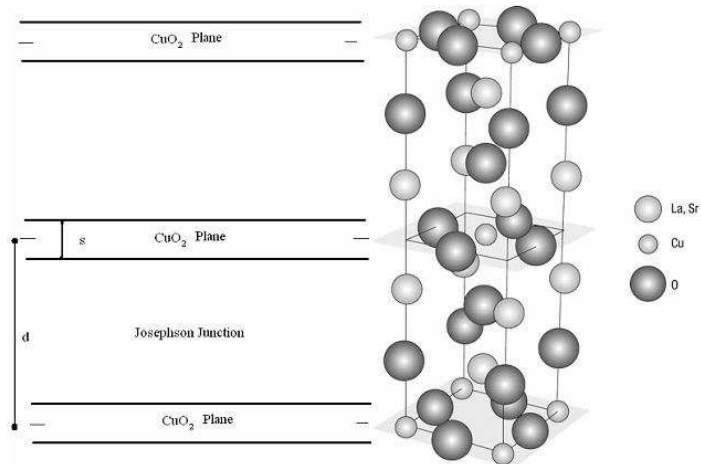


Figure 2.1: Crystal structure of  $La_{2-x}Sr_xCuO_{4+\delta}$  and the Lawrence - Doniach model.

The basic building block in Fig.2.1 is a perovskite structure consisting of the  $CuO_6$  octahedron seen in the centre of the unit cell, surrounded by eight  $La$  ions. The  $CuO_6$  octahedra are elongated, giving rise to a layered structure with quasi-two-dimensional  $CuO_2$  sheets. In this particular cuprate, a rocksalt-structured layer is stacked in between the perovskite cells, but there are many variations that give rise to different families of high-temperature superconductors. In  $La_{2-x}Sr_xCuO_{4+\delta}$ ,  $Sr$  substitution for  $La$ , or the addition of interstitial oxygen, changes the carrier concentration on the  $CuO_2$  planes, drastically altering the electronic properties of this compound.

To reflect the fact of layered structure, the simplest model is to assume infinitesimally thin superconducting layers which are coupled via order parameter tunneling, the Josephson coupling, through insulating layers of thickness  $d$ . The modified  $GL$  model is called Lawrence-Doniach ( $LD$ ) free energy functional,  $\mathcal{F}_{LD}$  [119]:

$$\mathcal{F}_{LD} = \sum_n d \int d^2\mathbf{r} \left[ \frac{\hbar^2}{2m_{ab}^*} \left| \left( \nabla - i \frac{e^*}{\hbar c} \mathbf{A}_\perp \right) \psi_n \right|^2 - a(T) |\psi_n|^2 + \frac{b'}{2} |\psi_n|^4 + \frac{\hbar^2}{2m_c^* d^2} \left| \psi_{n+1} \exp \left( -i \frac{e^*}{\hbar c} A_z \right) - \psi_n \right|^2 + \frac{(\mathbf{B} - \mathbf{H})^2}{8\pi} \right]. \quad (2.7)$$

The order parameter  $\psi_n$  has discrete dependence on the index  $n$  in  $\mathbf{z}$  direction and a continuous dependence on  $\mathbf{x}, \mathbf{y}$  directions; the total vector potential  $\mathbf{A}_\perp + A_z \hat{\mathbf{k}}$  is defined at all points, where  $\overline{A_z} = (1/d) \int_{ns}^{(n+1)d} A_z dz$ . The structure of this equation is similar to GL energy with respect to the in-plane components while the interplane coupling is seen on expanding the exponent to be the operator  $\partial_z - i(e^*/\hbar c) \mathbf{A}_z$  to the case of finite differences. The LD model is a practical tool for layered materials such as *LSCO*.

Suppose the temperature dependent coherence length( $\xi_c$ ) is larger then the layered distance ( $d$ ), system can be regarded as a continuous 3D system but has anisotropy in  $c$  direction. A commonly used phenomenological *GL* model is introducing an effective-mass  $m^*$ . The asymmetry factor is defined by the ratio of effective mass

$$\gamma = \sqrt{m_c^*/m_{ab}^*}. \quad (2.8)$$

For conventional superconductor, *Pb* ( $\gamma = 1$ ), *NbSe<sub>2</sub>* ( $\gamma = 11$ ) and unconventional superconductor, *YBa<sub>3</sub>Cu<sub>3</sub>O<sub>6.92</sub>* ( $\gamma = 5$ ), *YBa<sub>3</sub>Cu<sub>3</sub>O<sub>6.7</sub>* ( $\gamma = 13$ ), *La<sub>2-x</sub>Sr<sub>x</sub>CuO<sub>4+\delta</sub>* ( $\gamma = 15$ ) and *Bi<sub>2</sub>Sr<sub>2</sub>CaCu<sub>2</sub>O<sub>8+\delta</sub>* ( $\gamma = 70$ ) . With the anisotropy in  $c$  direction, the coherence length  $\xi_c(T)$  is typically much smaller

$$\xi_c^2(T) = \frac{\hbar^2}{2m_c \alpha T_c (1 - T/T_c)} = \xi_{ab}^2(T) / \gamma^2 \quad (2.9)$$

while the corresponding penetration depth  $\lambda_c(T)$  is larger:

$$\lambda_c^2(T) = \frac{m_c^* c^2 \beta}{4\pi e^{*2} \alpha T_c (1 - T/T_c)} = \lambda_{ab}^2(T) \gamma^2. \quad (2.10)$$

In slightly anisotropic layered SC such as *YBCO*-type,  $d \ll \xi_c$ , system can be described by the anisotropic 3D GL Model [119]. Its free energy functional has the form:

$$\mathcal{F}_{3D} = \int d^3x \frac{\hbar^2}{2m_{ab}} |\mathbf{D}\psi|^2 + \frac{\hbar^2}{2m_c} |\partial_z \psi|^2 + a(T) |\psi|^2 + \frac{b'}{2} |\psi|^4 + \frac{(\mathbf{B} - \mathbf{H})^2}{8\pi}. \quad (2.11)$$

In extreme layered high- $T_c$  materials such as  $Bi_2Sr_2CaCu_2O_{8+\delta}$ -type,  $d \gg \xi_c$ , system can be regarded as quasi-2D system (since the tunneling between nearby  $CuO_2$ -layered are negligible) [119]. A commonly used 2D GL model has the form:

$$\mathcal{F}_{2D} = \int d^2x \frac{\hbar^2}{2m_{ab}} |\mathbf{D}\psi|^2 + a(T) |\psi|^2 + \frac{b'}{2} |\psi|^4 + \frac{(\mathbf{B} - \mathbf{H})^2}{8\pi}. \quad (2.12)$$

Now we will consider the system which breaks the in plane  $O(2)$  rotational symmetry. It is an experimental fact that the for high  $T_c$  superconductors such as  $YBCO$  has a mixture of *d-wave* and *s-wave* components [38], newly discovered  $Sr_2RuO_4$  [37] has *p-wave* pairing and etc.. Experimentally evidences show those influences can result in different configurations of vortex matter. In  $YBCO$  both square and rhombic phases exists [18]. In overdoped  $LaSCO$ , at low temperatures, the square and rhombic lattices were observed in SANS experiments [16]. Asymmetry is not always related to the non *s-wave* nature of pairing, it can strongly relate to the structure of the Fermi surface, which is a consequence of the crystallographic symmetry group of the material. In borocarbides ( $RE = Lu, Y, Er$ )  $Ni_2B_2C$  [14],  $Nb$  [13], and  $V_3(Si)$  [15], square vortex lattice is observed using techniques such as decoration, STM, SANS or  $\mu$ SR etc.

Taking in to account the coupling with underlying material from microscopic theories is a formidable task. The current exist full microscopic models contain a large number of unknown parameters and are rather cumbersome to work with numerically [106][27]. To study it in phenomenological approach, several ideas are proposed [20][22][26].

To include the in-plan anisotropy to GL model one need to take into account higher order term. Since there is no quadratic in covariant derivative terms that break  $O(2)$ . In this study, we consider the material has fourfold ( $D_4$ ) symmetric. One can use four derivative terms to modify the model. There are three such terms

$$|(D_x^2 + D_y^2) \Psi|^2, D_z^2 \Psi^* (D_x^2 + D_y^2) \Psi, |(D_x^2 - D_y^2) \Psi|^2, \quad (2.13)$$

but only the last term which breaks the  $O(2)$  is irrelevant. This term leads to anisotropic shape of a vortex and an angle dependent vortex – vortex interaction thus the emergence of lattices other than hexagonal, a symmetric rhombic lattices. One therefore can add

the following gradient term for a in-plane 4-fold symmetric material:

$$\mathcal{F}_{ab-aniso} = \eta_m |(D_x^2 - D_y^2) \Psi|^2 \quad (2.14)$$

with dimensionless constant  $\eta_m$  characterizing the strength of the in-plan asymmetry. Since the ultimate microscopic theory is not known as yet, the coefficient  $\eta_m$  is considered as phenomenologically fixed parameters.

### 2.3 Applicability of Lowest Landau level approximation within the mean field approach

The most common additional assumption in most of theoretical studies is the lowest Landau level (LLL) approximation, namely, only the lowest Landau level (LLL) significantly contributes to physical quantities of interest [109, 107, 108, 48, 111, 112]. To understand the valid region of the LLL approximation, we will discuss the higher Landau level correction to the free energy of superconducting state. Due to symmetries of the problem leading to numerous cancellations the range of validity of the LLL approximation in the mean field approach is much wider than a naive range but extends all the way down to  $H = H_{c2}(T)/13$ . We will show that the contribution of higher Landau levels is significantly smaller compared to LLL.

Now we discuss the solution of the Ginzburg-Landau equations obtained from Eq. 2.12 a perturbation method expand in  $a_h$ , indicate as the distance near the mixed state - normal phase transition line. This has been done before in Ref. [114] to the second order and higher order by Li and Rosenstein [89]. Our starting point is the rescaled free energy functional density Eq.(3.10). The expansion parameter is  $a_h$  which is defined in Eq.(3.9). Rewriting the quadratic part in terms of operator (“Hamiltonian”)  $\mathcal{H} \equiv -\frac{1}{2}(D^2 + b)$  whose spectrum starts from zero, the equation of motion is therefore

$$\mathcal{H}\psi - a_h\psi + \psi|\psi|^2 = 0 \quad (2.15)$$

This equation is solved perturbatively in  $a_h$  by assuming



$$\Phi = (a_h)^{1/2} [\Phi_0 + a_h \Phi_1 + \dots] \quad (2.16)$$

It is convenient to represent  $\Phi_0, \Phi_1, \dots$  in the basis of eigenfunctions of  $\mathcal{H}$ ,  $\mathcal{H}\varphi^n = nb\varphi^n$ , normalized to unit "Cooper pairs density"  $\langle |\varphi_N|^2 \rangle_r \equiv \int_{cell} d^2x |\varphi_N|^2 \frac{b}{2\pi} = 1$ , the integration go over a unit cell of the vortex lattice. Assuming hexagonal lattice symmetry, one explicitly has

$$\varphi_N(x, y) = \sqrt{\frac{\sqrt{2\sigma}}{2^N N!}} \sum_{l=-\infty}^{+\infty} \exp [i\pi\rho(l^2 - l)] \exp [i\sqrt{2\pi\sigma}ly] H_N \left( \frac{x}{\sqrt{b}} - \sqrt{2\pi\sigma}bl \right) \times \exp \left[ -\frac{1}{2} \left( \frac{x}{\sqrt{b}} - \sqrt{2\pi\sigma}bl \right)^2 \right]. \quad (2.17)$$

with  $\sigma = \sqrt{3}/2$  and  $\rho = 1/2$ . Function  $H_N(x)$  is Hermite polynomials. Insert the Eq.(2.16) to Eq.(2.15). To the order  $a_h^{1/2}$ , one get

$$\mathcal{H}\Phi_0 = 0 \quad (2.18)$$

and  $\Phi_0$  is proportional to the Abrikosov vortex lattice solution  $\varphi_0$ , namely  $\Phi_0 = g_0^0 \varphi_0$ . The general form expanded in all Landau level for  $\Phi_i$  is

$$\Phi_i = g_0^i \varphi_0 + \sum_{N=1}^{\infty} g_N^i \varphi_N. \quad (2.19)$$

Inserting into Eq.(2.15) to order  $a_h^{3/2}$ , one obtains

$$\mathcal{H}\Phi_1 = g_0 \varphi_0 - g_0 |g_0|^2 \varphi_0 |\varphi_0|^2. \quad (2.20)$$

Taking the inner product with  $\varphi_0$  one finds that

$$g_0^0 = \frac{1}{\sqrt{\beta_A}}, \quad (2.21)$$

where the Abrikosov's constant is the following average over primitive cell:  $\beta_A \equiv \langle |\varphi_0|^4 \rangle_r \approx 1.159$ . Inner product with  $\varphi_N$  determines  $g_N^0$ :

$$g_N^0 = -\frac{\beta_N}{nb\beta_A^{3/2}}, \quad (2.22)$$

where  $\beta_N \equiv \langle |\varphi_0|^2 \varphi_N \varphi_0^* \rangle_r$ . To fix the  $g_0^1$  coefficient in  $\Phi_1$ , we need in addition also the order  $a_h^{5/2}$  equation:

$$\mathcal{H}\Phi_2 = \Phi_1 - (g_0)^2(2\Phi_1|\varphi_0|^2 + \Phi_1^*\varphi_0^2) \quad (2.23)$$

Inner product with  $\varphi_0$  gives:

$$g_0^1 = \frac{3}{2} \sum_{N=1}^{\infty} \frac{\beta_N^2}{Nb\beta_A^{5/2}}. \quad (2.24)$$

The mean field expression for the free energy to order  $a_h^3$  can be obtained by inserting the next correction  $\Phi_1$  in Eq.(2.16) into Eq.(2.15) one obtains the free energy density:

$$\frac{\mathcal{F}_{mf}}{T} = \frac{1}{\omega} \left( -\frac{a_h^2}{2\beta} - \frac{a_h^3}{\beta^3 b} \sum_{N=1}^{\infty} \frac{\beta_N^2}{N} \right) = \frac{1}{\omega} \left( -.43a_h^2 - .0078\frac{a_h^3}{b} \right). \quad (2.25)$$

Due to hexagonal symmetry of the vortex lattice [114],  $\beta_N \neq 0$  only when  $N = 6j$ , where  $j \in \mathbb{N}$ . For  $N = 6j$  it decreases very fast with  $j$ :  $\beta_6 = -.2787, \beta_{12} = .0249$ . Because of this the coefficient of the next to leading order is very small (additional factor of 6 in the denominator). We might preliminarily conclude therefore that the perturbation theory in  $a_h$  works much better than might be naively anticipated  $H = H_{c2}(T)/13$  and can be used very far from transition line.

## 2.4 Optimized perturbation approach and the Bore-Padé approximation

To solve the nonlinear problem Eq.(3.13) by field theory, we use optimized perturbation approach (OPA) to obtain a converged series and then apply resummation technique to extract more physics from the series. Resummation process we adopted here is a *Bore-Padé approximation* [118].

OPA is first developed in field theory, one introduces an auxiliary parameter  $\varepsilon$  as a variational parameter, then the free energy  $f$  can be interpolated as  $f = \varepsilon|\psi|^2 + \alpha(f - \varepsilon|\psi|^2)$ . The artificial parameter  $\alpha$  here is to generate a perturbation expansion by expanding the functional integral  $Z$  to order  $\alpha^n$  at  $\alpha = 1$ . The nonperturbative part is to

optimize the free energy with respect to  $\varepsilon$ . To calculate the free energy  $f_{eff} = -\omega_0 \log Z$ , one starts from expanding the logarithm of the statistical sum  $Z$  in  $\alpha$ ,

$$\begin{aligned} Z &= \iint D\psi \exp(-K) \exp(-\alpha V) \\ &= \iint D\psi \sum_{i=0}^{\infty} \frac{(-\alpha V)^i}{i!} \exp(-K) . \end{aligned} \quad (2.26)$$

For convenience in writing we defined  $\tilde{f}$  as  $f_{eff} = \frac{\omega_0}{V} \tilde{f}$ . In OPA, we have  $\tilde{f} \equiv \tilde{f}_n + O(\alpha^{n+2})$ , the  $n^{th}$  order of OPA,  $\tilde{f}_n$ , is

$$\tilde{f}_n = -\log \iint D\psi \exp(-K) - \sum_{i=1}^{n+1} \frac{(-\alpha)^i}{i!} \langle V^i \rangle_K . \quad (2.27)$$

where  $\langle \dots \rangle_K$  denotes the sum of all the connected Feynman diagrams. The first two order of  $\tilde{f}$  as a function of  $\varepsilon$  are

$$\tilde{f}_0 = 2 \left( \log \frac{\varepsilon}{4\pi^2} + \frac{a_\varepsilon}{\varepsilon} + \frac{1}{\varepsilon^2} \right) , \quad (2.28)$$

$$\tilde{f}_1 = \tilde{f}_0 - \frac{1}{\varepsilon^4} (18 + 8\varepsilon + a_\varepsilon^2 \varepsilon^2) , \quad (2.29)$$

where  $a_\varepsilon = a_T - \varepsilon$ . The solution of  $n^{th}$  order of OP denotes as  $\varepsilon_n$  is obtained from the minimization equations,

$$(\partial_\varepsilon - \partial_{a_\varepsilon}) \tilde{f}_n = 0 , \quad (2.30)$$

such that

$$f_n = \tilde{f}_n(\varepsilon_n) = \min \left[ \tilde{f}_n(\varepsilon) \right] .$$

The  $f_{eff}$  series are calculated by several groups. The original paper by Thouless and Ruggeri [110] reached 6<sup>th</sup> order; and expended to 13<sup>th</sup> order by Hu and MacDonald [115]. The free energy has the form

$$f_{eff} = 2 \log \frac{\varepsilon_1}{4\pi^2} + 2f_n(x) + \mathcal{O}(x^{n+1}) , \quad \text{with} \quad (2.31)$$

$$f_n(x) = \sum_{i=1}^n h_i x^i \quad \text{and} \quad x = \frac{1}{\varepsilon^2} \quad (2.32)$$

where  $\varepsilon = \left(a_T + \sqrt{a_T^2 - 4z_n}\right)/2$ . The coefficients  $h_k$  can be found in [116] and  $z_n$  can be found in [85]. The consecutive approximates are plotted on Fig.2.2. Dashed dotted lines represent a optimized perturbation theory (denoted by the order numbers). One can see clearly that the series are convergent with radius of convergence at  $a_T = -5$ .

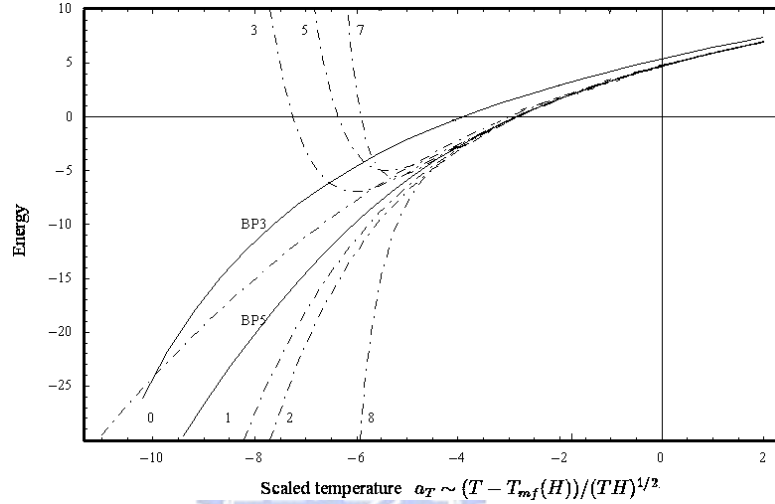


Figure 2.2: The free energy calculated using two different approximation schemes. Dashed dotted lines represent a optimized perturbation theory (denoted by the order numbers).

It is known that in the theory of critical phenomena one can extract more physical results from a divergent series by resummation processes. Bore-Pad é approximation is a good option. By applying Bore-Pad é approximation to perturbation expansion at “weak coupling” [118], an accurate description in the critical region is obtained, since there exists a renormalization group flow from the weak coupling fixed point towards the strongly couple one [117]. We use the following strategy: The factorial growth of  $h(x)$  is taken into account by means of Borel transformations, then Pad é approximation is used to approach the less divergent series. Observing that in our case the  $h_k$  of the asymptotic series growth factorial for large  $k$ , we divide each term in the expansion by a factor  $k!$ , a less divergent series is obtained. It is so called Borel sum:

$$B(x) \equiv \sum_k^{\infty} B_k x^k, \text{ with } B_k \equiv h_k/k!. \quad (2.33)$$

$i$	$h_n$	$z_{n-1}$
1	-2	-4
2	-1	-6
3	$\frac{38}{9}$	-12.239721181139888
4	$-39 - \frac{29}{30}$	-7.508888400035477
5	471.39659451659446	-7.349933383279474
6	-6471.5625749551446	-14.152646217045422
7	101279.32784597063	-9.961364397930787
8	-1779798.7875947522	-9.174960576928443
9	34709019.614363678	-15.232548389083844
10	-744093435.66822231	-11.629924499110746
11	17399454123.559521	-10.8399817525306
12	-440863989257.28510	-15.9366927661989
13	12035432945204.531	-12.753308785106007

Figure 2.3: Coefficients  $h_i$  and  $z_i$  in 2D.

The Padé approximation for a series expansion  $B(x) = \sum_{i=0}^k B_i x^i + \mathcal{O}(x^{k+1})$  up to the order  $k$  is given by

$$[k, k-1] \equiv \frac{\sum_{i=0}^k a_i x^i}{\sum_{i=1}^{k-1} b_i x^i} \quad (2.34)$$

where  $a_i$  and  $b_i$  are chosen such that the series expansion of  $[k, k-1]$  up to the order  $k$  equals to the original series,  $B(x) = [k, k-1] + \mathcal{O}(x^{k+1})$ , or

$$\sum_{i=0}^k B_i x^i = [k, k-1]. \quad (2.35)$$

By doing the Borel transformation, the Borel sum,  $B(x)$ , can be integrated to restore  $f(x)$ ,

$$h(x) = \iint_0^\infty dt e^{-t} B(xt). \quad (2.36)$$

The *Bore-Padé series* for different orders are shown in Fig. 2.2 with solid line denoted by "BP" plus the order number represent the  $[k, k-1]$  Borel - Pade series for  $k = 3, 4, 5$ .

The  $k = 4$  and  $k = 5$  practically coincide on the scale of the plot. For  $k = 4$  and  $k = 5$ , the liquid energy converges to required precision (0.1%). The liquid energy extract by *BP* approximation agrees with the optimized Gaussian expansion results [90] till its radius of convergence at  $a_T = -5$ .

## 2.5 Disorder

To describe the disorder (pinning) potential one adds a random component

$$\alpha T_c (1 - t) W(\mathbf{r}) |\psi(\mathbf{r})|^2$$

or

$$\alpha T_c (1 - t - b) W(\mathbf{r}) |\psi(\mathbf{r})|^2$$

to the GL functional. The first case is indicate the random pinning potential change the local critical temperature; the later includes the a random effective mass due to defects (in Lowest Landau level approximation). We assume that  $W(\mathbf{r})$  has a Gaussian random distribution with variance,

$$\overline{W(\mathbf{r})W(\mathbf{r}')} = n\delta^{(3)}(\mathbf{r} - \mathbf{r}'), \quad (2.37)$$

$n$  is related to the average number of pinning center per volume. The ensemble average of a quantity  $O$  on all possible disorders is read as

$$\langle O \rangle = \frac{\int_W O \exp \left[ - \int d\mathbf{r} \frac{W(\mathbf{r})^2}{2n} \right]}{\int_W \exp \left[ - \int d\mathbf{r} \frac{W(\mathbf{r})^2}{2n} \right]}. \quad (2.38)$$

Disorder can pin vortices therefore it affects both dynamic and statistical behaviors of the system. Thermal fluctuation of the individual vortex lines lead to a dynamic sampling and hence average the disorder potential over the spatial extent of the thermal displacement  $\langle u^2 \rangle_{th}^{1/2}$ . Thermal fluctuation effect reduce the effect of quenched disorder as thermal depinning which is a continuous crossover from a pinned to a an unpinned situation.

The number of pinning centers over the area of the sample  $L^2$  is  $N = n \cdot L^2$ . Potential of  $N$  small pinning centers located at  $x_i$  can be represented by a sum of delta functions:

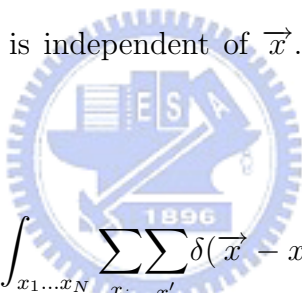
$$V(\vec{x}) = V_0 \sum_{i=1}^N \delta(\vec{x} - \vec{x}_i) \quad (2.39)$$

The constant  $V_0$  is proportional to the gap between normal and superconducting energy.

The average of the probability over disorder potential assumed random is:

$$\begin{aligned} \overline{V(\vec{x})} &= \left(\frac{1}{L^2}\right)^N \int_{x_1 \dots x_N} V_0 \sum_{i=1}^N \delta(\vec{x} - x_i) \\ &= \frac{1}{L^{2N}} V_0 \times L^{2(N-1)} \times N = \frac{1}{L^2} V_0 N = V_0 n \end{aligned} \quad (2.40)$$

We see that  $\overline{V(\vec{x})} \propto n$  is independent of  $\vec{x}$ . The correlator can be computed in similar way:



$$\begin{aligned} \overline{V(x)V(0)} &= (V_0)^2 \left(\frac{1}{L^2}\right)^N \int_{x_1 \dots x_N} \sum_{x_i} \sum_{x'_i} \delta(\vec{x} - x_i) \delta(-x_{i'}) \\ &= (V_0)^2 \left(\frac{1}{L^2}\right)^N \int_{x_1 \dots x_N} \left[ \sum_{x_i \neq x_{i'}} \delta(\vec{x} - x_i) \delta(-x_{i'}) + \sum_{x_i = x_{i'}} \delta(\vec{x} - x_i) \delta(-x_{i'}) \right] \\ &= (V_0)^2 \left(\frac{1}{L^2}\right)^N [L^{2(N-2)} \times (N^2 - N) + L^{2(N-1)} \times N \times \delta(\vec{x})] \\ &= (V_0)^2 \left[ \frac{N^2 - N}{L^4} + \frac{N \times \delta(\vec{x})}{L^2} \right] \end{aligned} \quad (2.41)$$

Since  $N \gg 1$ , we obtain

$$\overline{V(x)V(0)} \approx (V_0)^2 [n^2 + n\delta(\vec{x})] \quad (2.42)$$

It is convenient to define a shifted random disorder field:

$$W(x) = V(x) - \overline{V(x)} = V(x) - V_0 n. \quad (2.43)$$

Its correlator is proportional to a delta function (white noise):

$$\begin{aligned}\overline{W(x)W(0)} &= \overline{(V(x) - \overline{V(x)})(V(0) - \overline{V(0)})} \\ &= \overline{V(x)V(0)} - \overline{V(x)\overline{V(0)}} - \overline{\overline{V(x)}V(0)} + \overline{\overline{V(x)}\overline{V(0)}} \\ &= \overline{V(x)V(0)} - \overline{V(x)V(0)} = (V_0)^2[n^2 + n\delta(\vec{x})] - (V_0n)^2 \\ &= (V_0)^2n\delta(\vec{x})\end{aligned}\tag{2.44}$$





# Chapter 3

## Magnetization in Layered Superconductors

### 3.1 Introduction

Fluctuation diamagnetism is one of the characteristic feature of a strongly fluctuating superconductor. For high- $T_c$  superconductors, due to the enhanced thermal fluctuations, diamagnetism is observed even above the transition temperature,  $T_c(H)$  [59, 62]. At high field region  $\sim H_{c2}(T)$ , Thouless and Ruggeri [109, 110] demonstrated that thermodynamic and transport physical quantities have a good high-field scaling behavior as function of the dimensionless scaling temperature  $a_T \sim (T - T_{mf}(H)) / (TH)^r$ , for quasi- $2D$  system  $r = 1/2$ , while for  $3D$  system  $r = 2/3$ . This is a consequence of the dominant role of the Landau quantization: main contribution is coming from the lowest Landau level. It was studied and elaborated later by Tešanovic et al and others [48, 83]. For example, the magnetization experiments provide an evidence of the LLL scaling in of both  $3D$  and  $2D$  systems. Data shows that at different magnetic fields and temperatures magnetization curves collapse on a universal curve  $M / (HT)^r \propto f_{sc}(a_T)$  (see, for example, Fig.3.4) [29, 31, 44, 79].

Another striking feature is the magnetization curves  $M(T)$  is that they intersect at the same point  $(T^*, H^*)$  for a wide range of magnetic fields, see Fig.3.6. It was observed

both in extremely anisotropic quasi two dimensional (quasi- $2D$ ) layered materials such as  $BSCCO$  [29] and the  $Tl$  based high  $T_c$  superconductors [79] and in more isotropic quasi  $3D$  ones, such as the optimally doped  $YBa_2Cu_3O_{7-\delta}$  [44] and  $YBa_2Cu_4O_8$  [43]. However recently it was found that magnetization curves of several other classes of layered high  $T_c$  superconductors, including  $HgBa_2Ca_2Cu_3O_{8+\delta}$  [31], strongly underdoped  $YBa_2Cu_3O_{7-\delta}$  [86] and  $La_{1.92}Sr_{0.08}CuO_4$  [32], the intersection point is no longer the same for all the magnetic fields. It rather moves a bit from its “ $3D$ ” position at low fields to its “ $2D$ ” position at high fields.

Theoretically, the phenomenon of the intersection points in  $2D$  [48] and  $3D$  materials [113] was first described in the framework of Ginzburg - Landau theory based on the fluctuations dominance scenario. Later, using the systematic expansion, it was shown that although the magnetization curves do not intersect at the same point at all the fields, it can move a negligible distance on the phase diagram in both  $2D$  and  $3D$  [83]. For layered Lawrence-Doniach (LD) model [86], the theory shows a observable migration of the crossing points moving from  $2D$  to  $3D$  position while approach  $H_{c2}(T)$  from superconducting state.

Moreover recent measurement on the strongly underdoped  $La_{1.92}Sr_{0.08}CuO_4$  [32] shows the migration of crossing points move in an opposite direction, namely at low fields the intersection point is below  $T_c$ ; while increasing magnetic field, the intersection point moves in the opposite direction and eventually it exceeds  $T_c$ . In Ref. [32] the theoretical formulas of Ref. [86] in limits of quasi  $2D$  and quasi  $3D$  were used to quantify the data on  $LaSCO$ . While it was possible to fit the data in the optimally doped case, it was impossible to fit the data in the far underdoped cases.

In this study we will use  $LD$  for layered superconductor to investigate the movement of the intersection points. By following Hartree-Fock approximation in LLL approximation in Ref. [86], we mathematically defined the field dependent curve of “intersection point” for different coupling constant. Our result shows that with increasing magnetic field, the migration of the intersection points move from its  $3D$  position to  $2D$  position. More, the intersection doesn't exceed  $T_c$  is proved. Therefore, the results of strongly

underdoped *LaSCO* are very puzzling and irreconcilable with the general LD theory.

Another topic we will study here is inspired by the experiment done by Ong *et al* [30]. In which they claimed that for strongly layered superconductor *BSCCO*[30] the diamagnetism at the vicinity of the critical temperature in type II superconductors significantly differ from the behavior predicted by fluctuation diamagnetism theories based on Ginzburg-Landau model [80, 83, 48, 108, 84].

Theoretically, in the vortex liquid of 3D system, such as *YBCO*, the HLL contribution has been studied by Lawrie in the framework of the Gaussian (Hartree-fock like) approximation [49]. The result shows that the region of validity of LLL is very limited. Recently, the leading (Gaussian) contribution of HLL was combined with more refined treatment of the LLL modes in 3D system by Li and Rosenstein [87]. In the vortex liquid of 2D system, the phenomenon above  $T_c$  was studied by Prange [88] and later by [80]. The later study show the physical quantity is strongly dependence on the UV cut-off which is puzzling.

In this study, we extend previous theoretical result [80] to  $T < T_c$  region by the approach developed in Ref. [87]. Instead of using the traditional lowest Landau level approximation we integrated out higher Landau modes to obtain an effective lowest Landau level free energy functional and map it to existed lowest Landau result. Comparison with experimental results shows a good agreement with our theory for an optimally doped sample while underdoped sample differ from the theoretical results at low temperature.

## 3.2 Basic equations and assumptions

### **The Lawrence – Doniach model for layered superconducts (LSCO-like material)**

The material parameters of layered material *LSCO* are  $\xi_{ab} \approx 34\text{\AA}$ ,  $\gamma \approx 15$  and the interlayer spacing,  $d \approx 15\text{\AA}$ . The measurement temperature  $|1 - t| < 0.1$ , the  $\xi_c(T)$  which diverged as  $(1 - t)^{-1}$  will exceed the interlayer spacing. The proper model for the

system is the Lawrence-Doniach (LD) free energy functional, Eq.(2.7 ). We choice  $T_c$  as a unit of temperature,  $T = tT_c$ , and  $\frac{\Phi_0}{2\pi\xi^2}$  as a unit of magnetic field,  $B = b\frac{\Phi_0}{2\pi\xi^2}$ , the coherence length  $\xi_{ab} = \sqrt{\hbar^2/(2m_{ab}\alpha T_c)}$  as a unit of length in  $ab$  plane. The gauge is choice to be the Landau gauge,  $\mathbf{A} = (0, Hx, 0)$ . In  $c$  direction is in  $\xi_c = \xi_{ab}/\gamma$ . Namely,  $x \rightarrow \xi_{ab}x, y \rightarrow \xi_{ab}y$  and  $d \rightarrow \xi_c d$ . The order parameter is rescaled as  $\psi_n^2 \rightarrow \frac{2\alpha T_c}{b'}\psi_n^2$ . The Boltzmann factor of LD can be formulated as:

$$f_{LD} = \frac{\mathcal{F}_{LD}}{T} = \frac{1}{\omega t} \sum_n \int d^2x \frac{1}{2} |D\psi_n|^2 + \frac{1}{2d^2} |\psi_n - \psi_{n+1}|^2 - \frac{1-t}{2} |\psi_n|^2 + \frac{1}{2} |\psi_n|^4 \quad (3.1)$$

The dimensionless coefficient  $\omega$ ,

$$\omega = \sqrt{2Gi_{2D}\pi} \quad (3.2)$$

where the Ginzburg number is defined by

$$Gi_{2D} \equiv \frac{1}{2} \left( \frac{32\pi^2 e^2 \kappa^2 \xi T_c \gamma}{c^2 \hbar^2 d} \right)^2. \quad (3.3)$$

The nonlinear term  $|\psi_n|^4$  becomes very important in the temperature range  $|1-t| \sim Gi$ . We will make the following assumption: (1) lowest Landau level approximation: the essential contribution is from lowest landau level as we mentioned in the previous section. (2) the magnetic fluctuation is negligible due the superposition of the magnetic field from individual vortex. It is convenient to expand the order parameter in terms of the Landau levels eigenfunctions basis,  $\phi_{k_z, k_y}^N(\mathbf{r})$ [91]

$$\psi_n^N(\mathbf{x}) = \sum_{N, k, q} \phi_{k, q}^N(\mathbf{x}) \psi_{k, q}^N \quad (3.4)$$

where

$$\begin{aligned} \phi_{k, q}^N(\mathbf{x}) = & \frac{1}{\sqrt{L_z L_y}} \frac{1}{\pi^{1/4} \sqrt{2^N N!}} \exp \left[ i q y + i k d n - \frac{1}{2} \left( x\sqrt{b} - \frac{q}{\sqrt{b}} \right)^2 \right] \\ & \times H_N \left( x\sqrt{b} - \frac{q}{\sqrt{b}} \right) \exp \left[ -\frac{1}{2} \left( x\sqrt{b} - \frac{q}{\sqrt{b}} \right)^2 \right]. \end{aligned} \quad (3.5)$$

The  $N$  stands for the  $N^{th}$  Landau level,  $q$  is the momentum in  $ab$  plane and  $k$  is the one in  $c$  direction. For magnetic field is close the  $H_{c2}$ , the lowest Landau level modes ( $N = 0$ ) or in short LLL modes is a very good approximation[49]. The reason is that the

$e_{n=0} \ll e_{n \neq 0}$ , so any contribution from the  $\varphi_{n \neq 0}$  greatly increases the  $\psi^2$  contribution to  $f$ . The same reason for fluctuations, fluctuation with  $n \neq 0$  is not important. This is achieved by enforcing the constraint

$$-\frac{1}{2}\mathbf{D}^2\psi = \frac{b}{2}\psi. \quad (3.6)$$

Take  $N = 0$  limit, use the LLL constrain 3.6. The system now is missing one independent parameter, since there is no gradient term in directions perpendicular to the field and thus possesses the “LLL scaling” [109]. After additional rescaling  $x \rightarrow x/\sqrt{b}$ ,  $y \rightarrow y/\sqrt{b}$  and  $\psi^2 \rightarrow (bt\omega/\omega_0)^{1/2}\psi^2$  with  $\omega_0 = 4\pi$ . The Boltzmann factor of LD model becomes:

$$f_{LD} = \frac{\mathcal{F}_{LD}}{T} = \frac{1}{\omega_0} \sum_n \int d^2x \frac{\gamma_t}{2} |\psi_n - \psi_{n+1}|^2 + a_T |\psi_n|^2 + \frac{1}{2} |\psi_n|^4 \quad (3.7)$$

$$a_T = -a_h (bt\omega/\omega_0)^{-1/2} \quad (3.8)$$

with

$$a_h \equiv \frac{1-t-b}{2} \quad (3.9)$$

and  $\gamma_t = \frac{1}{d^2} \left( \frac{bt\omega}{\omega_0} \right)^{-1/2}$ .

## 2D Model for strongly anisotropic layered superconductors

The thermal fluctuation effect are particularly pronounced in *BSCCO* or *Tl* compounds (for *BSCCO*:  $\xi_{ab} \sim 30\text{\AA}$ ,  $\gamma \sim 70$  and  $d \sim 20\text{\AA}$ ) due to the greater effective spacing between near by two *CuO*-layer-group plane. Hence, the tunneling effect between two *CuO* groups are negligible. We assume that the material is rotational symmetric in-plane with strong anisotropy along the  $z$  axis. The system can be effectively described by 2D Ginzburg-Landau free energy functional Eq.(2.12). We choice the gauge  $\mathbf{A} = (-By, 0, 0)$  such that  $\mathbf{B} = (0, 0, B)$  describes magnetic field. More, we assume magnetic field is constant and nonfluctuating at the vicinity of  $H_{c2}(T)$ . It is base on the fact that the inhomogeneity of magnetic field is of order  $1/\kappa^2 < 10^{-4}$  which is due to superposition from many vortices. Even with fluctuations of the order parameter field, one can neglect completely the fluctuations of the electromagnetic field for very large  $\kappa$

[93, 92]. Moreover, we assume the effect of point-like disorder which appear as random pinning potential is negligible. Since the pounced thermal fluctuations influence in such a strong anisotropy martial like *BSCCO* will smear out the disorder effect.

Rescaled the 2D free energyfunctional , Eq.(2.12), by  $x \rightarrow \xi_{ab}x, y \rightarrow \xi_{ab}y$  and  $\psi^2 \rightarrow \frac{2\alpha T_c}{b'}\psi^2$ . The Boltzmann factor for 2D GL model becomes

$$f = \frac{\mathcal{F}_{2D}}{T} = \frac{1}{\omega t} \int dx \left[ \frac{1}{2} |\mathbf{D}\psi|^2 - (a_h + \frac{b}{2}) |\psi|^2 + \frac{1}{2} |\psi|^4 + \frac{\kappa^2 (\mathbf{b} - \mathbf{h})^2}{4} \right], \quad (3.10)$$

where  $\omega$ ,  $a_h$  and  $G_{i2D}$  are defined as Eq.(3.2), Eq.(3.9) and Eq.(3.3), respectively. In the liquid state, since it's homogeneity  $\langle \psi(x) \rangle = 0$ , the fluctuation is  $\psi(x)$  itself. As in basic lattice wave, we will construct an orthonormal set of functions suitable for treating the fluctuation excitation , $\psi(x)$  . According to the Bloch theory, one can use translation operator to construct a complete set from any solution of the Hamiltonian. In our case, it is convenient to use the eigenfunctions from noninteracting part, the kinetic term which is known as Landau basis. We choose the arbitrary solution to be the solution for triangular lattice. By doing magnetic translation, one get the so called quasimomentum basis  $\varphi_{N,k}$  for  $N^{th}$  Landau level and vector  $k \in \mathbb{R}^2$  is within the first Brillouin zone associated with the triangular lattice ( $\sigma = \sqrt{3}/2$  and  $\rho = 1/2$  ).

$$\begin{aligned} \varphi_{N,k}(x, y, z) = & \sqrt{\frac{\sqrt{2\sigma}}{2^N N!}} \sum_{l=-\infty}^{+\infty} \exp [i\pi\rho(l^2 - l)] \exp \left\{ i \left[ \sqrt{2\pi\sigma}l (yb^{1/2} + k_x b^{-1/2}) + yk_y \right] \right\} \\ & \times \exp \left[ -\frac{1}{2} \left( xb^{1/2} - \sqrt{2\pi\sigma}bl - k_y b^{-1/2} \right)^2 \right] H_N \left( xb^{1/2} - \sqrt{2\pi\sigma}bl - k_y b^{-1/2} \right) \end{aligned} \quad (3.11)$$

The corresponding eigenvalue is  $e_N = (N + 1/2)b$ . The fluctuations can be then expanded in  $\varphi_{N,k}$ :

$$\psi(x) = \frac{1}{2\pi} \int_k \sum_{N=0}^{\infty} \varphi_{\mathbf{k}}^N(\mathbf{x}) \psi^n(k). \quad (3.12)$$

Take  $N = 0$  limit, and use the LLL constrain Eq.(3.6). After the LLL scaling we mentioned in previous LD model. The Boltzmann factor becomes:

$$f = \frac{1}{\omega_0} \int d^3x \left[ a_T |\psi|^2 + \frac{1}{2} |\psi|^4 + (bt\omega/\omega_0)^{-1} \frac{\kappa^2 (\mathbf{b} - \mathbf{h})^2}{4} \right]. \quad (3.13)$$

the  $a_T$  defined in Eq. (3.8) is the LLL rescaled temperature. Since the magnetization  $-4\pi M = H - B$  is of order  $1/\kappa^2$ , thus the last term in Eq.(3.13) is negligible very small in high  $T_c$  superconductors. Free energy density in the newly scaled model is defined as:

$$f_{eff}(a_T) = -\frac{\omega_0}{V} \log \int D\psi \exp(-f). \quad (3.14)$$

To compare with experiments, the rescaled free energy  $f_{eff}$  is related to the free energy in physical units by

$$F = \frac{H_{c2}^2}{4\pi\kappa^2} \omega b t f_{eff}(a_T). \quad (3.15)$$

In conventional units Eq.(2.12) within the LLL, the magnetization in the presence of thermal fluctuations is determined from

$$\frac{\delta}{\delta \mathbf{B}} \mathcal{F} = Z^{-1} \int_{\Psi} \frac{\delta}{\delta \mathbf{B}} F[\Psi, \mathbf{B}] \exp \left[ -\frac{1}{T} \int F[\Psi, \mathbf{B}] \right] = 0. \quad (3.16)$$

The derivative results in

$$-Z^{-1} \int_{\Psi} \left[ \int_r \frac{\alpha T_c}{H_{c2}} |\Psi|^2 + \frac{\mathbf{B} - \mathbf{H}}{4\pi} \right] \exp \left[ -\frac{1}{T} \int \mathcal{F}[\Psi, \mathbf{B}] \right] \quad (3.17)$$

$$= -\frac{\alpha T_c}{H_{c2}} \langle |\Psi|^2 \rangle - \frac{(\mathbf{B} - \mathbf{H})}{4\pi} = 0, \quad (3.18)$$

where from now on  $\langle \dots \rangle$  denotes thermal average. The magnetization on LLL is therefore proportional to the superfluid density

$$M = -\frac{\alpha T_c}{H_{c2}} \langle |\Psi|^2 \rangle. \quad (3.19)$$

This motivates the definition of the scaled magnetization proportional to  $\langle |\Psi|^2 \rangle$ ,

$$m(a_T) = -\langle |\psi|^2 \rangle = -\frac{\partial}{\partial a_T} f_{eff}(a_T) \quad (3.20)$$

which is related to magnetization by

$$4\pi M = \frac{\pi H_{c2}}{4\kappa^2} (tbGi_{2D})^{1/2} m(a_T). \quad (3.21)$$

One can see consequently that  $M(TB)^{-1/2}$  depends on  $a_T$  only[48, 109]..

### 3.3 Dimensionality effects of layered superconductors

In momentum space, the LD Boltzman factor Eq.(3.7) is

$$f_{LD} = \frac{1}{\omega_0} \left\{ \sum_{kq} [\gamma_t (1 - \cos dk) |\psi_q|^2 + a_T |\psi_q|^2] + \sum_{k_i q_j} \frac{1}{2} \psi_{k_1, q_1}^* \psi_{k_2, q_2}^* \psi_{k_3, q_3} \psi_{k_4, q_4} \right\} \quad (3.22)$$

where  $k_1 + k_2 = k_3 + k_4$  and  $q_1 + q_2 = q_3 + q_4$ . In Hatree-Fock approximation, we assume  $\langle |\psi_q|^2 \rangle = \Delta_0$ . Applying the Wick theorem, the free energy is

$$f_{LD} \approx \frac{1}{\omega_0} \sum_{kq} \{ [\gamma_t (1 - \cos dk) + a_T + \Delta_0] |\psi_q|^2 \}. \quad (3.23)$$

According the definition of ensemble summation,

$$\langle |\psi_q|^2 \rangle = \iint \mathcal{D}\psi_q \{ |\psi_q|^2 \exp(-f_{LD}) \} \quad (3.24)$$

a self-consistent equations is read as

$$\Delta_0 = \frac{\omega_0}{\sqrt{(\gamma_t + a_T + \Delta_0)^2 - \gamma_t^2}}. \quad (3.25)$$

The magnetization calculated from the partition function  $Z$ , using the mean field Hamiltonian (2.7), is

$$4\pi M = -\frac{e^* \hbar}{cm_{ab}} \frac{2\alpha T_c}{b'} \sqrt{bt\omega/\omega_0} \Delta_0 \quad (3.26)$$

To show that free energy  $F$  can exhibit a  $3D \rightarrow 2D$  crossover as temperature or field are changed. We consider two limits for which the gap equation can be solved *analytically*.

$$\Delta_0 = \frac{\omega_0}{\sqrt{(\gamma_t + a_T + \Delta_0)^2 - \gamma_t^2}} \quad (3.27)$$

Here the coefficients  $\gamma_t \propto d^{-2} \sqrt{\frac{d}{bt}}$  and  $a_T \propto -\frac{1-t-b}{2} \sqrt{\frac{d}{bt}}$ . In  $2D$  system, the inter-layer distance is large ( $d \rightarrow \infty$ ), namely the coupling strength between two layers  $\gamma_t \rightarrow 0$ . The gap equations become analytical soluble  $\Delta_0 (a_T + \Delta_0) \approx \omega_0$  or  $\Delta_0 \approx$



$-\left(a_T + \sqrt{a_T^2 + 4\omega_0}\right)/2$ . The magnetization in this limit demonstrates a well pronounced  $2D$  scaling dependence

$$\frac{M}{\sqrt{HT}} \propto f_{2D} \left( \frac{T - T_c(H)}{\sqrt{HT}} \right). \quad (3.28)$$

For convenience, we define a dimensionless coupling constant  $g = \frac{T_c b'}{\pi \xi^2}$  characterizes the strength of the thermal fluctuations.

$$\Delta = g \frac{bt}{\sqrt{(b+t+\Delta+\gamma_t-1)^2 - \gamma_t^2}}, \quad (3.29)$$

In  $3D$  limit,

$$\gamma \gg b+t-1 + \frac{2((b+t-1)^3}{27}, \text{ and } V = \frac{4((b+t-1)^3\gamma}{27g^2(bt)^2} > \frac{1}{2}$$

namely for the experiments at relatively low fields. In this case,

$$\Delta = (bt)^{2/3} \left( \frac{g^2}{\gamma} \right)^{1/3} f_{3D}(V) \quad (3.30)$$

where

$$f_{3D}(V) = 2V^{1/3} \sin\left(\frac{\pi}{6} - \frac{\varphi}{3}\right) - \left(\frac{V}{2}\right)^{1/3}$$

and

$$\tan \varphi = \frac{\sqrt{2V-1}}{1-V}. \quad (3.31)$$

Apparently, the behavior of the magnetization in this case is caused by  $3D$  fluctuations:

$$\frac{M}{(HT)^{2/3}} \propto f_{3D} \left( \frac{T - T_c(H)}{(HT)^{2/3}} \right) \quad (3.32)$$

In both limits one clearly finds a scaling behavior, manifested in Figures 3 and 4. For an intermediate magnetic field, however, scaling is not expected even though the LLL approximation is still valid. In this intermediate case the scale is provided by the inter-layer spacing  $d$ .

Experimentalists often define the crossing point  $T^*(H)$  as the temperature at which two "successive" magnetization curves  $M(T, H)$  and  $M(T, H + \Delta H)$  cross [32]. Therefore, the curves satisfy the equation

$$\left. \frac{\partial M}{\partial H} \right|_{T=T^*} = 0, \quad (3.33)$$

i.e.  $\partial\Delta/\partial b=0$  (or equivalently  $\partial\Delta/\partial t=0$ ). Two equations Eq.(3.33) and Eq.(3.29) can be solved with respect to  $b$

$$b = -\frac{\Delta^2(t^* + \Delta + \gamma_t - 1)}{\Delta^2 - g^2 t^{*2}}, \quad (3.34)$$

where  $t^* = T^*/T_c$  is the reduced temperature of  $T^*$ . Substituting Eq.(3.34) back into Eq.(3.29) one obtains the relation between the crossing temperature and magnetization  $\Delta^*$ . This can be solved for  $\Delta^*$ :

$$\Delta^* = gt^* \frac{gt^*(1 - \gamma_t - t^*) + \gamma_t \sqrt{g^2 t^{*2} + \gamma_t^2 - (1 - t^* - \gamma_t)^2}}{g^2 t^{*2} + \gamma_t^2}. \quad (3.35)$$

The "motion" of the crossing points for  $g = 0.08$  and  $\gamma_t = 0.01, 0.05$  and  $0.1$  is depicted in Fig.3.1. Moreover, one easily sees from Eq.(3.35) that only for  $t^* < 1$  physical condition  $\Delta > 0$  is obeyed. Thus, in this model, the intersection point generally cannot move beyond  $T_c$ .

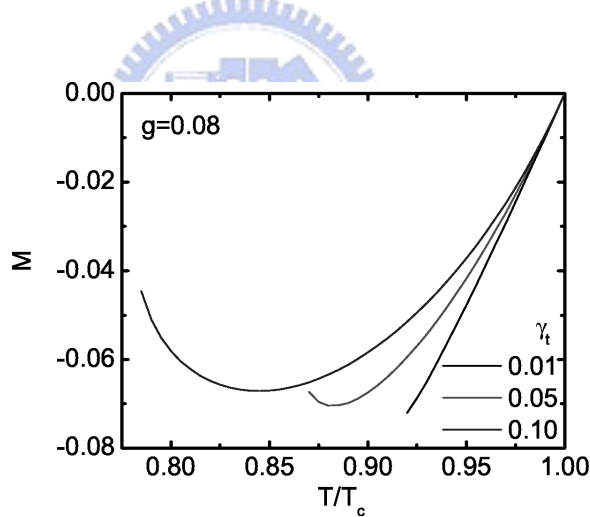


Figure 3.1: The evolution of the crossing points of the magnetization curves for the coupling  $g = 0.08$  and three copies of the anisotropy parameter  $\gamma_t=0.01, 0.05$  and  $0.1$ .

### 3.4 Sum of contributions of all Landau levels in quasi-2D systems. The 1<sup>st</sup> OPA method

Contributions of HLL are important phenomenologically in two sections of the phase diagram. The first is at temperature above the mean field critical temperature  $T_c(H)$

inside the liquid phase. The second is far below the melting point deep inside the solid phase. The first one is the interesting region. The first order approximation of the optimized perturbation approach which we mentioned above is a Hartree-Fock-like approximation. In the framework of this approximation, free energy, Eq.(3.10), is divided into an optimized quadratic part  $K$ , and a small part  $V$ . Then  $K$  is chosen in such a way that the Gaussian energy is minimal [49]. The Gaussian energy is a rigorous lower bound on energy. In liquid phase with an arbitrary homogeneous  $U(1)$  symmetric, one variational parameter  $\varepsilon$  is sufficient:

$$K = \frac{1}{\omega t} \int d^2x \left[ \psi^* \left( -\frac{1}{2} \mathbf{D}^2 - \frac{b}{2} + \varepsilon \right) \psi \right]. \quad (3.36)$$

The small perturbation is therefore:

$$V = \frac{1}{\omega t} \int d^2x \left[ (-a_h - \varepsilon) |\psi|^2 + \frac{1}{2} |\psi|^4 \right]. \quad (3.37)$$

The eigenvalue of  $N^{\text{th}}$  Landau level is  $-\frac{1}{2} \mathbf{D}^2 \varphi = (N + \frac{1}{2}) b \varphi$ . For simplified in writing, we introduce  $g_{gauss}(\varepsilon) = g_{tr \log}(\varepsilon) + \langle V(\varepsilon) \rangle_K$  which is relative to the free energy density as  $f_{eff} = -\omega t g_{gauss}$ , where

$$g_{tr \log} \equiv \log \left[ \int \mathcal{D}\psi \mathcal{D}\bar{\psi} \exp(-K) \right] = \frac{b}{2\pi} \sum_{N=0}^{\infty} \log(Nb + \varepsilon) \quad (3.38)$$

$$\langle V \rangle_K = (-a_h - \varepsilon) \frac{b}{2\pi} \sum_{N=0}^{\infty} \frac{1}{Nb + \varepsilon} + \omega t \left( \frac{b}{2\pi} \sum_{N=0}^{\infty} \frac{1}{Nb + \varepsilon} \right)^2. \quad (3.39)$$

(Magnetic field independent term appear in the free energy density is dropped because it is irrelevant to our study on magnetization.) Both terms has ultraviolet divergency, namely at large  $N$  the sums diverge. An UV momentum cutoff  $N_f + 1 = \frac{\Lambda}{b}$  are introduced for regulization. To extract the divergent part, one can interpolate the  $g_{tr \log}$  to two terms:

$$g_{tr \log} = \frac{b}{2\pi} \left\{ \sum_{N=1}^{N_f} \left[ \log(Nb + \varepsilon) - \int_{N-1/2}^{N+1/2} \log(xb + \varepsilon) dx \right] \right. \quad (3.40)$$

$$\left. + \log \varepsilon + \sum_{N=1}^{N_f} \int_{N-1/2}^{N+1/2} \log(xb + \varepsilon) dx \right\}. \quad (3.41)$$

The last term is divergent and for large  $N$ , it can be approximated by  $\log(1+x) \sim x$ :

$$\begin{aligned} & b \sum_{N=1}^{N_f} \int_{N-1/2}^{N+1/2} \log(xb + \varepsilon) dx \\ & \approx \Lambda (\log \Lambda - 1) + (\varepsilon - b/2) \log \Lambda + (\varepsilon + b/2) - (\varepsilon + b/2) \log(\varepsilon + b/2) \end{aligned} \quad (3.42)$$

Therefore one can divided  $g_{tr \log}$  to an infinite part with  $\Lambda$  and a finite part,  $u$ :

$$g_{tr \log} = \frac{1}{2\pi} \{ \Lambda (\log \Lambda - 1) + (\varepsilon - b/2) \log \Lambda \} + u(\varepsilon, b). \quad (3.43)$$

The finite part  $u$  can be simplified as

$$u(\varepsilon, b) = \frac{b}{2\pi} f_s(\varepsilon/b) + \frac{b}{2\pi} (1/2 - \varepsilon/b) \log b, \quad (3.44)$$

where the function  $f_s$  is defined as

$$\begin{aligned} f_s(x) = & \log x - (x + 1/2) (\log(x + 1/2) - 1) + \\ & \sum_{n=1}^{\infty} \left[ \log(n+x) - \int_{n-1/2}^{n+1/2} \log(y+x) dy \right]. \end{aligned} \quad (3.45)$$

which is basically  $-\ln \Gamma(x)$  plus a constant.

The interactions part, the "bubble" integral, diverges logarithmically:

$$\frac{b}{2\pi} \sum_{n=0}^{\infty} \frac{1}{nb + \varepsilon} = \frac{1}{2\pi} \log \Lambda + u' \quad (3.46)$$

where  $u' \equiv \frac{\partial}{\partial \varepsilon} u(\varepsilon, b) = \frac{1}{2\pi} [f'_s(\varepsilon/b) - \log b]$ , and the derivative of  $f_s$  is a polygamma function,  $\Psi(x)$ , i.e.

$$f'_s(x) = \sum_{n=1}^{\infty} \left[ \frac{1}{n+x} - \int_{n-1/2}^{n+1/2} \frac{1}{(y+x)} dy \right] + \left[ \frac{1}{x} - \log(x + 1/2) \right] = -\Psi(x). \quad (3.47)$$

The total free energy in Gaussian variational approximation for all Landau levels is obtained,

$$\begin{aligned} g_{gauss}(\varepsilon) = & \frac{1}{2\pi} \Lambda (\log \Lambda - 1) - \omega t \left( \frac{1}{2\pi} \log \Lambda \right)^2 - (a_h^r + b/2) \left[ \frac{1}{2\pi} \log \Lambda \right] \\ & - (a_h^r + \varepsilon) u' + u(\varepsilon, b) + \omega t (u')^2. \end{aligned} \quad (3.48)$$

Thus, the temperature  $T_c$  and vacuum energy will be renormalized:  $a_h^r = a_h - 2\omega t \frac{1}{2\pi} \log \Lambda$ . The first three terms are divergent, however, they will not contribute to physical quantities such as magnetization, specific heat ...etc. To find the minimum of  $g_{gauss}(\varepsilon)$ , we need to solve the gap equation:

$$\varepsilon = -a_h^r + 2\omega t u'(\varepsilon, b) \quad (3.49)$$

Substitute the solution  $\varepsilon_s$  to  $g_{gauss}(\varepsilon)$  one get the minimized free energy density  $f_{eff} = -\omega t g$ :

$$g = \frac{1}{2\pi} \Lambda (\log \Lambda - 1) - \omega_{2D} t \left( \frac{1}{2\pi} \log \Lambda \right)^2 - (a_h^r + b/2) \left[ \frac{1}{2\pi} \log \Lambda \right] + u(\varepsilon, b)|_{\varepsilon_s} - \omega t u'^2(\varepsilon, b)|_{\varepsilon_s} \quad (3.50)$$

In the "Prange" limit where only the normal part is taking in to account,

$$g_{prg} = \frac{1}{2\pi} \Lambda (\log \Lambda - 1) - (a_h^r + b/2) \left[ \frac{1}{2\pi} \log \Lambda \right] + u(-a_h^r, b). \quad (3.51)$$

### 3.5 All Landau level contributions in quasi-2D systems. An effective LLL model

As we mentioned in Chapter II, at the parameter range of interest for us, the coupling between HLL and LLL is important. Unfortunately the above used Gaussian variational approximation is not precise enough at low temperatures. (for example see free energy of various approximants in Fig 2.2 ) and one is forced to use a more sophisticated Borel-Pade approximation. A simple way to present it is via an effective LLL model in which one "integrates out" the HLL contributions. In the effective LLL model the coupling between LLL and HLL renormalizes the LLL functional as following. Consider the simplest case of the coupling of two different Landau layers in the interaction term  $|\psi|^4$ . We have

$$|\psi|^4 = \dots + 4(\psi_0^* \psi_0 \psi_1^* \psi_1 + \psi_0^* \psi_0 \psi_2^* \psi_2 + \dots) + \dots, \quad (3.52)$$

where only the most interesting quadratic in the  $\psi_i$  part is written. The index  $i > 0, i \in \mathbb{N}$  denotes the rest of Landau levels excluding the lowest one. Since coupling between the two different high Landau level correction,  $\langle \psi_i^* \psi_j \rangle_K$  for  $i \neq j$  is small, we effectively drop out the off-diagonal terms. We therefore extract the main coupling from the GL model:

$$f_{couple} [\psi_0, \psi_i] = 2 \sum_{i=1}^{\infty} |\psi_0|^2 |\psi_i|^2. \quad (3.53)$$

The correlation function is

$$\langle \psi_{n,k}^* \psi_{m,q} \rangle = \frac{2\pi}{b} \frac{1}{\varepsilon + nb} \delta(k+q) \delta_{n,m}. \quad (3.54)$$

For simplicity in the following we will neglect the fluctuations of the magnetic field because in lowest Landau level approximation it gives just a renormalization of the interaction term. Moreover, the high- $T_c$  superconductors are extremely type II superconductors and therefore even this renormalization is not essential. The total original action is

$$f [\psi_0, \psi_i] = f_{HLL} [\psi_i] + f_{LLL} [\psi_0] + f_{couple} [\psi_0, \psi_i]. \quad (3.55)$$

The effective LLL free energy is defined as  $f = -\omega t \log Z \equiv -\omega t g$

$$Z = \int \mathcal{D}\psi_0 Z_{eff} [\psi_0] \quad \text{with} \quad (3.56)$$

$$Z_{eff} [\psi_0] = \int \prod_{i=1}^{\infty} \mathcal{D}\psi_i \exp \{-f[\psi_0, \psi_i]\}. \quad (3.57)$$

To integrate out the high Landau level coupling parts, one can use Gaussian variational method within which one uses a decomposition

$$f_{HLL} [\psi_i] = K [\psi_i] + \alpha V [\psi_i], \quad (3.58)$$

and separates the main quadratic part

$$K_{HLL} [\psi_i] = \frac{1}{\omega t} \int d^2x \left[ \psi_i^* \left( -\frac{1}{2} \mathbf{D}^2 - \frac{b}{2} + \varepsilon \right) \psi_i \right] \quad (3.59)$$

and a small perturbation,

$$V_{HLL} [\psi_i] = \frac{1}{\omega t} \int d^2x \left[ (-a_h - \varepsilon) |\psi_i|^2 + \frac{1}{2} |\psi_i|^4 \right]. \quad (3.60)$$

The effective partition function, expanded to first order of  $\alpha$  is

$$Z_{eff}[\psi_0] = \int \prod_{i=1}^{\infty} \mathcal{D}\psi_i (1 - (V_{HLL}[\psi_i] + f_{couple}[\psi_0, \psi_i])) \exp[-(K_{HLL}[\psi_i] + f_{LLL}[\psi_0])]. \quad (3.61)$$

After integrating out high Landau level coupling terms, one gets

$$\begin{aligned} g(\varepsilon) &= \log \int \mathcal{D}\psi_0 Z_{eff}[\psi_0] \\ &= \frac{b}{2\pi} \sum_{N=1}^{\infty} \log(Nb + \varepsilon) + (-a_h - \varepsilon) \frac{b}{2\pi} \sum_{N=1}^{\infty} \frac{1}{Nb + \varepsilon} + \omega_{2Dt} \left( \frac{b}{2\pi} \sum_{N=1}^{\infty} \frac{1}{Nb + \varepsilon} \right)^2 \\ &\quad + \log \int \mathcal{D}\psi_0 \exp \left\{ - \left[ f_{LLL}[\psi_0] + 2 \frac{b}{2\pi} \sum_{n=1}^{\infty} \frac{1}{nb + \varepsilon} |\psi_0|^2 \right] \right\}. \end{aligned} \quad (3.62)$$

Alternatively, one can rewrite this as

$$g = g_{gauss}^{HLL}(\varepsilon) + \log \int \mathcal{D}\psi_0 \exp \left\{ f_{LLL}[\psi_0] + 2 \frac{b}{2\pi} \sum_{N=1}^{\infty} \frac{1}{Nb + \varepsilon} |\psi_0|^2 \right\} \quad (3.63)$$

$$= g_{gauss}^{HLL}(\varepsilon) + g_{bp}^{eff}(\varepsilon), \quad (3.64)$$

where  $f_{LLL}$  is the functional energy with lowest landau level constrain Eq. 3.13 and  $g_{gauss}^{HLL}(\varepsilon)$  is the free energy without contribution from lll and it's first order coupling with hlls. The summation

$$\frac{b}{2\pi} \sum_{N=1}^{\infty} \frac{1}{Nb + \varepsilon} = \frac{1}{2\pi} \log \Lambda + u'(\varepsilon, b) - \frac{b}{2\pi} \frac{1}{\varepsilon}.$$

The effective LLL free energy functional with the first order coupling with high landau level is,

$$f_{LLL}^{eff}[\psi_0] = \iint dx^2 \left\{ -a_h^A |\psi_0|^2 + \frac{1}{2} |\psi_0|^4 \right\} \quad (3.65)$$

with

$$a_h^A = a_h^r + 2\omega_{2Dt} \left( \frac{b}{2\pi} \frac{1}{\varepsilon} - u'(\varepsilon, b) \right). \quad (3.66)$$

High landau level coupling term renormalized the rescaled temperature  $a_h^r$ , therefore one modified the LLL result by Bore-Padé approximation. After substitution of the gap equation solution  $\varepsilon_s$  into the free energy, one gets:

$$g = g_{gauss}^{HLL}(\varepsilon_s) + g_{bp}^{eff}(\varepsilon_s). \quad (3.67)$$

Magnetization can be obtained by taking the first derivative of Gibbs energy with respect to magnetic field  $b$ .

$$M = -\frac{H_c^2}{4\pi\kappa^2}\omega t\partial_b g(b, t). \quad (3.68)$$

The theoretical curves of magnetization curves with various approaches are shown in Fig.3.2 where the scaled magnetization

$$m = -\partial_b g(b, t) \quad (3.69)$$

is used.

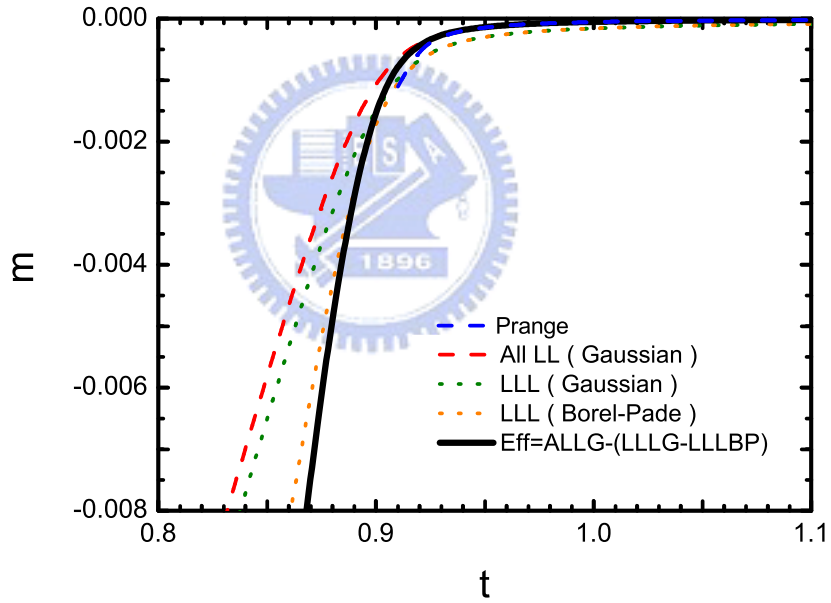


Figure 3.2: Theoretical magnetization curve in various approaches.

### 3.6 Results and Comparisons with Experiments

The high temperature part of the magnetization was fitted to a Curie law,  $M = \chi H = (\chi_0 + C/T)H$ , and extrapolated to temperatures below  $T_c$ . The extrapolated values



of  $M$  were subtracted from the raw data measured below  $T_c$ . Observing the scaling behavior of the experiments (see Fig. 3.4 and 3.5 ), one found  $Bi_2Sr_2Ca_3Cu_3O_y$  [81]  $TiBa_2Ca_3Cu_4O_y$  [79], three-layered  $HgBa_2Ca_3Cu_3O_{8+\delta}$  [31] and  $Bi_2Sr_1Ca_1Cu_2O_{8+\delta}^{OP}$  [30] has good scaling behavior in high field. The scaling theory suggest those are quasi-2D system. However, while the scaling function obtained from BP approximation describe accurate [79, 81] and [31], it doesn't go well as [30] since the diverse at the high temperature region at the vicinity of  $T_c$ . Especially for under doped  $Bi_2Sr_1Ca_1Cu_2O_{8+\delta}^{UD}$ , the scaling behavior doesn't exist.

	$T_c$ (K)	$H_{c2}^{fitting}$ (T/K)	$H_{c2}^{scaling}$ (T/K)	$Gi_{2D}$	$\kappa$
$Bi_2Sr_2Ca_3Cu_3O_y$	111	3.39	3.3 ~ 4.2	0.0011	140
$TiBa_2Ca_3Cu_4O_y$	127	2.20	2.24	0.0001	84.8
$HgBa_2Ca_3Cu_3O_{8+\delta}$	132	2.95	2.95	0.0011	55
$Bi_2Sr_1Ca_1Cu_2O_{8+\delta}^{OP}$	93.3	2.36	2.15	0.0035	72.3747
$Bi_2Sr_1Ca_1Cu_2O_{8+\delta}^{UD}$	57	2.98	1.8	0.31	97.183

Figure 3.3: fitting of the melting curve

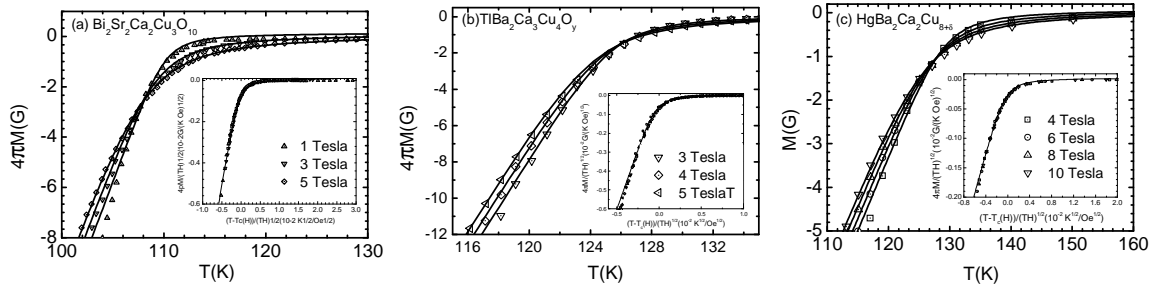


Figure 3.4: Magnetic moment versus temperature for quasi2D system, fitting by the with parameter discussed and given in the text. Materials are: (a)  $Bi_2Sr_2Ca_2Cu_3O_{10}$  (b)  $TiBaCaCuO_7$  (c)  $HgBa_2Ca_2Cu_3O_{8+\delta}$

The HLL correction will be calculated as follows. We numerically solve the gap equation (3.49) from which  $F(T, H)$  can be obtained. Then Eq.(3.68) is used to calculate the magnetization of the full GL model in Gaussian approximation. The HLL

correction is thus the magnetization of the full GL model in Gaussian approximation minus the magnetization of the LLL contribution in Gaussian approximation. We compare the experiments using following approximation. While the corrections due to HLL are calculated in Gaussian approximation, the LLL contribution will be calculated non-perturbatively. The comparison of the theoretical predictions with the experiments for optimized doped *BSCCO*[30], is shown on Fig.3.5. The fitting parameters  $T_c$ ,  $H_{c2}$ ,  $\kappa$  and  $G_i$  obtained from the fitting of the melting curve tabulated in Fig.3.3. The agreement is fair at intermediate magnetic fields and high temperature. It is expected that agreement is improved at higher temperature for all fields. One can tell that the theory of the full GL model (higher Landau levels included) beyond Gaussian approximation is required at low magnetic fields. Indeed experimentally it is often claimed that one can establish the LLL scaling for fields above 3 T for *YBCO* (see, for example, ref. [43] ) as at low magnetic fields, the HLL contribution will be significant. When go below low temperature region, the HLL contribution is expected to decrease, but the correction from theoretical curve is still strong.

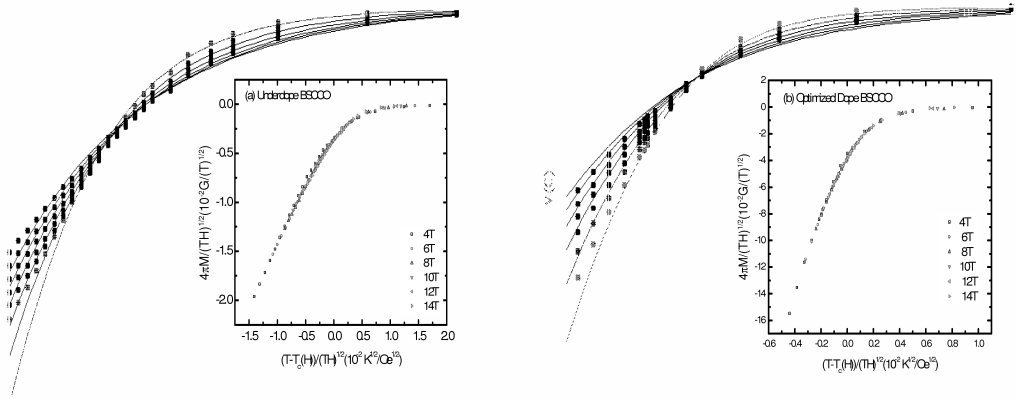


Figure 3.5:

Intersection points of magnetization curves of layered superconductors tells the dimensionality of the fluctuations. In this section the Lawrence - Doniach model was applied to describe the magnetization curves in *HgBCO* and *LaSCO* samples. Pre-

viously the data were analyzed by using either  $2D$  or  $3D$  Ginzburg - Landau models. However, unlike the optimally doped  $YBCO$  or  $BSCCO$ , these materials belong to a class of materials which are neither  $2D$  nor slightly anisotropic  $3D$  for which LD model, a simple generalization of GL models, described in section 2.2 is applicable.

They include layered superconductor  $HgBa_2Ca_2Cu_3O_{8+\delta}$  whose magnetization measured in ref. [31] is fitted by using the Lawrence - Doniach formulas is given above in 3.6(a). The transition temperature  $T_c$  derived directly from the magnetization data is  $132K$ . Although in the original paper the value of the slope  $\frac{dH_{c2}(T)}{dT}|_{T=T_c}$ , derived from the scaling field  $H_s$  was estimated as  $1.32$  Tesla/K indicating  $H_{c2} = 178.2$  Tesla, a much higher value  $H_{c2} = 390$  Tesla was applied. The dimensionless coupling constant  $g = 0.08$  and the interlayer-coupling parameter  $\gamma_t = 0.1$  give the best fit to experimental data. According to the result of the underdoped  $YBCO$  [86] at temperature exceeding the mean field transition temperature, the LLL approximation overestimated magnetization. This can be realized by including higher Landau levels. The evolution of the crossing point is also shown in 3.6(a).

Data for a sample close to the optimally doped  $La_{1.857}Sr_{0.143}CuO_4$  of ref. 7 are presented in 3.6(b). For magnetic fields from 2 Tesla to 7 Tesla, the crossing points move in the direction consistent with theory and are always below  $T_c$ . The transition temperature is  $T_c = 36.4 K$  [32]. The best fitting parameters are  $g = 0.019$ ,  $H_{c2} = 80$  Tesla and  $\gamma_t = 0.02$ . In the strongly underdoped samples, such as  $La_{1.92}Sr_{0.08}CuO_4$ , the experimental data were rather unusual. Two different well-defined crossing points were observed. As magnetic field increased from 0.3 Tesla to 7 Tesla the crossing point unexpectedly "jumped" from a temperature below  $T_c$  to another one well above  $T_c$ . The phenomenon obviously conflicts with our previous qualitative conclusion based on the Lawrence - Doniach model. Even though, the high magnetic field data can be fitted if slightly higher transition temperature  $T_c = 24.2 K$  is assumed. 3.6(c) shows the fit for  $La_{1.92}Sr_{0.08}CuO_4$  with  $g = 0.05$ ,  $H_{c2} = 44$  Tesla and  $\gamma_t = 0.02$ .

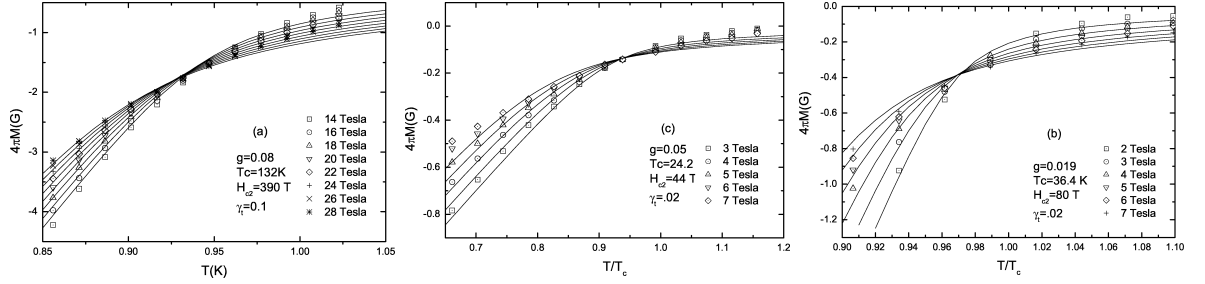


Figure 3.6: Magnetic moment versus temperature in the high-field region. The solid lines are fits using Eq. 3.26 with parameter discussed and given in the text. Materials are: (a)  $HgBa_2Ca_2Cu_3O_{8+\delta}$  (b) the optimally doped  $La_{1.857}Sr_{0.143}CuO_4$  (c) the strongly underdoped  $La_{1.92}Sr_{0.08}CuO_4$ .

### 3.7 Discussion

The order parameter may be considered as an average of the localized quantity over a few lattice spacings, or a microscopic length scale  $a$ . Only for distance much larger than  $a$  can a field-theoretic description of the system in terms of order field be meaningful. Below the microscopic length  $a$  microscopic properties of the material begin to become relevant. Such that one can classify the thermal fluctuation to the microscopic thermal fluctuations and two kinds of mesoscopic thermal fluctuations.

On the microscopic level, temperature modifies properties of the electron gas and the pairing interaction responsible for the creation of Cooper pairs. When “integrating out” the microscopic (electronic) degrees of freedom, one obtains an effective mesoscopic GL free energy with temperature dependent parameters,  $m^*$ ,  $\alpha$  and  $\beta$ , in terms of the distributions of the order parameter  $\Psi(\mathbf{x})$  with a lower limit on the length scale,  $a$ , over which the order parameter field can vary, or an upper limit to the momentum,  $\Lambda = 2\pi/a$ , of the Fourier components of the field. In practice, if one decompose  $\Psi(\mathbf{x})$  to a bases, for example Fourier components, with amplitude  $\varphi_{\mathbf{k}}$ , the measure,  $\mathcal{D}\Psi$ , of a path integral in partition function of the system can be written as

$$\mathcal{D}\Psi = \prod_{k>0;|k|<\Lambda} d^2\varphi_k \quad (3.70)$$

The remaining part of the statistical sum can be view as the mesoscopic fluctuations. Therefore, unlike the theory proposed in ref.[80], for measurable quantity such as magnetization, the  $UV$  cut-off dependence should cancel out with the by renormalization of the bare mass, i.e. the mean field transition temperature.

The mean field lowest Landau level theory of thermal fluctuation is able to describe magnetization curves near  $T_c$ , including the intersection point, in both the quasi 2D superconductors like *BSCCO* and the 3D superconductors like *YBCO*. It is therefore expected that the natural generalization of the model to include the coupling between layers, the Lawrence - Doniach model, should describe sufficiently well the thermal fluctuations in a wide range of layered materials, which exhibit neither the 2D nor the 3D behavior. A characteristic general feature is that the magnetization curves intersect always below  $T_c$ . While we show that the theory is consistent with the recent very detailed studies on *HgBCCO* and earlier studies on *LaSCO*, the results on the strongly underdoped *LaSCO*, which show the intersection point above  $T_c$ , are incompatible with the theory. Despite the fact that the theory has a number of assumptions like effects of disorder and contributions of higher Landau levels, the discrepancy is real. Since the description of the layered superconductors by the Lawrence - Doniach is a very important part of the physics of the high  $T_c$  superconductors this question should be addressed experimentally.

# Chapter 4

## Structural Phase transition in Fourfold Symmetric Superconductors



### 4.1 Introduction

The symmetry of the order parameter in superconductor is strongly related to the crystallographic symmetry group of the material, the structure of the Fermi surface and the nature of the pairing mechanism. In *YBCO*, the in-plane  $O(2)$  is breaking due to the *d*-wave character of pairing. It has both a square and a rhombic phases [18]. In overdoped *LaSCO*, at low temperatures, the square and rhombic lattices were observed using SANS by Gilardi *et al* [16]. Asymmetry is not always related to the non s-wave nature of pairing. In borocarbides ( $RE : Y, Lu, Er$ )  $Ni_2B_2C$  [14], *Nb* [13], and  $V_3(Si)$  [15], square vortex lattice is observed using techniques such as decoration, STM, SANS or  $\mu$ SR etc.

The precise location in the  $T-H$  plane of the square-rhombohedral SPT in the vortex crystal is still a matter of discussion. Earlier experiments on  $LuNi_2B_2C$  indicate a very small positive slope of the transition line in the  $T-H$  plane  $H_2(T)$  till it reaches the  $H_{c2}(T)$  region. According to some experiments, it abruptly turns up and even acquires a

negative slope at high fields, while in other experiments experiments in a closely related material  $YNi_2B_2C$ , it continues the gradual increase even near  $H_2(T)$ . The results at low temperatures was first explained in the framework of the nonlocal London  $NLL$  theory proposed by Kogan *et al* [20]. The  $NLL$  theory includes four derivative terms which bring in the anisotropy effects essential to trigger the SPT between the vortex lattice phases. The more symmetric square vortex crystal, stable at a stronger magnetic field higher density of vortices, transforms into a less symmetric rhombic vortex crystal as the magnetic field decreases. Thus the square-to-rhombus SPT is associated with a spontaneous breaking of the fourfold symmetry of the system. The transition has also been understood theoretically on the basis of the Ginzburg-Landau functional which had to be extended in a similar fashion, by including an asymmetric four derivative term. Such higher derivatives Ginzburg-Landau HDGL theories are applicable, strictly speaking, not far from  $T_c$ , but they generally work well in a much larger part of the  $T - H$  plane, including fields and temperatures well below the  $H_{c2}(T)$  line. Although temperature might be introduced into these phenomenological models via a temperature dependence of their coefficients, the resulting slope of the transition line is typically very small and, more importantly, is of higher order in the relevant expansion parameter and therefore cannot be predicted.

It should be emphasized at this point that both  $NLL$  and  $HDGL$  were solved at the mean-field level only in the papers mentioned above and only recently in Refs. [20] and [24], respectively, were attempts made to take into account thermal fluctuations on the “mesoscopic” scale. Although thermal fluctuations are dominant in high- $T_c$  superconductors, leading, they are negligible in low- $T_c$  materials for which the Ginzburg number, characterizing the strength of the thermal fluctuations, is several orders of magnitude lower. In high- $T_c$  superconductors the square-to-rhombus transition was observed directly via neutron scattering in  $YBa_2Cu_3O_{7+\delta}$ , and  $La_2Sr_{1-x}Cu_xO_4$ , and indirectly via the peak effect in  $LaSCO$ .

In this study, we will consider both thermal fluctuations and disorder in both perturbation and nonperturbation method. We suggest that for low- $T_c$  material such as

borocarbides, the disorder influence is pronounced and result in the reentrance of rhombic lattice near the  $H_{c2}$ .

## 4.2 Basic equations and symmetries

The system is phenomenologically described by the anisotropy Ginzburg–Landau free energy functional with 4-fold symmetry,  $\mathcal{F}_{4-fold} = \mathcal{F}_{3D} + \mathcal{F}_{ansio}$ :

$$f = \frac{\mathcal{F}_{4-fold}}{T} = \frac{1}{\omega} \int d^3x \left[ \frac{1}{2} \psi^* \mathcal{H} \psi - \frac{1-t}{2} |\psi|^2 + \frac{1}{2} |\psi|^4 \right], \quad (4.1)$$

where the gradient part of the free energy  $\mathcal{H} = \mathcal{H}_0 + \mathcal{H}'$ [26]: The isotropic

$$\mathcal{H}_0 = -\vec{D}^2 - \partial_z^2, \quad (4.2)$$

and the anisotropic parts  $\mathcal{H}'$  is chosen to have a combination from terms in Eq.(2.13) which preserve the  $H_{c2}(T)$  line produced by  $\mathcal{H}_0$  (up to first order of  $\tilde{\eta}$ ).

$$\begin{aligned} \mathcal{H}' = & -\frac{\tilde{\eta}}{4} \left[ \cos(4\Theta) \left\{ (D_x^2 - D_y^2)^2 - (D_x D_y + D_y D_x)^2 \right\} \right. \\ & \left. + \sin(4\Theta) \left\{ (D_x^2 - D_y^2) (D_x D_y + D_y D_x) + (D_x D_y + D_y D_x) (D_x^2 - D_y^2) \right\} \right] \end{aligned} \quad (4.3)$$

where  $\Theta$  is the angle between the rhombic lattice and the atomic lattice and  $D_x = \partial_x - iby$ ,  $D_y = \partial_y$ . Within the gauge, the rescaled magnetic field is in  $c$  direction,  $\mathbf{b} = (0, 0, b)$ . The properties of a particular material are encoded into the phenomenological coefficient  $\eta_m$ . Due to GL expansion,  $\eta_m$  is a constant but in fact it can depend weakly on temperature and other external parameters. It can be positive (usually in low  $T_c$  materials) or negative (usually in high  $T_c$  materials). In terms of operators of creation and annihilation of Landau levels,

$$\hat{a}^\dagger \equiv -\frac{1}{\sqrt{2b}} (D_x - iD_y), \quad \hat{a} \equiv \frac{1}{\sqrt{2b}} (D_x + iD_y), \quad (4.4)$$

The commutation relations is

$$[a^+, a] = -1, \quad (4.5)$$

$$[a, a^+] = 1. \quad (4.6)$$



It is simply

$$\mathcal{H}_0 = ba^\dagger a - \frac{1}{2}\partial_z^2 \quad (4.7)$$

$$\mathcal{H}' = -b^2\eta_m \left[ (a^\dagger)^4 e^{4i\Theta} + a^4 e^{-4i\Theta} \right]. \quad (4.8)$$

The effective magnitude of the four-fold anisotropy depends also on the magnetic induction and should be specified by a parameter that is proportional to  $b\eta_m$ .

### 4.3 Structure of the vortex lattice in the clean system and its phase transition

In mean field approach, one must find the order parameter which minimizes the total free energy of the system, namely to solve the nonlinear equation

$$\mathcal{H}\psi - a_h\psi + \psi|\psi|^2 = 0. \quad (4.9)$$

One can first solves the linearized GL equation  $\mathcal{H}\psi = a_h\psi$  to obtain an nontrivial solution,  $\psi \neq 0$ . If  $b\eta_m \ll 1$ , the anisotropic part of  $\mathcal{H}'$  can be treated as a perturbation [66], the presence of anisotropy modifies the eigenfunctions of the isotropic part  $\varphi_{N,k}(x, y, z)$  by

$$\phi_{Nk} = \varphi_{Nk} - b^2\tilde{\eta} \sum_{M \neq N} \frac{\langle \varphi_{M,k} | (a^\dagger)^4 e^{4i\Theta} + a^4 e^{-4i\Theta} | \varphi_{N,k} \rangle}{b(N-M)} \varphi_{Mk} + \dots \quad (4.10)$$

where the eigenfunctions

$$\begin{aligned} \varphi_{N,k}(x, y, z) = & \sqrt{\frac{\sqrt{2\sigma}}{2^N N!}} e^{ik_z z} \sum_{l=-\infty}^{+\infty} \exp\{i[\pi\rho(l^2 - l)]\} \exp\left\{i\left[\sqrt{2\pi\sigma}l(yb^{1/2} + k_x b^{-1/2}) + yk_y\right]\right\} \\ & \times \exp\left[-\frac{1}{2}\left(xb^{1/2} - \sqrt{2\pi\sigma}l - k_y b^{-1/2}\right)^2\right] \cdot H_N\left(xb^{1/2} - \sqrt{2\pi\sigma}l - k_y b^{-1/2}\right) \end{aligned} \quad (4.11)$$

,  $\sigma = \frac{1}{2} \tan \theta$  where  $\theta$  is the apex angle between vortex lattice basis  $\mathbf{d}_1$  and  $\mathbf{d}_2$  chosed as Eq.(4.14) (see Fig. 4.2). The first order correction of  $H$  is

$$\phi_{0k} \equiv \phi_k = \varphi_k + \eta e^{4i\Theta} \varphi_{4k}, \quad (4.12)$$

$$\eta = \sqrt{3/2} b\eta_m \quad (4.13)$$

called the modified lowest Landau level (MLLL) which will be employed as LLL approximation in previous topic. Note that the magnetic translation operator had been applied on the eigenfunction of  $N^{th}$  Landau level to get a complete basis for functions belonging to each Landau level as we mentioned in previous chapter. The normalization factor is defined by the average over a unit cell of  $|\varphi_{N,k}(x, y, z)|^2 = 1$ . To simplify the notation, from now on  $\langle \dots \rangle$  denotes the average over a unit cell in real space.  $H_N(x)$  is Hermite Polynomials. The components of the vectors that determine the unit cell are

$$\begin{aligned} \mathbf{d}_1 &= \left( \sqrt{2\pi\sigma}, \frac{1}{2}\sqrt{\frac{2\pi}{\sigma}} \right) \\ \mathbf{d}_2 &= \left( 0, \sqrt{\frac{2\pi}{\sigma}} \right) \end{aligned} \quad (4.14)$$

In the above formulas we measure all distances between the vertices with magnetic length  $\ell$  which are related to the magnetic field by  $\Phi_0 = 2\pi H\ell^2$ .

To solve the GL equation, one can expand  $\psi$  on  $a_h - \frac{1-t-b}{2}$ , the distance from  $H_{c2}$  line. The solution of GL equation (4.9) has the form

$$\begin{aligned} \psi &= \sqrt{a_h} (\Psi_0 + a_h \Psi_1 + \dots), \\ \Psi_0 &= c\phi_0, \quad \Psi_1 = \sum_N c_N \phi_N, \quad \dots, \end{aligned} \quad (4.15)$$

which is formally identical to the case of the isotropic GL model. The normalization coefficient  $c^{-2} = \langle |\phi_0|^4 \rangle$  is fixed by the nonlinear terms of the GL equation. We use  $\langle \dots \rangle$  for spatial average. In lowest order expansion in  $a_h$ , the mean field solution is

$$\Psi = \sqrt{\frac{a_h}{\langle |\phi_0|^4 \rangle}} \phi_0 \quad (4.16)$$

Expand in first order of  $\eta$ ,

$$\begin{aligned} \langle |\phi_0|^4 \rangle &= \langle |\varphi_0|^4 \rangle + 2\eta(Re) (e^{4i\Theta} \langle \varphi_4 \varphi_0^* |\varphi_0|^2 \rangle) + \mathcal{O}(\eta^2) \\ &\equiv \beta_0(\theta) + 4\eta\beta_4(\theta) \cos(4\Theta) + \mathcal{O}(\eta^2) \end{aligned} \quad (4.17)$$

where  $\beta_0(\theta) = \langle |\phi_0|^4 \rangle$ ,  $\beta_4(\theta) = \langle \phi_4 \phi_0^* |\phi_0|^2 \rangle$  are real function since  $(Im)\beta_4 = 0$ . In general, apex angle,  $\theta$ , dependent  $\langle \varphi_N^* \varphi_M \varphi_O \varphi_P^* \rangle$  for any landau level is

$$\begin{aligned}
& \langle \varphi_N^* \varphi_M \varphi_O \varphi_P^* \rangle \\
&= \sqrt{\frac{2^M 2^P P! M!}{2^N 2^O N! O!}} \sum_{m_1, m_2} \left\{ \exp \left[ -\frac{\pi}{4\sigma} \left( (2m_1 - m_2)^2 + 4m_2^2 \sigma^2 \right) \right] \right. \\
& \quad \left[ \sqrt{2\pi\sigma m_2} - i\sqrt{\frac{\pi}{2\sigma}} (2m_1 - m_2) \right]^{N-M} \left[ \sqrt{2\pi\sigma m_2} + i\sqrt{\frac{\pi}{2\sigma}} (2m_1 - m_2) \right]^{O-P} \\
& \quad \left. L_M^{N-M} \left[ \frac{1}{2} \left( 2\pi\sigma m_2^2 + \frac{\pi}{2\sigma} (2m_1 - m_2)^2 \right) \right] L_P^{O-P} \left[ \frac{1}{2} \left( 2\pi\sigma m_2^2 + \frac{\pi}{2\sigma} (2m_1 - m_2)^2 \right) \right] \right\}
\end{aligned} \tag{4.18}$$

where  $L_q^r(x)$  is Legendre Polynomials. In the derivation, we use the fact

$$\begin{aligned}
& \int_{X=-\infty}^{\infty} e^{-X^2} H_M(X+Y) H_N(X+Z) \\
&= \sqrt{\pi} 2^N M! Z^{N-M} L_M^{N-M}(-2YZ) \quad (M \leq N).
\end{aligned} \tag{4.19}$$

The mean field free energy density which depends on the geometrical parameters  $\theta$  and  $\Theta$  of the vortex lattice has the form

$$F_0(\theta, \Theta) = -\frac{a_h^2}{2 \langle |\phi_0|^4 \rangle} + \mathcal{O}(a_h^3). \tag{4.20}$$

The minimization with respect to  $\Theta$  and  $\theta$  determines the orientation and shape of the vortex lattice at equilibrium, respectively. Since  $\beta_4 < 0$  for  $\pi/4 < \theta < \pi/3$ , thus the minimize condition is  $\cos 4\Theta = \eta/|\eta|$ . Therefore for positive  $\eta^{GL}$ ,  $\Theta = 0$  and for negative  $\eta$ ,  $\Theta = \pi/4$ . The energy density is

$$F_0(\theta) = -\frac{a_h^2}{2} \frac{1}{\beta_0 + 4|\eta| \beta_4(\theta)}. \tag{4.21}$$

The minimization with respect to  $\theta$  was performed numerically in [26]. The phase transformation between the square and rhombic lattices found in this way is continuous. Therefore, in order to find the boundary between these phases it is also possible, and more convenient in this case, to study the conditions for the stability of the more symmetric square phase. The condition for stability reads

$$\frac{d^2 F_{mf}(\theta)}{d\theta^2} \Big|_{\theta=\frac{\pi}{4}} = 0 \tag{4.22}$$

or

$$\beta_0''(\theta = \frac{\pi}{4}) + 4|\eta_c|\beta_4''(\theta = \frac{\pi}{4}) = 0 \quad (4.23)$$

which yields  $|\eta_c| = 0.02923$  i.e. the phase transition line  $b_{SPT}$  on H-T diagram is:

$$b_{SPT} = \frac{0.02387}{|\eta_m|}. \quad (4.24)$$

In this approximation the line of square–rhomb structural phase transformation (SPT line) is parallel to the reduce temperature axis,  $t$ . Note however that some weak temperature dependence can appear through the parameter  $\eta_m$ . The small magnitude of  $\eta_c$  means that the SPT occurs well below  $H_{c2}(T = 0)$  that consistent with our approach in which in  $\mathcal{H}$  of Eq.(4.8)  $\mathcal{H}'$  is treated as a perturbation.

## 4.4 Effects of weak disorder on structural phase transition

In the following we discuss the quenched disorder correction to the STP. Quenched ( or static ) disorder is essentially unavoidable for any material especially for low- $T_c$  superconductor whose thermal fluctuation depinning is small. In naive way, disorder change the local critical temperature and change the effective mess of the local cooper pair. As we mentioned in Disorder section. An random pinning potential  $W(x)$  is introduce, in the rescaled model, the disorder potential  $a_h W(\mathbf{r}) |\psi(\mathbf{r})|^2$  is added to the GL functional, Eq. (4.1). Disorder potential  $W(\mathbf{r})$  is assumed to be independent of temperature and magnetic field.

If a weak disorder potential is present in the system, vortex lattice distorts to take advantage of the places where the local  $T_c$  (at given magnetic field  $H$ ) is higher and to avoid the places with lower  $T_c$ . The complete energy reads

$$F = F_0(W = 0) + F_{dis} \quad (4.25)$$

The free energy correction  $F_{dis}$  of the GL equation is  $a_h W(x) |\psi|^2$ . Following the same strategy, one can minimize the disorder GL functional to obtained the order parameter

$\psi(\mathbf{r}; W)$  and then averaging over the disorder to obtain the effective free energy of the system:

$$F = -\frac{1}{2} \overline{\langle |\psi(\mathbf{r}; W)|^4 \rangle}_{u.c.} = F_0 + \overline{F_{dis.}}$$

It is convenient to introduce a new random potential  $U(\mathbf{r}) = \frac{W(\mathbf{r})}{\sqrt{n}}$  with the correlator  $\overline{U(\mathbf{r})U(\mathbf{r}')} = \delta^{(3)}(\mathbf{r} - \mathbf{r}')$ . We rewrite the HDGL Eq. (4.9) as

$$\mathcal{H}\psi - a_h\psi + \psi|\psi|^2 + a_h r U(\mathbf{r})\psi = 0, \quad (4.26)$$

where we introduced the new perturbation parameter  $r = \sqrt{n}$ .

Expanding in  $\gamma$ , one gets

$$\psi(\mathbf{r}; U) = \sqrt{a_h} \left[ \Psi_0 + \sum_{m=1}^m r \Psi_m \right]. \quad (4.27)$$

The first term is given by linearized GL equation:  $\Psi_0 = c\phi_0$  with  $c = 1/\sqrt{B_0}$ . The equations for the next two terms are

$$\begin{aligned} \left( 1 - \frac{1}{2a_h} \partial_z^2 - 2|\Psi_0|^2 \right) \Psi_1 - \Psi_0^2 \Psi_1^* &= U \Psi_0, \\ \left( 1 - \frac{1}{2a_h} \partial_z^2 - 2|\Psi_0|^2 \right) \Psi_2 - \Psi_0^2 \Psi_2^* &= 2|\Psi_1|^2 \Psi_0 + \Psi_1^2 \Psi_0^* + U \Psi_1, \end{aligned} \quad (4.28)$$

The unknown functions are found using the expansion in  $\phi_k$  basis:  $\Psi_1 = \int_k d_k \phi_k$ ,  $\Psi_2 = \int_k e_k \phi_k$ . The coefficients of these expansions read:

$$\begin{aligned} d_0 &= -\frac{c}{2} U_0, \\ d_k &= \frac{c}{\Delta_k} \left[ \left( 1 - 2\frac{B_k}{B_0} - \frac{k_z^2}{2a_h} \right) U_k + \frac{G_k^*}{B_0} U_{-k}^* \right], \quad k \neq 0, \end{aligned} \quad (4.29)$$

$$\begin{aligned} e_0 &= -\frac{1}{2c} \int_k |d_k|^2, \\ \Delta_k &= \left[ 2\frac{B_k}{B_0} - 1 - \frac{|G_k|}{B_0} + \frac{k_z^2}{2a_h} \right] \left[ 2\frac{B_k}{B_0} - 1 + \frac{|G_k|}{B_0} + \frac{k_z^2}{2a_h} \right], \end{aligned} \quad (4.30)$$

where  $U_k = \langle U(\mathbf{r}) \phi_k^*(\mathbf{r}) \phi_0(\mathbf{r}) \rangle_{u.c.}$ . The coefficients  $e_k$  with  $k \neq 0$  are not needed for our purposes.

The correction to the free energy density due to disorder is given by:

$$\begin{aligned}
\overline{F_{dis}} &= -\frac{a_h^2 \gamma^2}{2(2\pi L_z)} \int_x \left\{ 4|\overline{\Psi_1}|^2 |\Psi_0|^2 + \left[ 2\overline{\Psi_2^*} \Psi_0 |\Psi_0|^2 + \overline{(\Psi_1^*)^2} \Psi_0^2 + cc \right] \right\} \\
&= -\frac{a_h^2 \gamma^2}{2} \left\{ 4c\overline{c_0} + \int_k \left[ 4\frac{B_k}{B_0} \overline{|d_k|^2} + \left( \frac{G_k^*}{B_0} \overline{d_k d_{-k}} + cc \right) \right] \right\} \\
&= -\frac{a_h^2 \gamma^2}{2} \int_k \left[ -2|d_k|^2 + 4\frac{B_k}{B_0} \overline{|d_k|^2} + \left( \frac{G_k^*}{B_0} \overline{d_k d_{-k}} + cc \right) \right] \\
&= \frac{a_h^2 \gamma^2}{2} c \int_k (\overline{d_k^* U_k} + cc)
\end{aligned} \tag{4.31}$$

At the last step the equation for  $d_k$  has been used. Performing disorder averages we obtain:

$$\begin{aligned}
\overline{F_{dis}} &= \frac{a_h^2 r^2 c}{2} \int_k (\overline{d_k^* U_k} + cc) \\
&= \frac{a_h^2 r^2}{2} c \left[ \int_k \frac{1}{\Delta_k} \left( \left( 1 - 2\frac{B_k}{B_0} \right) \overline{U_k U_k^*} + \frac{G_k}{B_0} \overline{U_k^* U_{-k}} + cc \right) \right] \\
&= \frac{a_h^2 r^2}{2} c^2 \left[ \int_k \frac{1}{\Delta_k} \left( \left( 1 - 2\frac{B_k}{B_0} \right) B_k + \frac{G_k}{B_0} G_k^* \right) \right] \\
&= -\frac{a_h^2 r^2}{2} \left[ \int_k \frac{\frac{B_k}{B_0} - \frac{|G_k|}{B_0}}{2\frac{B_k}{B_0} - 1 - \frac{|G_k|}{B_0} + \frac{k_z^2}{2a_h}} + \int_k \frac{\frac{B_k}{B_0} + \frac{|G_k|}{B_0}}{2\frac{B_k}{B_0} - 1 - \frac{|G_k|}{B_0} + \frac{k_z^2}{2a_h}} \right]
\end{aligned} \tag{4.32}$$

Performing the  $k_z$  integration we arrive at the formula Eq.(4.33) in which the numerator was expressed via dispersion relations. The disorder correction of free energy is negative:

$$F_{dis} = -\frac{a_h^{5/2} n}{B_0 8\sqrt{2}\pi^2} \int_{BZ} d^2 k \left( \frac{B_k - |G_k|}{\sqrt{\epsilon_k^A}} + \frac{B_k + |G_k|}{\sqrt{\epsilon_k^O}} \right), \tag{4.33}$$

with

$$B_k \equiv \langle |\phi_0|^2 \phi_k \phi_k^* \rangle = \beta_k + 4\eta\beta_k^4 + \mathcal{O}(\eta^2), \tag{4.34}$$

$$G_k \equiv \langle (\phi_0^*)^2 \phi_{-k} \phi_k \rangle = \gamma_k + 4\eta\gamma_k^4 + \mathcal{O}(\eta^2) \tag{4.35}$$

The phonon spectrum dispersion functions  $\epsilon_k^A$  and  $\epsilon_k^O$  are:

$$\epsilon_k^A = 2\frac{B_k}{B_0} - 1 - \frac{|G_k|}{B_0}, \tag{4.36}$$

$$\epsilon_k^O = 2\frac{B_k}{B_0} - 1 + \frac{|G_k|}{B_0} \tag{4.37}$$

The energy of the acoustic branch vanishes at  $\mathbf{k} = 0$  since they are the Goldstone bosons associated with disappearance of the continuous translation symmetry at the homogeneous – vortex lattice transition. Note that expanding in  $\eta$  preserves the property  $\epsilon_{\mathbf{k}=0}^A = 0$ .

The location of the SPT line is now obtained by minimization of the corrected free energy Eq.(4.33). The results for several values of the disorder strength are given in Fig.5. Square-to-rhomb transition line for different dimensionless disorder strength  $n$  defined by  $R = n\xi_{ab}^2\xi_c$ . One observes again that the slope is positive.

## 4.5 Spectrum of rhombic lattice in a clean system

To go beyond the mean-field approach, we include the fluctuation of  $\psi$  close its minimum  $\Psi$ . In this section we will use study the thermal fluctuations influence on the structural phase transition of clean system and disordered system. Before going to variational approach, we will first study the *One-loop perturbation*. We expected that the low temperature limit variational perturbation approach should consistent with perturbation approach.

The effective probability for each possible state  $\psi$  is base on the usual Boltzmann probability distribution  $P[\psi] = \frac{1}{Z} \exp(-\beta F[\psi])$ . To find an excitation spectrum in harmonic approximation, one expands free energy functional around the Abrikosov solution. In isotropic clean system, it has been done by [71][67] in LLL approximation. Recently a low temperature perturbation theory around Abrikosov solution was developed and shown to be consistent up to the two loop order in both 3D and 2D [112][82]. If the thermal fluctuations were absent, the Abrikosov solution has the form  $\Psi(x) \equiv v_0 \varphi_{\mathbf{k}=\mathbf{0}}(\mathbf{x})$ . The normalization factor  $v_0$  is determined by minimizing the mean field free energy  $f = a_T v^2 + \frac{1}{2} \beta_A v^4$  where  $\beta_A = 1.16$ . This results in  $v_0^2 = -\frac{a_T}{\beta_A}$ . Since all interest physics are base on the variation from the minimum, namely it mean field solution 4.16, we separate the trial wavefunction to two parts: the main field solution part  $\Psi(x)$  and function  $\chi(x)$  describes the deviation due to thermal fluctuations at every point  $x$ . Parameter

$v$  can be found by minimize the free energy.

$$\psi(x) = v\varphi(\mathbf{x}) + \chi(x). \quad (4.38)$$

First we diagonalize the quadratic term of free energy of Eq. (4.1) to obtain the harmonic excitation spectrum. Instead of a complex field  $\chi_k$ , two “real” fields  $O$  and  $A$  (indicating as “optical” and “acoustic” phonon modes respectively) is used. The “real” in the sense that it preserves the degree of freedom of a complex field  $\chi_k$ . An additional constrain between two complex fields  $O$  and  $A$  is included as  $O_{\mathbf{k}}^* = O_{-\mathbf{k}}$  and  $A_{\mathbf{k}}^* = A_{-\mathbf{k}}$ . ( For example, one can think of it as  $O_{\mathbf{k}} \equiv (\chi_{\mathbf{k}} + \chi_{-\mathbf{k}}^*)/2$  and  $A_{\mathbf{k}} \equiv (\chi_{\mathbf{k}} - \chi_{-\mathbf{k}}^*)/2$ .) We choice a complete basis  $\phi_{\mathbf{k}}(x)$ , the modified LLL basis 4.12, to expend the deviation  $\chi(x)$ :

$$\chi(x) = \sum_{\mathbf{k}=B.Z.} \gamma_{\mathbf{k}} \phi_{\mathbf{k}}(x) (O_{\mathbf{k}} + iA_{\mathbf{k}}) \quad (4.39)$$

$$\chi^*(x) = \sum_{\mathbf{k}=B.Z.} \gamma_{\mathbf{k}}^* \phi_{\mathbf{k}}^*(x) (O_{-\mathbf{k}}^a - iA_{-\mathbf{k}}^a), \quad (4.40)$$

Moreover, the coefficient  $\gamma_{\mathbf{k}}$  is defined as  $\gamma_{\mathbf{k}}^2 \equiv \frac{1}{2} \frac{G_{\mathbf{k}}^*}{|G_{\mathbf{k}}|}$  to diagonalize the quadratic part of the  $F_{GL}$ . In clean isotropic system,  $\eta = 0$  and  $r = 0$ , the eigenvalues first found by Eilenberger in [71] are  $\epsilon_A^{3D}(k) = \epsilon_A(k) + k_z^2/2$  correspond to the acoustic phonon mode and  $\epsilon_O^{3D}(k) = \epsilon_O(k) + k_z^2/2$  correspond to the optical phonon mode, where

$$\epsilon_A(k) = -a_T \left( 2 \frac{\beta_k}{\beta_0} - 1 - \frac{|\zeta_k|}{\beta_0} \right), \quad (4.41)$$

$$\epsilon_O(k) = -a_T \left( 2 \frac{\beta_k}{\beta_0} - 1 + \frac{|\zeta_k|}{\beta_0} \right). \quad (4.42)$$

The function  $\beta_k \equiv \langle \varphi_0^* \varphi_0 \varphi_k^* \varphi_k \rangle$  and  $\zeta_k \equiv \langle \varphi_0^* \varphi_0^* \varphi_k \varphi_{-k} \rangle$ . Note that the energy of the acoustic branch vanishes at  $k = 0$ . The acoustic phonons are the Goldstone bosons associated with the disappearance of continuous (gauge) symmetry at the normal state – vortex lattice transition. When  $k \rightarrow 0$ ,

$$\epsilon_A(k) \approx -0.12a_T |k|^4. \quad (4.43)$$



The optical mode  $\epsilon_O(k)$  has a finite gap. However the Goldstone mode is much softer, namely at small momentum they behave like powers of  $k$ ,  $|k|^4$  instead of  $|k|^2$ . This exceptional "softness" apparently should lead to an instability of the vortex lattice against thermal fluctuations. Indeed naive calculation of the correlator in perturbation theory shows that certain quantities including superfluid density are infrared (IR) divergent. This was even considered an indication that the vortex lattice does not exist. One could argue that real physics is dominated by the small mass  $1/\kappa^2$  of the shear mode, acting as a cutoff that prevents IR divergencies, but basic physical properties related to thermal fluctuations near  $H_{c2}(T)$  seemed to be independent of the cutoff, especially for high  $T_c$  superconductors. In the IR divergencies were reconsidered and it was found that they all cancel exactly at each order in physical quantities like free energy, magnetization etc. This means apparently that for the infinite infrared cutoff fluctuations destroy the inhomogeneous ground state, namely the state with lowest energy is a homogeneous liquid.

To produce result for the anisotropy, one can replace the  $\beta$  and  $\zeta$  function with  $B_k$  4.34 and  $G_k$  4.35 respectively. In the presence of anisotropy,  $\epsilon_A(k=0) = 0$  is preserved. The spectrum is positive for triangular lattice in isotropic system and a rhombic lattice in anisotropic system.

While including the fluctuations of lattice motion around its static solution, the essential requirement is the rhombic lattice solution is stable, namely its spectral function  $\epsilon_A(k)$  is positive. It is our criterion that for the existence of solid solution. The finite part for the Gibbs free energy to one loop (finite parts of the integrals were calculated numerically). Up to two loops the calculation (extending the one carried in ref.[112] to umklapp processes) gives:

$$f(\theta) = -\frac{a_T^2}{2B_0} + \int d^2k \left( \sqrt{\epsilon_k^A} + \sqrt{\epsilon_k^O} \right). \quad (4.44)$$

The integration is angle dependent and is proportion to  $\sqrt{a_T}$ . For  $\theta = 60^\circ$ ,

$$f(60^\circ) = -\frac{a_T^2}{2B_0} + 2.848\sqrt{a_T}. \quad (4.45)$$

## 4.6 Hartree-Fock-like approximation and Replica trick in disordered system

In disorder system, the functional  $F[\psi, W]$  has a random potential  $W$  which increase the complicity of disorder system. Since it is not trivial how to calculate the ensemble average  $\overline{\ln Z}$  over all possible state. The replica method is a useful tool to do the ensemble average. The manipulation are greatly facilitated by a mathematical identity

$$\ln Z = \lim_{m \rightarrow 0} \frac{1}{m} (Z^m - 1) \quad (4.46)$$

One prepares  $m$  replicas of the original system, evaluates the ensemble average of the product of their partition functions  $Z^m$ , and then take the limit  $m \rightarrow 0$ . A problem in actual replica calculation is that one often evaluate  $\overline{Z^m}$  with positive integer  $m$  in mind and then extrapolates the result to  $m \rightarrow 0$ . The discussion of the significance of the replica calculations can be fine in [78]. Applying it to the disorder average of the statistical sum one obtains:

$$\overline{Z^m} = \int_{\psi} \exp \left[ \frac{1}{2} \left( \frac{ra_h}{T} \right)^2 \int_x \sum_{i,j} |\psi^i|^2 |\psi^j|^2 - \frac{1}{T} \sum_i F_{GL} [\psi^i] \right] \quad (4.47)$$

where  $\psi^i$  are the  $i$  th replica and it will interact with different filed  $\psi^j$ .

We consider the case on the ground state. After the “LLL scaling”, one parameter

$$a_T \equiv (bt\omega/\omega_0)^{-2/3} \left( \frac{1-t-b}{2} \right) \quad (4.48)$$

is left ( $\omega_0 = 4\pi\sqrt{2}$ ). One get

$$\overline{Z^m} = \int_{\psi_1, \dots, \psi_n} \exp \left\{ \frac{1}{\omega_0} \left[ \frac{R}{2} \int_x \sum_{i=1}^n \sum_{j=1}^n |\psi^i|^2 |\psi^j|^2 \right. \right. \quad (4.49)$$

$$\left. \left. - \int_x \sum_{i=1}^n \left( \frac{1}{2} |\partial_z \psi^i|^2 - a_T |\psi^i|^2 + \frac{1}{2} |\psi^i|^4 \right) \right] \right\} \quad (4.50)$$

where  $R = \frac{(ra_T)^2}{T_{re}}$ .

To go beyond perturbation, one can calculate the partition function via Hartree-Fock approximation. In solid phase, it is more complicate to optimize the quadratic

part since our system doesn't have translation symmetry. Moreover, with disorder we take into account the interaction between two replica system. Here we assume that two phonon modes will not couple together. Instead of a single variational parameter in liquid phase, there are four variational functions. We introduce variational matrix  $G^{-1}$  and expand

$$\overline{Z^m} \approx \int_{O,A} (1 - \eta (G_0^{-1} - G^{-1}) \eta^T - \text{quartic}) \exp [-\eta G^{-1} \eta^T]. \quad (4.51)$$

For each  $\eta_k = (O_k^1 \dots O_k^m, A_k^1 \dots A_k^m)$  in  $\eta$  and  $G_0^{-1} = \frac{\alpha_T}{4\pi\sqrt{2}} \delta_{ij} \delta_{k_1, k_2}$ . The variational matrix  $(G_k^{-1})_{2m \times 2m}$  is defined as

$$G_{k,OO,i=j}^{-1} = \frac{1}{4\pi\sqrt{2}} \left( \epsilon_O(k) + \frac{k_z^2}{2} \right) \quad (4.52)$$

$$G_{k,AA,i=j}^{-1} = \frac{1}{4\pi\sqrt{2}} \left( \epsilon_A(k) + \frac{k_z^2}{2} \right) \quad (4.53)$$

the coupling between replica fields are

$$G_{k,OO,i \neq j}^{-1} = \frac{1}{4\pi\sqrt{2}} h_O(k), \quad (4.54)$$

$$G_{k,AA,i \neq j}^{-1} = \frac{1}{4\pi\sqrt{2}} h_A(k). \quad (4.55)$$

Since optical mode has a finite gap, thus we assume the coupling between two phonon mode is negligible in a replica field and therefore it is reasonable to assume that the coupling between two phonon mode of two different field is zero. We have

$$G_{k,OA}^{-1} = 0, G_{k,AO}^{-1} = 0. \quad (4.56)$$

For simplify the notation, the inverse matrix element of  $G_k^{-1}$  are defined:

$$p_O(k) = \frac{1}{\sqrt{\epsilon_O(k) - h_O(k)}} - \frac{h_O(k)}{2(\epsilon_O(k) - h_O(k))^{3/2}}, \quad (4.57)$$

$$q_O(k) = \frac{-h_O(k)}{2(\epsilon_O(k) - h_O(k))^{3/2}}. \quad (4.58)$$

To calculate the average over disorder free energy we recalled the mathematical identity,

$$f \equiv -4\pi\sqrt{2} \ln Z = -4\pi\sqrt{2} \lim_{m \rightarrow 0} \frac{\overline{Z^m} - 1}{m}. \quad (4.59)$$

After carry out the integration over  $k_z$  and drop the constant term in the free energy, we get the free energy density with variational functions  $\epsilon_A, \epsilon_o, h_O, h_A$  and  $v$ , and the external parameter  $a_T$  which is  $b$  and  $t$  dependent, and the effective anisotropy  $\eta$  which dependent on  $b$ , and  $n$  is disorder density per unit cell:

$$f(a_T, \eta, n; \theta, v, \epsilon_A, \epsilon_o, h_O, h_A) = f_0 + f_{tr \log} + f_2 + f_4 \quad (4.60)$$

where the “mean field” part is

$$f_0 = a_T v^2 + \frac{1}{2} v^4 B_0, \quad (4.61)$$

the trlog term is

$$f_{tr \log} = - \left\langle \sqrt{\epsilon_O(k) - h_O(k)} + \sqrt{\epsilon_A(k) - h_A(k)} \right\rangle_k \quad (4.62)$$

$$- \left\langle \frac{h_O(k)}{2\sqrt{\epsilon_O(k) - h_O(k)}} + \frac{h_A(k)}{2\sqrt{\epsilon_A(k) - h_A(k)}} \right\rangle_k, \quad (4.63)$$

the quadratic part is

$$\begin{aligned} f_2 = & a_T \langle p_O(k) + p_A(k) \rangle_k \\ & + v^2 (2 - R) \langle B_k (p_O(k) + p_A(k)) \rangle_k \\ & + v^2 (1 - R) \langle |G_k| (p_O(k) - p_A(k)) \rangle_k \\ & + v^2 R \langle B_k (q_O(k) + q_A(k)) \rangle_k + v^2 R \langle |G_k| (q_O(k) - q_A(k)) \rangle_k \end{aligned}$$

the interaction part is

$$f_4 = \frac{1}{2} \langle g_1 - R g_2 \rangle_{k,l}$$

where the “clean” part is

$$g_1 = 2B_{k-l} (p_O(k) + p_A(k)) (p_O(l) + p_A(l)) + \frac{|G_k| |G_l|}{B_0} (p_O(k) - p_A(k)) (p_O(l) - p_A(l))$$

and the “disorder” part is

$$\begin{aligned} g_2 = & B_{k-l} (p_O(k) + p_A(k)) (p_O(l) + p_A(l)) - B_{k-l} (q_O(k) + q_A(k)) (q_O(l) + q_A(l)) \\ & + \frac{|G_k| |G_l|}{B_0} (p_O(k) - p_A(k)) (p_O(l) - p_A(l)) - \frac{|G_k| |G_l|}{B_0} (q_O(k) - q_A(k)) (q_O(l) - q_A(l)). \end{aligned}$$

Note the intergration  $B_k = B_k(\theta, \eta)$  and  $G_k = B_k(\theta, \eta)$  are function of angle. We numerically minimize the free energy  $f$  with respect to  $\theta$  and those variational functions to obtained the SPT line.

Optimizing 4.60 has been solved numerically with the help of what we called mode expansion. For  $n = 0$  case, thermal fluctuations influence in pure sample, the amoeba method is used to minimize the free energy  $f$  with respect to variational parameter  $v$  and variational functions  $\epsilon_A, \epsilon_O, h_O, h_A$ . For the case  $n \neq 0$ , both disorder and thermal fluctuation are taken into account, iteration method is used to solve the set of equation obtained from functional derivatives  $df(a_T, \eta; \theta) / d\Omega = 0$ ,  $\Omega \in \{v, \epsilon_A, \epsilon_O, h_O, h_A\}$ . An important external parameter  $a_T$  depends on  $b$  and  $t$ . The effective anisotropy,  $\eta$ , is proportional to  $b$ ; and effective disorder strength,  $R$ , is  $b$  and  $t$  dependent. ( Material parameters  $G_i$  characterize the thermal fluctuation strength and  $\tilde{\eta}$  present anisotropy and  $n$  is disorder density. ) In both case, to locate the structural phase transition line, we need to locate the boundary between square and rhombic lattice phase.

To understand how to simplified the functional problem to algebra problem by mode expansion, one can observe the gap equations. Minimize with respect to variational functions we got a set of equations, so called gap equations:

$$v^2 = -\frac{a_T}{B_0} - (2 - R) \frac{1}{B_0} \langle B_k (p_O(k) + p_A(k)) \rangle_k - R \frac{1}{B_0} \langle B_k (q_O(k) + q_A(k)) \rangle_k - R \frac{1}{B_0} \langle G_k (q_O(k) - q_A(k)) \rangle_k - (1 - R) \langle G_k (p_O(k) - p_A(k)) \rangle_k \quad (4.64)$$

and

$$\epsilon_{A/O}(k) = E(k) \mp G_k \Delta, \quad (4.65)$$

$$h_{A/O}(k) = H(k) \mp G_k \delta, \quad (4.66)$$

where

$$E(k) = a_T + v^2 (2 - R) B_k + (2 - R) \langle B_{k-l} (p_O(l) - p_A(l)) \rangle_l \quad (4.67)$$

$$H(k) = -R (v^2 B_k + \langle B_{k-l} (q_O(l) + q_A(l)) \rangle_l) \quad (4.68)$$

and

$$\Delta = (1 - R) \left( v^2 + \left\langle \frac{G_l}{B_0} (p_O(l) - p_A(l)) \right\rangle_l \right) \quad (4.69)$$

$$\delta = -R \left( v^2 + \frac{1}{B_0} \langle G_l (q_O(l) - q_A(l)) \rangle_l \right). \quad (4.70)$$

To effectively solve the gap equations, we simplified it to algebra equations in the following way. By observing the equations, we found that  $E(k)$  has the same periodicity as  $B_k$ . Two major contributions of  $B_k$ ,  $\beta_k$  and  $\beta_{4,k}$ , has the same periodicity in  $k$  space. In general, we can expand  $\beta_{N,k} \equiv \langle |\varphi_0|^2 \varphi_k \varphi_{N,k}^* \rangle$  of arbitrary landau level  $N$  in  $\exp[i\mathbf{k} \bullet \mathbf{X}_n] \equiv \tilde{\beta}_n(k)$ , namely

$$\beta_{N,k} = \sum_n \varkappa_n^N \tilde{\beta}_n(k). \quad (4.71)$$

The integer set  $n \equiv (n_1, n_2) \in Z^2$  determines the distance of a points on lattice from the origin,  $\mathbf{X}_n = n_1 d_1 + n_2 d_2$ .  $k$  can be present with reciprocal lattice constants  $\tilde{\mathbf{d}}_1 = (\sqrt{4\pi/\tan\theta}, 0)$  and  $\tilde{\mathbf{d}}_2 = (-\sqrt{\pi/\tan\theta}, \sqrt{\pi \tan\theta})$ ,  $k = k_1 \tilde{d}_1 + k_2 \tilde{d}_2$  where  $k_i \in (0, 1)$ . The coefficient  $\varkappa_n^N$  is different for each Landau level  $N$ ,

$$\varkappa_n^N = \left( \frac{1}{\sqrt{2}} \right)^N \frac{1}{\sqrt{N!}} \sum_n (-iX^*)^N \exp\left[-\frac{|\mathbf{X}_n|^2}{2}\right]. \quad (4.72)$$

The first 6 mode are listed in the table of Fig.4.1. (We denote two dimension vector  $(x, y)$  by bold latter  $\mathbf{X}$ . Normal latter  $X$  denote  $x + iy$ .)

Expand the  $E(k)$  and  $H(k)$  in  $\tilde{\beta}_n(k)$ , where  $\chi_n = \varkappa_n^0 + \eta \varkappa_n^4$ , one get

$$E(k) = E_0 + E_1 \chi_1 \tilde{\beta}_1(k) + \dots E_n \chi_n \tilde{\beta}_n(k) \dots + \quad (4.73)$$

$$H(k) = H_0 + H_1 \chi_1 \tilde{\beta}_1(k) + \dots H_n \chi_n \tilde{\beta}_n(k) \dots + \quad (4.74)$$

where

$$E_n = a_T \delta_{n0} + (2 - R) v^2 + \frac{(2 - R)}{C_n} \langle (p_A(l) + p_O(l)) \beta_n(l) \rangle \quad (4.75)$$

$$H_n = -R v^2 + \frac{R}{C_n} \langle (p_A(l) + p_O(l)) \beta_n(l) \rangle \quad (4.76)$$

$n$	lattice site $n = (n_1, n_2)$	modes $\tilde{\beta}_n = \exp[-ik \cdot \mathbf{X}]$	$ \mathbf{X} ^2$
0	(0, 0)	1	0
1	(1, 0), (-1, 0), (1, -1), (-1, 1)	$\cos 2\pi k_1, \cos 2\pi(k_1 - k_2)$ .	$2\pi\sigma + \frac{\pi}{2\sigma}$
2	(0, 1), (0, -1)	$\cos 2\pi k_2$	$\frac{2\pi}{\sigma}$
3	(2, -1), (-2, 1)	$\cos 2\pi(2k_1 - k_2)$	$8\pi\sigma$
4	(-2, 2), (2, -2), (2, 0), (-2, 0)	$\cos 2\pi(2k_1 - 2k_2), \cos 4\pi k_1$	$\frac{2\pi}{\sigma} + 8\pi\sigma$
5	(1, 1), (-1, -1), (1, -2), (-1, 2)	$\cos 2\pi(k_1 + k_2), \cos 2\pi(k_1 - 2k_2)$	$\frac{9\pi}{2\sigma} + 2\pi\sigma$

Figure 4.1: For triangle lattice, 2 modes is sufficient:  $\beta_0^1(\theta = 60^\circ) = 1 + 0.0265 \times 6 + 12 \times 10^{-19} = 1.159$ ; for square lattice, 5 modes gives  $\beta_0^1(\theta = 45^\circ) = 0 - 4 \times 0.348239 + 2 \times 0.0601951 + 2 \times 0.0601951 - 4 \times 0.000449644 + 4 \times 8.5010 \times 10^{-6} = -1.1539$ . The coefficients decrease exponentially with  $n$ .

where  $C_n$  is the number of points with same  $|\mathbf{X}|^2$ . One way to do the functional minimization of the free energy for a given angle is to simplified it to algebra equations, namely to solve interactively (4.75) and (4.64) with (4.73), (4.69), (4.70), (4.65), (4.66), (4.57) and (4.58). Another way we used to seek for minimum is so called Amoeba method.

## 4.7 Results

For clean sample, in the mean field approach, for a given effective anisotropy  $\eta$ , the system will prefer a rhombic lattice with apex angle  $\theta$ . The numerical results of transition condition (4.22) are presented in Figs.4.2. We found that for a given  $\eta_m$ , the magnetic field enhance the anisotropy strength  $\eta$ , the apex angle  $\theta$  deviates from  $60^\circ$  and decrease to  $45^\circ$  continuously and situate till the magnetic field destroy the superconductivity. The system undergo a second order phase transition.

The free energy with disorder correction 4.33 is plotted in Fig. 4.3. The system undergo a *1st order phase transition*, square lattice is not stable while dimensionless temperature  $t$  increasing. When effective anisotropy is stronger, it suppresses the barrier between two angle, the phase transition became continuous. The phenomenon happens

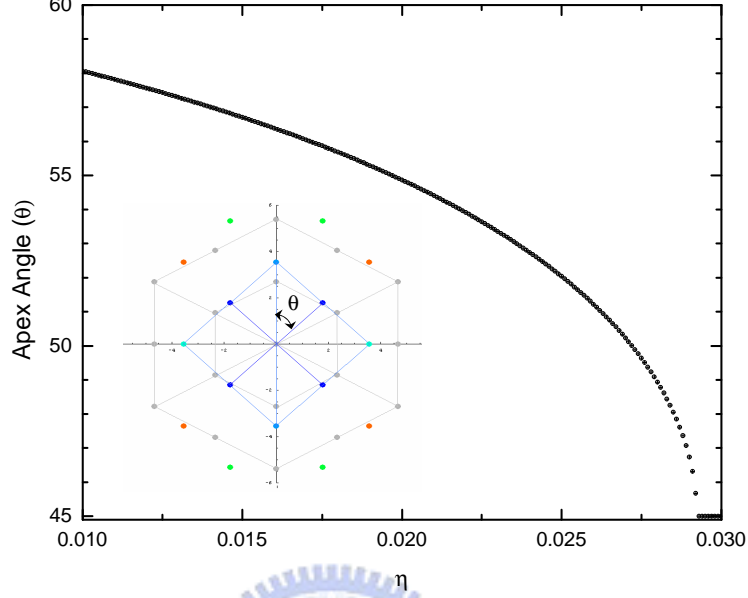


Figure 4.2: Evaluation of rhombic lattice in magnetic field. In mean field approach, the square to rhomb phase transition occurs at  $\eta = \tilde{\eta}b = 0.02932$ . After the critical field, the vortex exhibits perfect square vortex lattice till the upper critical field.

at the vicinity of the S-N phase transition line, one notices that the square lattice is not stable while temperature increases. The SPT transition happens at  $\partial_{\theta}^2 F(\theta)|_{45^\circ} = 0$ , where  $F$  are the free energy of clean sample plus disorder correction,  $F = F_{clean} + F_{dis}$ . Thus, it is convenient to collect all the coefficients to  $p(t, b) = \frac{n\gamma}{4\pi} b \sqrt{1-t-b}$ , such that  $(\partial_{\theta}^2 F'_{clean} + p(b, t) \partial_{\theta}^2 F'_{dis})_{45^\circ} = 0$ . The notation  $F'_{clean} = \frac{1}{B_0}$  and  $F'_{clean}$  is the integration in  $F$ . One finds that  $\partial_{\theta}^2 F'_{dis}$  has a different sign as  $\partial_{\theta}^2 F'_{clean}$ . The structural phase transition lines with various disorder  $n$  are plotted in Fig. 4.4. Unlike the case in a clean sample where the SPT line is  $t$  independent, at low temperature, disorder enhances the anisotropic effect. Near the S-N transition line where the microscopic fluctuations coupled with disorder smear out the effect of anisotropy, the system restores the rhombic lattice from square lattice. Indeed, when near the S-N phase transition, the higher order correction in the free energy functional, the  $D_4$  symmetric correction, is less important than its isotropic part. However, due to the applicability of the perturbation approach, the



theoretical line failed when in strong disorder.

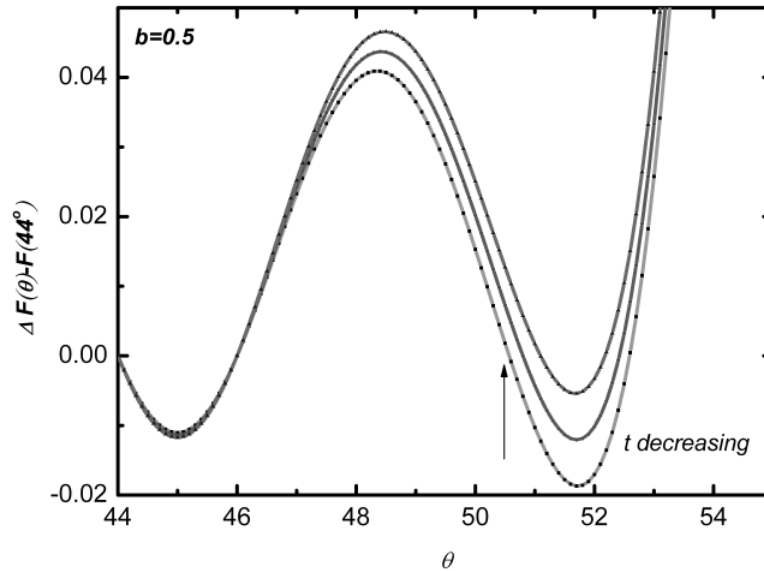


Figure 4.3: Energy difference between  $\theta = 44$  and other angle. The material parameter for anisotropy  $\tilde{\eta} = 0.5$ , disorder strength  $n = 0.8$ . Magnetic field is fixed at  $b = .5$ , system undergoes 1<sup>st</sup> phase transition while decreasing temperature: the preference angle jumps from rhombic ( $\theta \sim 52^\circ$ ) to perfect square ( $\theta = 45^\circ$ ).

Now we turn to the thermal fluctuations influences on structural phase transition in a clean system. In fig. 4.6 we show both perturbation (one loop) result and Gaussian variational approach. The latter approach is minimizing the free energy  $f(\theta, n = 0, \tilde{\eta})$  with respect to variational functional which we use the mode expansion to simplify the functional equation to algebra equations. It is interesting that at low temperature two methods show the same tendency, however, while temperature increases, two SPT lines depart from each other and result in totally different curvature. In both methods, they don't cross the melting line before the acoustic spectrum becomes negative. In spite of the different curvature, both of them show that for strong  $Gi$  the influence area increases. It is known that at the vicinity of critical the perturbation method is not valid. Moreover, for strong anisotropy case, the system undergoes SPT at low field and

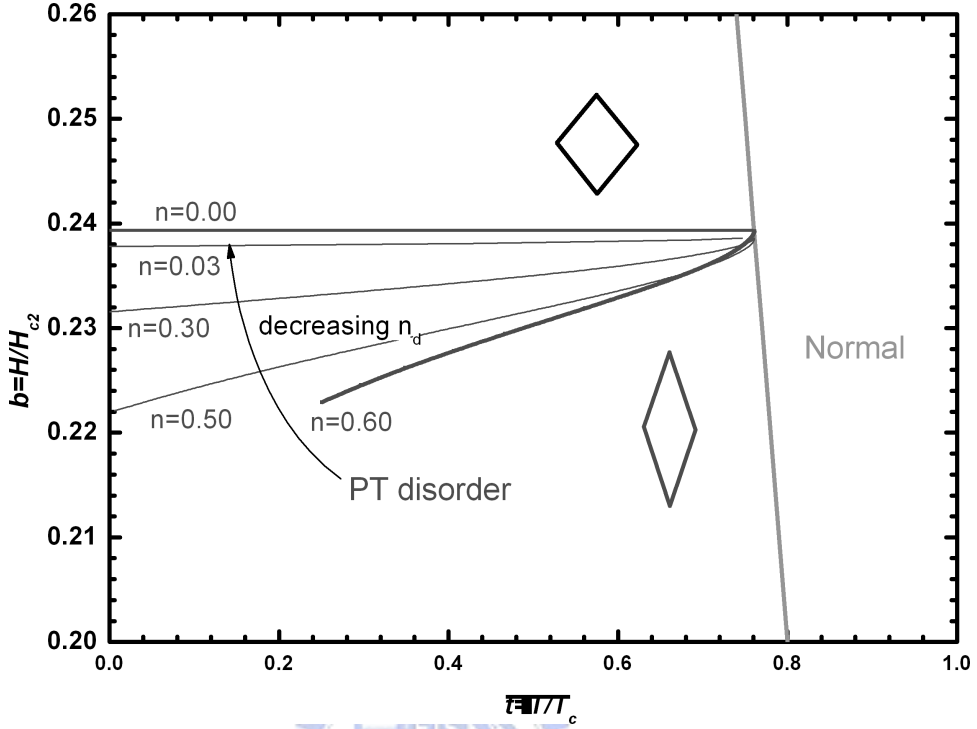


Figure 4.4: The phase diagram of structural phase transition. The vortex lattice structure of the system with  $b, t$  at the upper plane of the diagram are square lattice, while at the lower plane are rhombic lattice. The material anisotropy  $\tilde{\eta} = 0.5$ . System with stronger disorder depart further from the SPT line for clean sample ( $n = 0$ ).

the thermal fluctuation influence is suppressed.

When disorder influence are considered via ensemble average over all possible state, we expected that the variational method will be able to give better result than perturbation.

## 4.8 Discussion

We analyze the rhombic to square vortex lattice phase transition in anisotropic superconductors using a variant of Ginzburg-Landau theory. The mean-field phase diagram is determined to first order in the anisotropy parameter, and shows a reorientation transition of the square vortex lattice with respect to the crystal lattices. introduce both

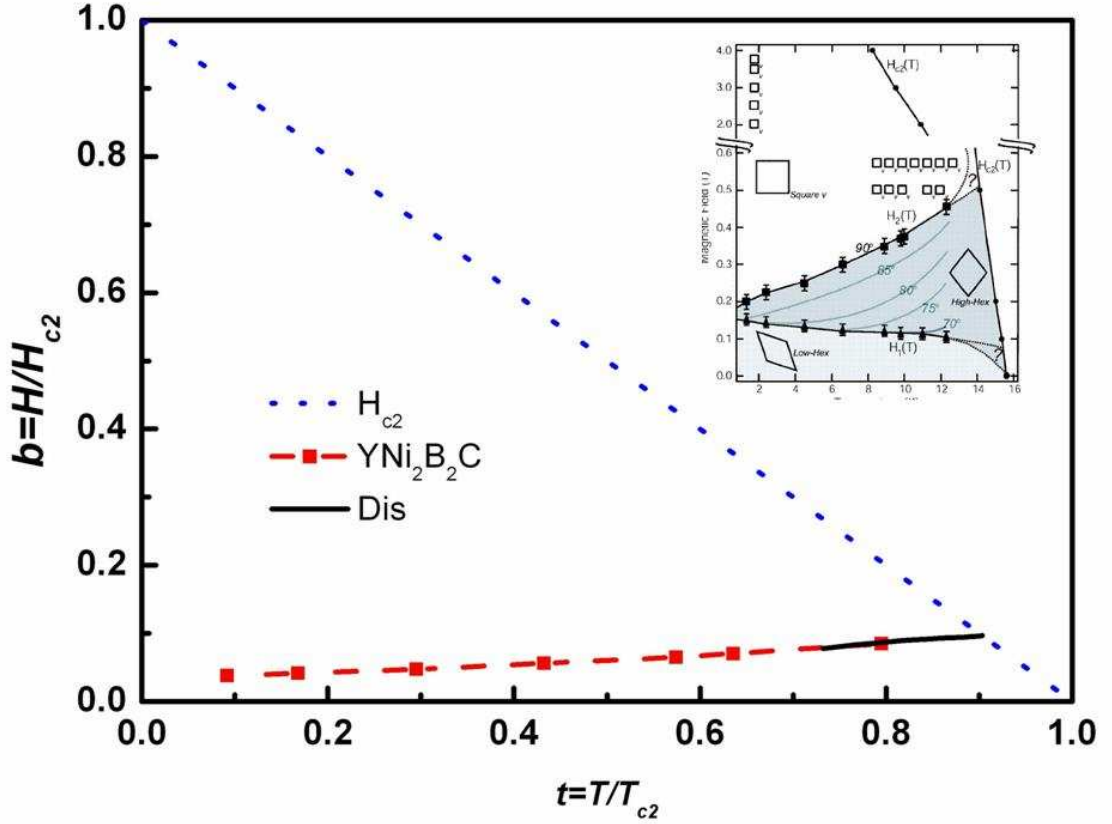


Figure 4.5: Comparison with experiment Dewhust's experiment. The fitting parameter  $n = 3.7$  and  $\tilde{\eta} = .5$ .

thermal fluctuation effect and disorder effect by both perturbation and variational approach to show that thermal fluctuations and disorder produce a reentrant rhombic to square lattice transition line at the vicinity of S-N phase transition line, similar to recent studies which used a nonlocal London model. Moreover, we show that for material with small  $Gi$  the reentrant rhombic is due to the quench disorder.

An in-plane anisotropic superconductor has a potential to have vortex lattice configuration other than hexagonal lattice. The coupling strength between vortex lattice and the underlying material properties depend not only on the material anisotropy coefficient  $\eta_m$  but also strongly depends on the external magnetic field. For a given anisotropy material with 4-fold symmetry, the field induced structural distortion will eventually reach a square lattice at high field ( $H > H_2$ ). It should be noted that at low temperature,

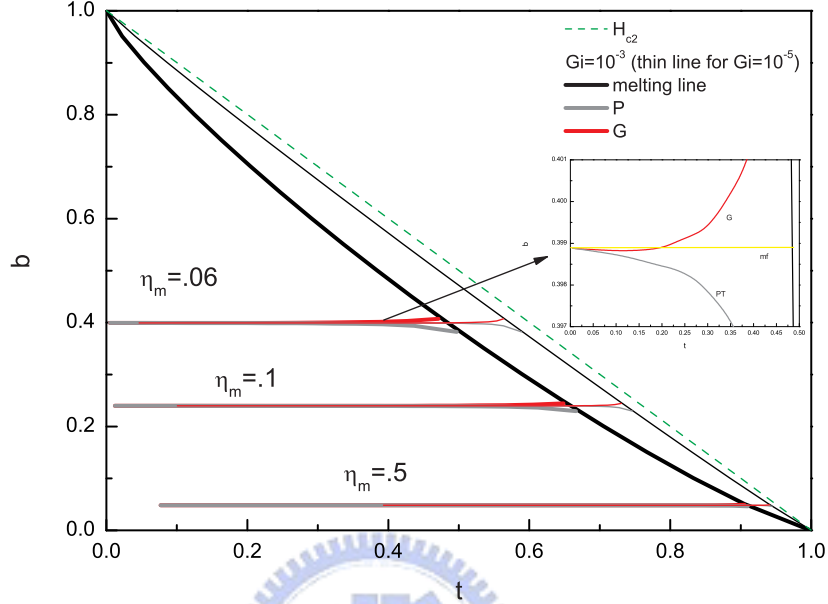


Figure 4.6: Structural Phase Transition with thermal fluctuations influence at  $\tilde{\eta} = .1$ . Result of both one loop perturbation result ( $P$ ) and variational gaussian ( $G$ ) are shown. The insert shows material with different  $Gi$ .

the structural phase transition is hardly depend on temperature. In the presence of disorder which is introduced as a random pinning potential  $a_h W(x) |\psi(x)|^2$ , the system has irregularity of minority vortices. We average all possible configuration of disorder, namely we take into account all possible system with different disorder distribution in space,  $W(x)$ , and make ensemble average. The result shows the temperature dependency appear on the SPT line. The physical interpretation is that the disorder coupled with microscopic thermal fluctuations in the quadratic term smears out the field induced anisotropy. Hence, the vortices rearranged themselves according to the effective coupling with underlying crystal which now has temperature dependency. This model works successfully explain the SPT characteristic line for low temperature superconductors (with small  $Gi$ ).

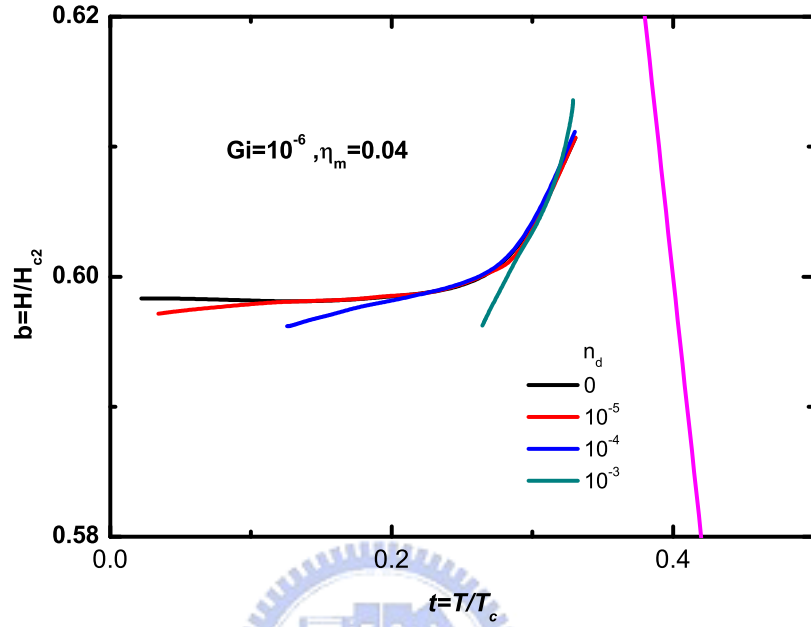


Figure 4.7:

Considering the thermal motion of vortices, at low temperature, the system appears to follow the symmetry of Hamiltonian, therefore, at the vicinity of SPT line, rhombic lattice could become square lattice due to the thermal fluctuation. And indeed, with larger  $Gi$  which characterize the thermal fluctuations strength of a material, the influence area on the phase diagram is larger. However, at high temperature when it approach the melting line, the dramatic vibration of vortex smear the anisotropic effect from the symmetry of underlying structure, the repulsion force became less anisotropic and restore the rhombic lattice structure and the apex angle increase as temperature increase. The anomaly in the dynamic magnetic susceptibility and paramagnetic [20] on borocarbides crystals is associated with a structural transition in the vortex lattice and satisfied with this picture. Theoretical results proposed by Dorsey *et al* [24], Kogan *et al* [20] proposed that the appear of rhombus at the vicinity of  $H_{c2}$  line is due to the thermal fluctuation smear out the anisotropic effect of underlying vortex. For borocarbides the  $Gi \sim 10^{-5}$ , it

is questionable if the thermal fluctuations plays the major role.



# Chapter 5

## Summary

Mesoscopic vortex motions influence the thermodynamic properties of superconducting state dramatically. Reduced symmetries of the underlying material lead non-trivial and complicate phenomena. Thermodynamic phase diagram of vortex matter includes: liquid state, solid state, glass state and other subregion. The complexity mainly depends on the intrinsic material properties ( $G_i$ ,  $H_{c2}$ ,  $T_c$  and  $\kappa$ ) and the density of disorder of a system. In a GL model, various approaches are proposed to understand the physics. In a liquid state, one can start from a solvable “noninteracting” field theory at very high temperatures and develop a theory of liquid by resummation of Feynman diagram and other resummation technique [90] [118] [63]. In solid state, one can study the “harmonic” solid at low temperatures and trace its destruction by fluctuations [48][113][112]. These two approaches are consequently the one phase theories. Direct numerical simulation can provides a valuable information on both the liquid and the solid side of the transition line.

In this work, by considering the thermal fluctuations and quenched disorder, we show non-trivial consequence of anisotropic effects on vortex matters. The anisotropic effect of layered superconductor ruins the high field scaling behavior in liquid phase because the effective dimensionality of the layered superconductor have crossover between 2D to 3D which can be influenced by the external field. For strongly 2D system, the thermal fluctuations excitation can go beyond lowest Landau level. We show that the higher

Landau level contribution around  $T_c$  is important, it is responsible for the failure of the LLL scaling.

The microscopic theory for a system with 4-fold in-plane anisotropy is not yet established, and nor does the direct link from non-Local Landon model to 4-fold symmetric Ginzburg-Lanau model. From the phenomenological GL we adopted here, at certain point in parameter space, a structural phase transition between rhombus and square can occur. The field dependent coupling between vortex lattice and atomic crystalline lattice will be enhanced by increasing magnetic field. At high field it will saturate with square lattice before  $H_{c2}(T)$ . In our theory we assume the coupling  $\eta_m$  between vortex lattice and atomic lattice is temperature independent, for a clean low- $T_c$  superconductor which mean field approach is valid, we show that the temperature dependence of SPT is not expected. The temperature dependency of SPT for small  $G_i$  material is not a result of mesoscopic thermal fluctuations, but due to the microscopic fluctuations from quench disorder.

Because of the ability to tune the interaction forces between individual vortex can be easily done by changing applied magnetic field and temperature of the system, I believe that the physics of structure phase transition can be study in vortex lattice while lack of the ability to control the interaction between atoms in materials. Such a system is very interesting, and due to possible realization of the system it may serve as an excellent experimental tool to examine well-developed theories with experiment.



# Bibliography

- [1] H. Kammerlingh Onnes, Leiden Comm. **120b**, **122b**, **124c**, (1911).
- [2] J. M. Casimir-Jonker and W. J. De Haas, Physica 2, 943 (1935).
- [3] V. L. Ginzburg and L. D. Landau, Zh. Eksp. Teor. Fiz. **20**, 1064 (1950).
- [4] A. A. Abrikosov, Sovjet Physics – JETP 5, 1174 (1957). [Sov. Phys. - JETP **5**, 1174 (1957)].
- [5] F. and H. London, Proc. Roy. Soc. (London) **A149**, 71 (1935).
- [6] F. London, *Superfluids, vol. I*, Wiley, New York, (1935).
- [7] W. Meissner and R. Ochsenfeld, Naturwissenschaften **21**, 787 (1933).
- [8] Bednorz, J. G. & Müller, K. A. Z. Phys. B 64, 189–193 (1986).
- [9] M. K. Wu *et al.* Phys. Rev. Lett. 58, 908–910 (1987).
- [10] A. B. Pippard, Proc. Roy. Soc. (London) **A216**, 547 (1953).
- [11] D. Cribier, B. Jacrot, L. M. Rao and B. Farnoux, Phys, Lett. 9, 106 (1964).
- [12] L. Neumann and L. Tewordt, Z. Phys. 191, 73 1966.
- [13] J. Schelten *et al.*, J. Low Temp. Phys. 14, 213 (1974); M. Laver, E. M. Forgan, S. P. Brown, D. Charalambous, D. Fort, C. Bowell, S. Ramos, R. J. Lycett, D. K. Christen, J. Kohlbrecher, C. D. Dewhurst, and R. Cubitt, Phys. Rev. Lett. 96, 167002 (2006).

- [14] (*Er*)M. R. Eskildsen, P. L. Gammel, B. P. Barber, U. Yaron, A. P. Ramirez, D. A. Huse, D. J. Bishop, C. Bolle, C. M. Lieber, S. Oxx, S. Sridhar, N. H. Andersen, K. Mortensen, and P. C. Canfield, Phys. Rev. Lett. 78, 1968 (1997); (*Y*)D. McK. Paul, C. V. Tomy, C. M. Aegerter, R. Cubitt, S. H. Lloyd, E. M. Forgan, S. L. Lee, and M. Yethiraj, Phys. Rev. Lett. **80**, 1517 (1998);M. Yethiraj, D. McK. Paul, C. V. Tomy, and J. R. Thompson, Phys. Rev. **B 58** R14767 (1998) C.D. Dewhurst, S.J. Levett and D.McK. Paul, Phys. Rev. **B 72**, 014542 (2002);(*Lu*)Y. De Wilde, M. Iavarone, U. Welp, V. Metlushko, A. E. Koshelev, I. Aranson, G. W. Crabtree, and P. C. Canfield, Phys. Rev. Lett. 78, 4273 (1997); L.Ya. Vinnikov, T. L. Barkov, P. C. Canfield, S. L. Bud'ko, and V. G. Kogan, Phys. Rev. **B64**, 024504 (2001); P. L. Gammel and D. J. Bishop, M. R. Eskildsen, K. Mortensen, and N. H. Andersens, I. R. Fisher, K. O. Cheon, P. C. Canfield, and V. G. Kogan, Phys. Rev. Lett. **82**, 4082 (2001); L. Ya. Vinnikov, T. L. Barkov, P. C. Canfield, S. L. Bud'ko, J. E. Ostenson, F. D. Laabs, and V. G. Kogan, Phys. Rev. **B 64** 220508 (2001); M R Eskildsen *et al*, Phys. Rev. Lett. 86, 5148 (2001);M. R. Eskildsen, A. B. Abrahamsen, V. G. Kogan, P. L. Gammel, K. Mortensen, N. H. Andersen, and P. C. Canfield, Phys. Rev. Lett., **86**, 5148 (2001);A. N. Price, R. I. Miller, R. F. Kiefl, J. A. Chakhalian, S. R. Dunsiger, G. D. Morris, J. E. Sonier, and P. C. Canfield Phys.Rev. **B 65** 214520 (2002).
- [15] M. Yethiraj, D. K. Christen, D. McK. Paul, P. Miranovic, and J. R. Thompson, Phys. Rev. Lett. 82 5112 (1999); C. E. Sosolik, Joseph A. Stroschio, M. D. Stiles, E. W. Hudson, S. R. Blankenship, A. P. Fein, and R. J. Celotta, Phys. Rev. **B 68**, 140503 (2003); M. Yethiraj, D. K. Christen, A. A. Gapud, D. McK. Paul, S. J. Crowe, C. D. Dewhurst, R. Cubitt, L. Porcar, and A. Gurevich, Phys. Rev. **B 72** 060504 (2005)
- [16] R. Gilardi, J. Mesot, A. Drew, U. Divakar, S. L. Lee, E. M. Forgan, O. Zaharko, K. Conder, V. K. Aswal, C. D. Dewhurst, R. Cubitt, N. Momono, and M. Oda, Phys. Rev. Lett. 88, 217003 (2002)

- [17] (*LSCO*)B. Rosenstein, B. Ya. Shapiro, I. Shapiro, Y. Bruckental, A. Shaulov, and Y. Yeshurun, Phys. Rev. **B 72**, 144512 (2005); (*Lu*)T. Park, A. Malinowski, M. F. Hundley, J. D. Thompson, Y. Sun, M. B. Salamon, E. Choi, H. Kim, S. Lee, P. C. Canfield, and V. G. Kogan Phys. Rev. **B 71** 054511 (2005);(*Y, Lu*)D. Jaiswal-Nagar, A. D. Thakur, S. Ramakrishnan, A. K. Grover, D. Pal, and H. Takeya, Phys. Rev. **B 74** 184514 (2006); R. Prozorov et al., Phys. Rev. B 76, 094520 (2007).
- [18] S. P. Brown, D. Charalambous, E. C. Jones, E. M. Forgan, P. G. Kealey, A. Erb, and J. Kohlbrecher, Phys. Rev. Lett. 92, 067004 (2004);B. Keimer *et al.*, Phys. Rev. Lett. 73, 3459 (1994)
- [19] R. Gilardi, J. Mesot, S. P. Brown, E. M. Forgan, A. Drew, S. L. Lee, R. Cubitt, C. D. Dewhurst, T. Uefuji, and K. Yamada, Phys. Rev. Lett. 93, 217001 (2004); Watanabe *et al.*, Phys. Rev. B 70, 020506 (2004); M. R. Eskildsen, C. D. Dewhurst, B. W. Hoogenboom, C. Petrovic, and P. C. Canfield, Phys. Rev. Lett. 90 187001 (2003)
- [20] V. G. Kogan, S. L. Bud'ko, I. R. Fisher, and P. C. Canfield, Phys. Rev. B 62 9077 (2000); Gurevich and Kogan, Phys. Rev. Lett. 87, 177009 (2001); P. Miranović and V. G. Kogan Phys. Rev. Lett. 87 137002 (2001); V. G. Kogan, M. Bullock, B. Harmon, P. Miranovic , Lj. Dobrosavljevic-Grujic, P. L. Gammel, D. J. Bishop, Phys. Rev. **B 55**, R8693 (1997).
- [21] B. Rosenstein, B. Ya. Shapiro, I. Shapiro, Y. Bruckental, A. Shaulov, and Y. Yeshurun, Phys. Rev. **B 72**, 144512 (2005).
- [22] I. Affleck, M. Franz, and M. H. Sharifzadeh Amin, Phys. Rev. B 55, R704 (1997);Masanori Ichioka, Akiko Hasegawa, and Kazushige Machida, Phys. Rev. **B 59** 8902 (1999);Nakai, Muranovic, Ichioka and Machida Phys. Rev. Lett. 89,237004(2002);
- [23] K. Park and D. A. Huse, Phys. Rev. **B 58** 9427 (1998).

- [24] A.D. Klironomos and A.T. Dorsey, Phys. Rev. Lett. **91**, 097002 (2003).
- [25] D. P. Li, P.-J. Lin, B. Rosenstein, B. Ya. Shapiro, and I. Shapiro, Phys. Rev. B **74**, 174518 (2006)
- [26] D. Chang, C.Y.Mou, B. Rosenstein, and C.L. Wu, Phys. Rev. Lett. **80**, 145 (1998); Phys. Rev. **B 57**, 7955 (1998).
- [27] K. Takanaka, Prog. Theo. Phys. **46** (1971); K. Takanaka, Prog. Theo. Phys. **5**, 365(1973); K. Fischer and H. Teichler, Phys. Lett. **58A**, 402( 1976).
- [28] U. Welp, S. Fleshler, W. K. Kwok, R. A. Klemm, V. M. Vinokur, J. Downey, B. Veal, and G. W. Crabtree, Phys. Rev. Lett. **67**, 3180 (1991).
- [29] Q. Li, M. Suenaga, T. Hikata and K. Sato, Phys. Rev. B **46**, 5857 (1992).
- [30] N.P. Ong *et al*, Phys. Rev. Lett. **95**, 247002(2005).
- [31] M. J. Naughton, Phys. Rev. B **61**, 1605 (2000).
- [32] Y. M. Huh and D. K. Finnemore, Phys. Rev. B **65**, 092506 (2002); **65**, 024523 (2002); Y. M. Huh, J. E. Ostenson, F. Borsa, V. G. Kogan, D. K. Finnemore, A. Vietkin, A. Revcolevschi, and M. H. Julien, *ibid.* **63**, 064512 (2001).
- [33] A. Schilling *et al*, Nature **382**, 791 (1996); A. Schilling *et. al.*, Phys. Rev. Lett. **78**, 4833 (1997).
- [34] H. Pastoriza, M. F. Goffmann, A. Arribere and F. Cruz, Phys. Rev. Lett. **72**, 2951 (1994); X. Liang, D. A. Bonn and W. N. Hardy, Phys. Rev. Lett. **76**, 835 (1996).
- [35] R. Lortz, F. Lin, N. Musolino, Y. Wang, A. Junod, B. Rosenstein, and N. Toyota, Phys. Rev. B **74**, 104502 (2006)
- [36] F. P-J. Lin and B. Rosenstein, Phys. Rev. B **71**, 172504 (2005)
- [37] D. F. Agterberg, T. M. Rice, and M. Sigrist, Phys. Rev. Lett. **78**, 3374 (1997).

- [38] Y. Ren, J. H. Xu, C. S. Ting, Phys. Rev. Lett. **74**, 3680 (1995); A.J. Berlinsky *et al.*, Phys. Rev. Lett. **75**, 2200 (1995); D.Chang *et al.*, Phys. Rev. Lett. **80**,145 (1998).
- [39] U. Welp *et. al.*, Phys. Rev. Lett. **76**, 4809 (1996).
- [40] M. Willemin *et al*, Phys. Rev. Lett. **81**, 4236 (1998).
- [41] T. Nishizaki *et al*, Physica **C341-348**, 957 (2000).
- [42] T. Sasagawa, K. Kishio, Y. Togawa, J. Shimoyama and K. Kitazawa, Phys. Rev. Lett. **80**, 4297( 1998).
- [43] J. Sok, Ming Xu, Wei Chen, B.J. Suh, J. Gohng, D.K. Finnemore, M.J. Kramer, L.A. Schwartzkopf, and B. Dabrowski, Phys. Rev.**B 51**, 6035 (1995).
- [44] Safar H, Gammel P L, Huse D A, Bishop D J, Rice J P and Ginsberg, Phys. Rev. Lett. **69**, 824 (1992); Kwok W K, Flesher S, Welp U, Vinokur V M, Downey J,Crabtree G W and Miller, Phys. Rev. Lett. **69**, 3370 (1992);Kwok W K, Fendrich J, Welp U, Flesher S, Downey J and Crabtree Phys. Rev. Lett. **72**, 1088 (1994);Kwok W K, Fendrich J, Flesher S, Welp U, Downey J and Crabtree Phys. Rev. Lett. **72**, 1092 (1994); Charalambous M, Chaussy J and Lejay Phys. Rev. B, **45**, 5091 (1992).
- [45] G. F. Sun,K. W. Wong, B. R. Xu, Y. Xin, D. F. Lu, Phys. Lett. A **192**, 122 (1994).
- [46] K. Kim, H. Kim, S. Lee, A. Iyo, Y. Tanaka, K. Tokiwa, and T. Watanabe, Phys. Rev. B **70**, 092501 (2004)
- [47] Dingping Li, B. Rosenstein, V. M. Vinokur, arXiv:cond-mat/0505663v1 (2005).
- [48] (*LLL*)Z. Tešanović, L. Xing, L. Bulaevskii, Q. Li, and M. Suenaga, Phys. Rev. Lett. **69**, 3563 (1992); Z. Tesanovic and A.V. Andreev, Phys. Rev. **B 49**, 4064 (1994);S.W Pierson, O.T. Valls, Z. Tesanovic, M.A. Lindemann, Phys. Rev. **B57**, 8622 (1998).

- [49] I. D. Lawrie, Phys. Rev. **B50**, 9456 (1994); D. Li and B. Rosenstein, Phys. Rev. **B60** 9704, 10460 (1999).
- [50] L. D. Landau, Phys. Z. Sowjet **11**, 129 (1937).
- [51] D. C. Baird and B. K. Mukherjee, Phys. Lett. **25A**, 137 (1967) and references therein.
- [52] L. P. Gor'kov, Zh. Eksperim. i Teor. Fiz. 37, 833 (1959); [English transl.: Soviet Phys.—JETP 10, 593 (1960)].
- [53] E. A. Shapoval, Zh. Eksperim. i Teor. Fiz. 41, 877 (1961) [CAS]; [English transl.: Soviet Phys.—JETP 14, 628 (1962)].
- [54] K. Maki, Physics 1, 21 (1964) [CAS].
- [55] A. M. Clogston, Phys. Rev. Letters 9, 266 (1962); B. S. Chandrasekhar, Appl. Phys. Letters 1, 7 (1962).
- [56] E. Helfand and N. R. Werthamer, Phys. Rev. 147, 288 (1966); N. R. Werthamer, E. Helfand, and P. C. Hohenberg, Phys. Rev. 147, 295 (1966)
- [57] A. P. Mackenzie et al., Phys. Rev. Lett. 71, 1238 (1993)
- [58] S. A. Brazovskii et al., Sov. Phys. JETP 41, 85 (1975); see also T. J. Newman and M. A. Moore, Phys. Rev. B 54, 6661 (1996).
- [59] E. Brezin, D. R. Nelson, and A. Thiaville, Phys. Rev. B 31, 7124 (1985)
- [60] M. A. Moore et al., Phys. Rev. B 58, 936 (1998)
- [61] W. A. Little and R. D. Parks, Phys. Rev. Lett. **9**, 9 (1962); Phys. Rev. **133**, A97 (1964).
- [62] G. Blatter, M.V. Feigel'man, V.B. Geshkenbein, A.I. Larkin, V.M. Vinokur, Rev. Mod. Phys. 66, 1125 (1994).

- [63] J. Yeo and M.A. Moore, Phys. Rev. B **54**, 4218 (1996); *ibid* **64**, 024514 (2001); Phys. Rev. Lett. **76**, 1142 (1996).
- [64] J. Bardeen, L. N. Cooper, and J. R. Schrieffer, Phys. Rev. **108**, 1175 (1957).
- [65] L. N. Cooper, Phys. Rev. **104**, 1189 (1956).
- [66] L. D. Landau and E. M. Lifshitz, *Quantum Mechanics*, Oxford (1997).
- [67] G. M. Eliashberg, Zh. Eksperim. i Teor. Fiz. **38**, 966 (1960); [English transl.: Soviet Phys.—JETP **11**, 696 (1960)].
- [68] V.L. Ginzburg Sov. Phys.-JETP **36** 571.
- [69] G. E. Volovik and L. P. Gorkov, Zh. Eksp. Teor. Fiz. **88**, 1412 (1985) [Sov. Phys. - JETP **61**, 843 (1985)].
- [70] K. Ueda and T. M. Rice, Phys. Rev. B **31**, 7144 (1985). E. I. Blount, Phys. Rev. B **32**, 2935 (1985). L. P. Gorkov, Sov. Sci. Rev. A **9**, 1 (1987). M. Sigrist and K. Ueda, Rev. Mod. Phys. **63**, 239 (1991). V. P. Mineev and K. V. Samokhin, *Introduction to Unconventional Superconductivity*, Gordon and Breach (1999).
- [71] G.Eilenberger, Phys. Rev. **164**, 628 - 635 (1967)
- [72] K. Maki and H. Takayama, Prog. Theor. Phys. **46**, 1651 (1971).
- [73] M.A. Moore, Phys. Rev. B **39**, 136 (1989); Phys. Rev. B **45**, 7336 (1992). V. Zhuravlev and T. Maniv, Phys. Rev. B **60**, 4277 (1999); B **66**, 014529 (2002); B (2007).
- [74] L. P. Gor'kov, Zh. Eksp. Teor. Fiz. **36**, 1918 (1959) [Sov. Phys. - JETP **9**, 1364 (1959)].
- [75] R. P. Groff and R. D. Parks, Phys. Rev. **176**, 567 (1968).
- [76] A. Knigavko, B. Rosenstein, Y. F. Chen, Phys. Rev. B **60**, 550 (1999); A. Knigavko and B. Rosenstein, Phys. Rev. Lett. **82**, 1261 (1999).

- [77] J. Zinn-Justin, *Quantum Field Theory and Critical Phenomena*, *International Series of Monographs on Physics*, **92** (1996).
- [78] Hideetoshi Nishimori, *Statistical physics of spin glasses and information processing* (2001).
- [79] Kyung-Hee Kim, Heon-Jung Kim, Sung-Ik Lee, A. Iyo, Y. Tanaka, K. Tokiwa, and T. Watanabe *Phys. Rev. B* **70**, 092501 (2004)
- [80] C. Carballerisa *et al*, *Phys. Rev. Lett.* **84**, 3157(2000); *ibid*, *Physica* **384C**, 185 (2003); J.P. Gollub *et al*, *Phys. Rev. B* **7**, 3039(1973); D.C. Johnston and J. H. Cho, *Phys. Rev. B* **42**, 8710 (1990)
- [81] S. Salem-Sugui Jr., A. D. Alvarenga, K. C. Goretta, V. N. Vieira, B. Veal, and A. P. Paulikas, *Journal of Low Temperature Physics*, Vol. 141, Nos. 1/2, 83 (2005)
- [82] D. Li and B. Rosenstein, *Phys. Rev. B* **65**, 024514 (2002)
- [83] D. Li , B. Rosenstein, *Phys. Rev. B* **65**, 220504 (**R**) (2002).
- [84] A.E. Koshelev, *Phys. Rev. B* **50**, 506 (1994)
- [85] D. Li and B. Rosenstein, *Phys. Rev. B* **65**, 024513 (2002); *Phys. Rev. Lett.* **86**, 3618 (2001)
- [86] B. Rosenstein, B. Ya. Shapiro, R. Prozorov, A. Shaulov, and Y. Yeshurun, *Phys. Rev. B* **63**, 134501 (2001).
- [87] D. Li, B. Rosenstein, *Phys. Rev. B* **70**, 144521(2004).
- [88] R. E. Prange, *Phys. Rev. B* **1**, 2349 (1970).
- [89] D. Li and B. Rosenstein, *Phys. Rev. B* **60**, 9704 (1999).
- [90] D. Li and B. Rosenstein, *Phys. Rev. Lett.* **86**, 3618 (2001).
- [91] R. Ikeda, T. Ohmi, and T. Tsuneto, *J. Phys. Soc. Jpn.* **58**, 1377 (1989)



- [92] C. J. Lobb, Phys. Rev. B **36**, 3930 (1987).
- [93] B. I. Halperin, T. C. Lubensky, and S. K. Ma, Phys. Rev. Lett. **32**, 292 (1974).
- [94] E. Zeldov *et. al.*, Nature **375**, 373 (1995); R. Liang, D.A. Bonn, W.N. Hardy, Phys. Rev. Lett. **76**, 835 (1996); A. Schilling, R. A. Fisher, N. E. Phillips, U. Welp, D. Dasgupta, W. K. Kwok, and G. W. Crabtree, Nature **382**, 791 (1996).
- [95] R. Gilardi, J. Mesot, A. Drew, U. Divakar, S. L. Lee, E. M. Forgan, O. Zaharko, K. Conder, V. K. Aswal, C. D. Dewhurst, R. Cubitt, N. Momono, and M. Oda, Phys. Rev. Lett. **88**, 217003 (2002); S.P. Brown, D. Charalambous, E. C. Jones, E. M. Forgan, P. G. Kealey, A. Erb and J. Kohlbrecher, Phys. Rev. Lett. **92**, 067004 (2004).
- [96] U. Divakar, A.J. Drew, S.L. Lee, R. Gilardi, J. Mesot, F.Y. Ogrin, D. Charalambous, E.M. Forgan, G.I. Menon, N. Momono, M. Oda, C.D. Dewhurst, and C. Baines, Phys. Rev. Lett. **92**, 237004 (2004);
- [97] Y. Radzyner, A. Shaulov, Y. Yeshurun, I. Felner, K. Kishio, and J. Shimoyama, Phys. Rev. **B 65**, 100503(R) (2002).
- [98] N. Avraham, B. Khaykovich, Y. Myasoedov, M. Rappaport, H. Shtrikman, D.E. Feldman, T. Tamegai, P.H. Kes, M. Li, M. Konczykowski, K. van der Beek, and E. Zeldov, Nature **411**, 451 (2001).
- [99] E.H. Brandt, J. Low Temp.Phys. **26**, 709;735 (1977); Phys. Rev. B **34**, 6514 (1986); Rep.Prog.Phys. **58**, 1465 (1995).
- [100] M. C. Dai, T. J. Yang, Physica C, **305**, 301 (1998).
- [101] T. Giamarchi and P. LeDoussal, Phys. Rev. B **52**, 1242 (1995); T. Nattermann, Phys. Rev. Lett. **64**, 2454 (1990); T. Natterman and S. Scheindl, Adv. Phys. **49**, 607 (2000)

- [102] C.E. Sosolik, J.A. Stroschio, M.D. Stiles, E.W. Hudson, S.R. Blankenship, A.P. Fein, and R.J. Celotta, Phys.Rev.**B 68**, 140503(R) (2003).
- [103] M.R. Eskildsen, C.D. Dewhurst, B.W. Hoogenboom, C. Petrovic and P.C. Canfield, Phys.Rev.Lett. **90**, 187001 (2003);
- [104] B. Rosenstein and A. Knigavko, Phys. Rev. Lett. **83**, 844 (1999).
- [105] D. Jaiswal Nagara,, T. Isshikia, N. Kimuraa, H. Aokia, S. Ramakrishnan and A.K. Grover, Physica C to be published, D. Jaiswal Nagara, A.D. Thakur, H. Aokia, S. Ramakrishnanb and A.K. Grover (to be published), and private communication;
- [106] H. Won and K. Maki, Phys. Rev. **B 53**, 5927 (1996).
- [107] G. Eilenberger, Phys. Rev. **164**, 628 (1967); K. Maki and H. Takayama, Prog. Theor. Phys. **46**, 1651 (1971).
- [108] M.A. Moore, Phys. Rev. **B41**, 7124 (1996), M. A. Moore, Phys. Rev. **B 39**, 136 (1989); Phys. Rev. **B31**, 7336 (1992); Phys. Rev. **B 55**, 14136 (1997);J. Yeo and M.A. Moore, Phys. Rev. Lett. 76, 1142 (1996).
- [109] G.J. Ruggeri and D.J. Thouless, J. Phys. **F6**, 2063 (1976).
- [110] G.J. Ruggeri, Phys. Rev. **B20**, 3626 (1978); G. J. Ruggeri, J. Phys. **F9**, 1861 (1979).
- [111] R. Sasik and D. Stroud, Phys. Rev. Lett. **75**, 2582 (1995).
- [112] B. Rosenstein, Phys. Rev. **B 60**, 4268(1999).
- [113] B. Zhou *et al*, Phys. Rev. **B 47**, 11631 (1993) ; S.W Pierson *et al*, Phys. Rev. Lett. **74**, 1887 (1995); Phys. Rev. **B 53**, 8638 (1996) .
- [114] G. Lascher, Phys. Rev. **A140**, 523 (1965).
- [115] J. Hu, A. H. Mcdonald and B. D. Mckay, Phys. Rev **B49**, 15263 (1994).

- [116] S. Hikami, A. Fujita and A.I. Larkin, Phys. Rev. **B44**, R10400 (1991); E. Brezin, A. Fujita and S. Hikami, Phys. Rev. Lett. **65**, 1949 (1990), **65**, 2921(E) (1990).
- [117] D. J. Amit, *Field Theory, the Renormalization Group, and Critical Phenomena* (World Scientific, Singapore, 1984).
- [118] G. A. Baker, *Quantitative Theory of Critical Phenomena* (Academic Press, Boston, 1990).
- [119] M. Tinkham, *Introduction to Superconductivity*, (McGraw - Hill, New York, 1996).
- [120] R. Brout, *“Phase Transitions”*, *University of Brussels, New York - Amsterdam*, (1965). JLTP (1991).

